pISSN 2234-0637 I eISSN 3140-0663

JASS | Journal of Advanced Spine Surgery

JASS | Journal of Advanced Spine Surgery
Vol. 16 • No. 1 • June 2026
Page 1–67

JASS | Journal of Advanced Spine Surgery

Vol. 16 • No. 1 • June 2026

Korean Society for the Advancement of Spine Surgery

www.e-jass.org

JASS
Journal of Advanced Spine Surgery

pISSN 2234-0637 I eISSN 3140-0663

Vol. 16 · No. 1 · June 2026

Aims and scope

Journal of Advanced Spine Surgery (JASS), the official journal of the Korean Society for the Advancement of Spine Surgery (KOSASS), is a peer-reviewed journal which publishes articles related to basic and clinical researches of all fields of advanced spinal surgery.

The journal aims to promote communications among spine surgeons especially who are interested in advanced spine surgery and its related basic research. All manuscripts should be creative, informative and useful for the diagnosis and treatment of spine problems. Manuscripts regarding advanced spinal technology would be preferable. Every researcher who has interested in the aims and scope of Journal of Advanced Spine Surgery is encouraged to submit the papers from all over the world.

Open access

Editor-in-Chief Jae Keun Oh

Published on June 30, 2026

Editorial office
The Korean Society for the Advancement of Spine Surgery
50-1, Yonsei-ro, Seodaemun-gu, Seoul 03722, Korea
Tel: +82-2-2228-0582 Fax: +82-2-393-9979
E-mail: office@e-jass.org

Printing office
M2PI
#805, 26 Sangwon 1-gil, Seongdong-gu, Seoul 04779, Korea
Tel: +82-2-6966-4930 Fax: +82-2-6966-4945
E-mail: support@m2-pi.com

JASS | Journal of Advanced Spine Surgery

JASS
Journal of Advanced Spine Surgery

Contents

Original Articles

Technical Note

Case Reports

Original Article

J Adv Spine Surg 2026;16(1):1-8
https://doi.org/10.63858/jass.26.0024
pISSN 2234-0637 • eISSN 3140-0663

JASS
Journal of Advanced Spine Surgery

Impact of Percutaneous Vertebroplasty on Vertebral Height and Sagittal Alignment in Thoracolumbar Osteoporotic Compression Fractures: A Retrospective Observational Study

Junho Oh, M.D.[1], Gi Jeong Park, M.D.[2], Kwang-Ryeol Kim, M.D.[2]

[1]Department of Neurosurgery, International St. Mary's Hospital, Catholic Kwandong University College of Medicine, Incheon, Korea
[2]Department of Neurosurgery, Daegu Catholic University School of Medicine, Daegu, Korea

Purpose: This study aimed to evaluate whether percutaneous vertebroplasty (PVP) contributes to vertebral height restoration and sagittal alignment correction in osteoporotic vertebral compression fractures (OVCF), focusing on thoracolumbar junction fractures.
Methods: A retrospective review of 40 patients with single-level OVCF at T10–L2 treated with PVP was performed. Vertebral heights (anterior, middle, and posterior) and sagittal alignment (thoracic kyphosis, lumbar lordosis, sagittal vertical axis, and segmental Cobb's angle) were measured preoperatively, at 3 months, and at 6 months. Clinical outcomes included visual analog scale and EuroQol-5 Dimensions.
Results: Significant pain relief and improvement in quality of life were observed at 6 months postoperatively. Vertebral height restoration, particularly in the anterior and middle portions, was noted at 3 months; however, partial loss of the restored height occurred by 6 months. Most sagittal alignment parameters showed no significant postoperative change, although lumbar lordosis significantly increased, resulting in a reduced pelvic incidence–lumbar lordosis mismatch.
Conclusion: PVP provides meaningful clinical improvement in thoracolumbar OVCFs and offers early vertebral height restoration; however, this radiologic benefit is not sustained over time. While limited improvement in lumbar lordosis was observed, PVP does not substantially correct global sagittal alignment. These findings suggest that PVP should be considered primarily a pain-relieving and stabilizing procedure rather than a deformity-correcting intervention.

Keywords: Vertebroplasty, Spinal curvatures, Spinal fractures, Body height

Introduction

Osteoporotic vertebral compression fracture (OVCF) is among the most common fragility fractures in the aging population, with more than half of individuals over 80 years of age experiencing at least one fracture during their lifetime. These fractures often lead not only to acute mechanical back pain but also to progressive vertebral body collapse, segmental kyphosis, and global sagittal imbalance, ultimately reducing mobility, independence, and quality of life.[1,2] The thoracolumbar junction (T10–L2) is particularly vulnerable to osteoporotic fractures because it constitutes a biomechanical transition zone between the rigid, kyphotic thoracic

Received: December 19, 2025; Revised: February 4, 2026; Accepted: February 10, 2026
Corresponding author: Kwang-Ryeol Kim, M.D.
Department of Neurosurgery, Daegu Catholic University School of Medicine, 33 Duryugongwon-ro 17-gil, Nam-gu, Daegu 42472, Korea
TEL: +82-53-650-4539, FAX: +82-53-650-4932, E-mail: ianremedios@cu.ac.kr

spine and the more flexible, lordotic lumbar spine.[3] Accordingly, OVCFs most frequently occur in this region, and fractures at T10–L2 tend to cause more pronounced deformity and instability than those at other spinal levels.[4,5]

Conservative management remains the first-line treatment for most OVCFs. Standard care involves 1–2 weeks of absolute bed rest with back support, followed by using a rigid thoracolumbar orthosis.[6,7] However, pain control may be insufficient in a considerable proportion of patients, especially those with severe collapse or progressive kyphosis. In such cases, surgical options including percutaneous vertebroplasty (PVP) or kyphoplasty (KP) are considered.[8,9]

Previous studies have shown heterogeneous results, partly due to variation in fracture levels, inclusion of multilevel fractures, differences between PVP and KP, inconsistent follow-up periods, and the confounding effect of osteoporosis pharmacotherapy.[10-12] There have even been reports that PVP has no significant effect in pain control.[13,14] On the other hand, there are also reports that it is helpful not only in controlling early pain but also in controlling chronic pain and reducing mortality.[15-18]

Although PVP is widely accepted as an effective method for rapid pain relief, its impact on vertebral height restoration and correction of segmental kyphosis remains controversial.[19,20] Thus, the true radiologic and clinical impact of PVP in OVCFs, particularly at the anatomically critical thoracolumbar junction remains unclear.

Therefore, this study evaluates whether PVP meaningfully restores vertebral height and improves global or segmental alignment in thoracolumbar OVCF.

Methods

1. Study population

This retrospective observational study included patients who underwent PVP or KP for OVCFs at a single institution between March 2020 and February 2023. A total of 157 consecutive patients were initially identified. To minimize confounding effects on radiologic outcomes, patients were excluded if they had multilevel fractures or previous adjacent-level fractures (n = 27), underwent KP (n = 25), had a follow-up duration of less than 6 months or lacked follow-up whole-spine standing radiographs (WSXR) (n = 17), received anabolic osteoporosis agents such as romosozumab or teriparatide (n = 15), or had pathologic fractures due to metastatic disease or Kümmell's disease (n = 14).

After applying these exclusion criteria, 59 patients who underwent PVP for a single-level OVCF were eligible for analysis. To focus specifically on fractures occurring at the biomechanically vulnerable thoracolumbar junction, only patients with fractures at T10–L2 were included in the final study population (n = 40). Patients with mid-thoracic (T6–8, n = 9) or lower lumbar (L3–5, n = 10) fractures were excluded from the primary analysis.

2. Procedural technique

All PVP procedures were performed by a single experienced spine surgeon under biplanar fluoroscopic guidance.

All procedures were performed with the patient in the prone position under sterile conditions. After routine skin preparation and surgical draping, the target pedicle was identified using a C-arm fluoroscope in the anteroposterior (AP) view. The superolateral margin of the target pedicle was infiltrated with 1% lidocaine to achieve local anesthesia of the skin and paraspinal muscles. A 0.5-cm skin incision was made using a No. 15 blade, and a Jamshidi needle was advanced through the pedicle under fluoroscopic guidance.

Needle advancement was monitored using alternating AP and lateral fluoroscopic views. Once the needle tip was confirmed to be positioned within the anterior one-third of the vertebral body on the lateral view, polymethylmethacrylate (PMMA) cement was prepared and injected during the doughy phase under continuous fluoroscopic monitoring. Cement injection was terminated immediately upon adequate filling of the vertebral body or when any sign of cement leakage was detected (Fig. 1).

For the unilateral transpedicular approach, the needle tip was directed slightly more medially compared with the bilateral approach to facilitate cement distribution across the midline.[21] In addition, a relatively lower-viscosity PMMA cement was used to promote bilateral intravertebral spread. If adequate cement distribution to the contralateral side was not achieved during injection via the unilateral approach, an additional transpedicular procedure on the contralateral side was considered to ensure sufficient vertebral body filling and stabilization.

A unilateral transpedicular approach was used in 22 cases, while a bilateral transpedicular approach was employed in 18 cases, depending on fracture morphology and cement distribution.

Postoperatively, patients were maintained on absolute bed rest for 4 hours and were subsequently mobilized with a rigid thoracolumbar orthosis on the same or following day. The brace was worn during ambulation and daily activities for 3 months after the procedure.

3. Clinical assessment

Clinical outcomes were evaluated at baseline (preoperatively)

https://doi.org/10.63858/jass.26.0024

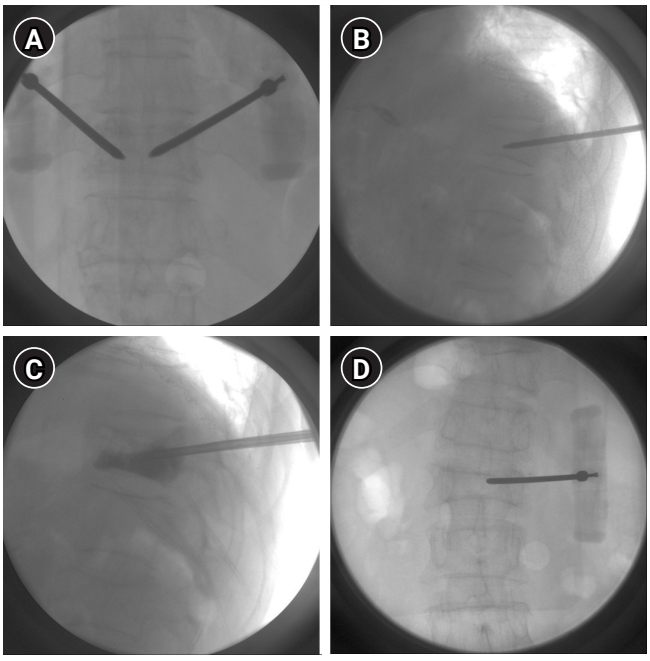

Fig. 1. Intraoperative C-arm fluoroscopic images demonstrate the percutaneous vertebroplasty procedure. (A) Anteroposterior (AP) fluoroscopic view confirming bilateral pedicle localization under C-arm guidance and advancement of Jamshidi needles through the bilateral pedicles. (B) Lateral fluoroscopic view showing the Jamshidi needle positioned within the anterior one-third of the vertebral body. (C) Polymethylmethacrylate cement injection under continuous fluoroscopic monitoring via a bilateral transpedicular approach. (D) AP fluoroscopic view of unilateral transpedicular approach.

and at 6 months postoperatively. Back pain intensity was assessed using the visual analog scale (VAS), and health-related quality of life was evaluated using the EuroQol-5 Dimensions (EQ-5D) index. Changes in clinical outcomes were analyzed in relation to radiologic findings to assess the association between symptomatic improvement and structural changes following PVP.

4. Radiologic assessment

Radiologic evaluations were performed at three times: preoperatively (within 1 week before PVP), and at 3 months and 6 months postoperatively. WSXR were obtained at each time point and used for all measurements.

Vertebral body height was assessed at the fractured level by measuring anterior, middle, and posterior vertebral heights. Measurements were recorded as absolute values and, when applicable, expressed as a percentage of the estimated normal height based on adjacent intact vertebrae.

Sagittal alignment parameters included thoracic kyphosis (TK) measured as the Cobb angle from T5 to T12, lumbar lordosis (LL) measured from L1 to S1, sagittal vertical axis (SVA), and the segmental Cobb angle (SCA) at the fractured level representing local kyphosis. All radiologic parameters were independently measured by two spine surgeons using a Picture Archiving and Communication System–based digital measurement system, and the mean of the two measurements was used for statistical analysis.

5. Statistical analysis

Continuous variables are presented as mean ± standard deviation, and categorical variables are expressed as frequencies and percentages. Normality of continuous variables was assessed using the Shapiro-Wilk test. Changes in clinical outcomes (VAS and EQ-5D scores) and radiologic parameters (sagittal alignment variables) before and after PVP were analyzed using paired t-tests. For variables that did not meet the assumption of normality, the Wilcoxon signed-rank test was applied. Changes in vertebral body height (anterior, middle, and posterior) across three points (preoperative, 3 months, and 6 months) were analyzed using one-way repeated-measures analysis of variance (ANOVA). When a significant overall effect was detected, post hoc pairwise comparisons were performed with Bonferroni correction. Statistical analyses were performed using SPSS software version 19.0 (IBM Corp., Armonk, NY, USA). All tests were two-tailed and a p-value < 0.05 was considered statistically significant.

6. Ethics statement

This retrospective study was approved by the Institutional Review Board of our institution (IRB No. IS25RISI0074) and was conducted in accordance with the principles of the Declaration of Helsinki. Because of the retrospective design of the study and the use of de-identified data, the requirement for informed consent was waived by the Institutional Review Board.

Results

1. Patient characteristics

The patient cohort in this study comprised nine men and 31 women, with median age of 82.20 years (range, 39 to 107 years). The L1 vertebral level was the most commonly affected level, with 16 patients (40.0%), followed by L2 in 10 patients (25.0%) and T12 in eight patients (20.0%). Mean injected PMMA volume was 5.53 mL (range, 3 to 9 mL), mean time to surgery 9.58 days (range, 1 to 47 days), and mean operative time 29.73 minutes (range, 15 to 50 minutes). Bone mineral density T-scores were −3.19 (lumbar spine) and −3.02 (femoral neck) (Table 1).

2. Clinical outcomes

The mean VAS scores for back pain before PVP were 7.80 ± 1.47. At 6 months after PVP, the mean VAS scores decreased to 3.30 ± 1.47. The VAS score decreased by approximately 4.5 points before and after the procedure.

The mean EQ-5D score was 0.51 ± 0.23 before PVP. It increased by 0.21 to 0.72 ± 0.18 after PVP (Table 2).

3. Radiologic outcomes

1) Vertebral height

Radiographic analysis demonstrated early improvement in vertebral body height following PVP. At 3 months postoperatively, the mean anterior vertebral height increased from 21.13 mm preoperatively to 23.94 mm, and the mean middle height increased from 17.23 mm to 19.90 mm. A modest increase was also observed in the posterior vertebral height, from 28.55 mm to 29.68 mm.

However, at the 6-month follow-up, partial loss of the restored vertebral height was observed. The mean anterior height decreased to 22.35 mm, and the middle height decreased to 18.64 mm, while the posterior height slightly decreased to 28.94 mm. Although vertebral heights at 6 months remained higher than preoperative values, the initial postoperative gains were not fully maintained over time (Fig. 2).

2) Sagittal alignment

Assessment of sagittal alignment revealed minimal changes following PVP. The mean TK angle showed a slight decrease from 29.84° preoperatively to 29.53° at follow-up. LL demonstrated a small increase from 29.84° to 31.13°. The SVA decreased marginally from 66.45 mm to 65.11 mm. The SCA at the fractured level increased slightly from 7.11° to 7.78°. Among these, LL significantly increased and pelvic incidence minus lumbar lordosis (PI–LL) significantly decreased (Table 3).

4. Correlation between radiologic and clinical outcomes

Correlation analysis was performed to determine whether the degree of vertebral height restoration influenced clinical improvement. No significant correlation was observed between the restoration of anterior, middle, or posterior heights and changes in VAS or EQ-5D scores at any follow-up interval (Table 4).

5. Subgroup analysis based on baseline sagittal balance

To further investigate whether the preoperative sagittal profile influences radiologic outcomes, patients were categorized into subgroups based on SVA and PI–LL mismatch. For SVA, a cutoff of 50 mm was used as it represents the threshold for normal sagittal balance.[22] Regarding PI–LL mismatch, while a 10° threshold is often considered the upper limit of normal, applying this cutoff resulted in a significant disproportion in sample sizes between groups. Therefore, a cutoff of 20° was adopted to represent severe sagittal imbalance, ensuring a more balanced distribution for statistical comparison.[23] Based on these criteria, subgroup analysis was performed to compare changes in TK and SCA (Table 5).

Discussion

The present study demonstrates that PVP provides significant

Table 1. Baseline demographic and clinical characteristics of the study participants

Variable	Value
Age (years)	82.20 ± 6.37
Sex	
Male	9 (22.5)
Female	31 (77.5)
Bone mineral density (T-score, L spine)	–3.19 ± 0.94
Bone mineral density (T-score, Femur)	–3.02 ± 0.85
Operation	
Days to OP (days)	9.58 ± 9.94
OP time (min)	29.73 ± 10.65
PMMA (mL)	5.53 ± 1.37
Fracture level	
T10	2 (5.0)
T11	4 (10.0)
T12	8 (20.0)
L1	16 (40.0)
L2	10 (25.0)

Values are presented as mean ± standard deviation or number (%). OP: operation, PMMA: polymethylmethacrylate.

Table 2. Changes in VAS scores and EQ-5D before and after PVP

Variable	Pre-PVP (n = 40)	6 months (n = 40)	Changes	p-value
VAS	7.80 ± 1.47	3.30 ± 1.81	–4.50 ± 1.78	0.006
EQ-5D	0.51 ± 0.23	0.72 ± 0.17	0.21 ± 0.16	< 0.001

Values are presented as the mean±standard deviation. p-values were obtained by generalized estimating equation. VAS: visual analog scale, EQ-5D: EuroQol-5 Dimensions, PVP: percutaneous vertebroplasty.

https://doi.org/10.63858/jass.26.0024

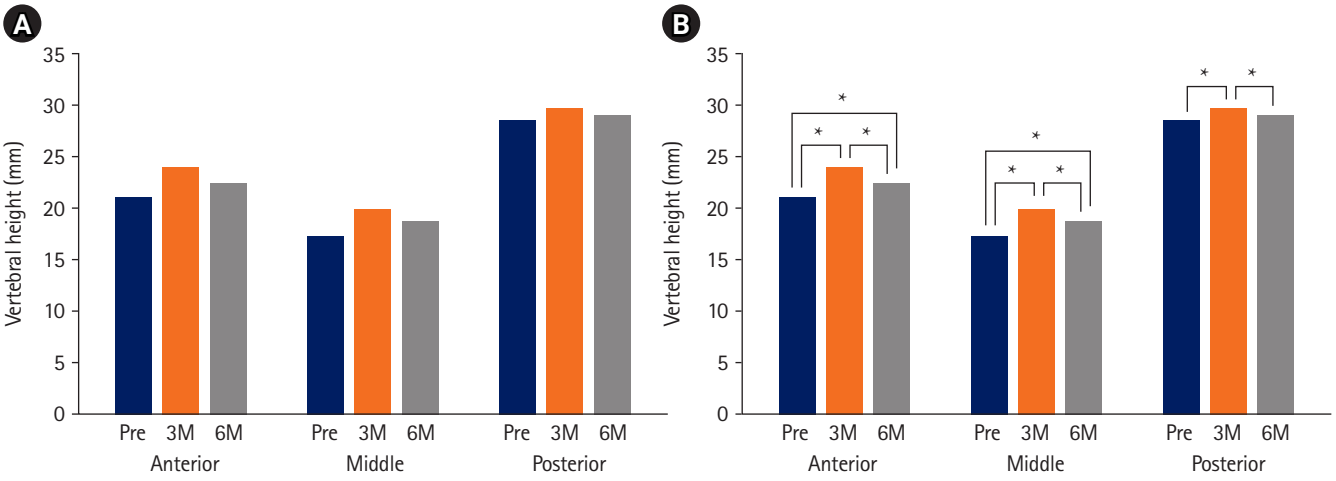

Fig. 2. Changes in vertebral body height following percutaneous vertebroplasty. (A) Mean anterior, middle, and posterior vertebral body heights are shown at the preoperative baseline (Pre), 3 months (3M), and 6 months (6M) after the procedure. Anterior and middle vertebral heights increased significantly at 3 months, with partial loss of restoration observed at 6 months, whereas posterior height remained relatively stable over time. (B) Statistical comparisons were performed using one-way repeated-measures analysis of variance with Bonferroni post hoc correction. An asterisk (*) indicates a statistically significant difference between the indicated time points ($p<0.05$).

Table 3. Changes (°) in sagittal alignment before and after PVP

Variable	Preoperative (n = 40)	Postoperative (n = 40)	Changes	p-value
Thoracic kyphosis	29.84 ± 13.09	29.53 ± 12.96	–0.30 ± 5.17	0.715
Lumbar lordosis	29.84 ± 8.31	31.13 ± 7.99	1.29 ± 3.70	0.001
Sagittal vertical axis	66.45 ± 26.90	65.11 ± 27.45	–1.34 ± 7.03	0.236
Pelvic incidence	56.62 ± 10.86	56.77 ± 10.55	0.14 ± 2.60	0.727
Pelvic tilt	23.69 ± 10.51	23.69 ± 10.14	–0.00 ± 5.56	> 0.99
Sacral slope	32.93 ± 9.56	33.07 ± 9.22	0.14 ± 4.79	0.849
PI–LL	26.78 ± 11.15	25.63 ± 11.02	–1.14 ± 4.70	0.004
Segmental Cobb's angle	7.11 ± 9.03	7.78 ± 10.28	0.68 ± 5.64	0.453

Values are presented as the mean±standard deviation. p-values were obtained by generalized estimating equation. PVP: percutaneous vertebroplasty, PI–LL: pelvic incidence minus lumbar lordosis.

Table 4. Correlation between vertebral height restoration and patient-reported outcomes

Radiologic change	Time	VAS change		EQ-5D change	
		Correlation coefficient	p-value	Correlation coefficient	p-value
Anterior height	3 months & immediate	0.191	0.237	–0.152	0.351
	6 months & 3 months	–0.096	0.557	0.080	0.623
	6 months & immediate	0.113	0.487	–0.086	0.596
Middle height	3 months & immediate	0.037	0.822	–0.025	0.880
	6 months & 3 months	0.110	0.500	–0.182	0.262
	6 months & immediate	0.102	0.530	–0.127	0.436
Posterior height	3 months & immediate	0.035	0.828	–0.224	0.166
	6 months & 3 months	–0.243	0.130	0.020	0.901
	6 months & immediate	–0.180	0.266	–0.159	0.327

VAS: visual analog scale, EQ-5D: EuroQol-5 Dimensions.

Table 5. Subgroup analysis based on baseline sagittal imbalance

Variable	SVA		p-value	PI–LL		p-value
	< 50 mm (n = 10)	≥ 50 mm (n = 30)		< 20° (n = 10)	≥ 20° (n = 30)	
TK change	0.24 ± 5.82	–0.48 ± 5.03	0.707	0.75 ± 4.31	–0.65 ± 5.44	0.463
SCA change	3.54 ± 8.75	–0.28 ± 3.91	0.063	3.13 ± 8.39	–0.14 ± 4.3	0.113

Values are presented as the mean±standard deviation. SVA: sagittal vertical axis, PI–LL: pelvic incidence minus lumbar lordosis, TK: thoracic kyphosis, SCA: segmental Cobb's angle.

clinical improvement in patients with thoracolumbar OVCFs. Meaningful reductions in pain scores and improvements in health-related quality of life were observed at 6 months postoperatively. Radiologic evaluation revealed modest and transient restoration of vertebral body height, which was not fully maintained over time. With respect to sagittal alignment, most global and segmental parameters, including TK, SVA, and SCA, showed no substantial postoperative change; however, LL demonstrated a significant postoperative increase, accompanied by a corresponding reduction in the PI–LL mismatch. Despite these limited alignment-related changes, the overall findings suggest that the primary benefits of PVP are derived from pain relief and mechanical stabilization rather than from durable anatomic restoration or global sagittal realignment.

The substantial pain relief observed in this study is consistent with previous reports supporting the analgesic efficacy of PVP. The mechanism underlying this improvement is likely related to mechanical stabilization of the fractured vertebral body, reduction of micro-motion at the fracture site, and thermal or chemical effects of PMMA cement.[24,25] Our correlation analysis further reinforces this, as no significant association was found between the magnitude of height restoration and clinical outcomes (Table 4). Importantly, the observed clinical benefits occurred despite the absence of meaningful sagittal realignment, reinforcing the concept that pain relief after PVP is not dependent on restoration of vertebral geometry or global spinal balance.[26,27]

With respect to vertebral height, our results demonstrate a clear early postoperative increase, particularly in the anterior and middle portions of the vertebral body. However, this restoration was only partially maintained for 6 months, indicating gradual settling of the fractured vertebra over time. These findings align with biomechanical and clinical studies suggesting that while PVP increases local stiffness, it does not reconstitute the trabecular architecture or load-bearing capacity of osteoporotic cancellous bone. Consequently, progressive collapse may occur even after technically successful cement augmentation.[28,29] This observation is particularly noteworthy when considering the natural course of untreated OVCFs. While untreated fractures typically undergo progressive and irreversible collapse, our data showed an initial significant height restoration followed by only partial loss. This suggests that while PVP may not permanently 'fix' the anatomy to a pre-fracture state, it potentially alters the natural history of vertebral collapse by providing early mechanical stabilization.

Despite early height restoration, sagittal alignment parameters, including TK, LL, SVA, and SCA, remained largely unchanged. Several factors may account for this observation. First, the thoracolumbar junction is subject to high transitional biomechanical stress, limiting the impact of localized vertebral height changes on global alignment.[30] Second, PVP does not restore disc height, ligamentous tension, or posterior column integrity, all of which play critical roles in sagittal balance.[31] Finally, the magnitude of vertebral height restoration observed in this study was relatively small and likely insufficient to translate into measurable changes in global or segmental alignment. Furthermore, our subgroup analysis demonstrated that even in patients with significant baseline sagittal imbalance (SVA ≥ 50 mm or PI–LL ≥ 20°), the corrective impact of single-level PVP on local or global alignment remained negligible (Table 5).

From a clinical perspective, these findings indicate that PVP should be regarded primarily as a procedure for pain control and fracture stabilization rather than a deformity-correcting intervention. Although early vertebral height restoration may be observed, it is not reliably sustained, and meaningful correction of kyphotic deformity or sagittal imbalance should not be expected. Accordingly, patient counseling should emphasize the symptomatic benefits of PVP while setting realistic expectations regarding radiologic and alignment outcomes, particularly in fractures involving the thoracolumbar junction.

Despite the clinical relevance of our findings, this study has several limitations that should be acknowledged. First, the follow-up duration was relatively short, which may be insufficient to fully capture long-term changes in vertebral height, sagittal alignment, and fracture progression after PVP. Second, the most significant limitation is the absence of a control group treated conservatively. Without a comparative cohort, it is difficult to definitively distinguish the therapeutic effects of PVP from the natural radiographic

https://doi.org/10.63858/jass.26.0024

progression of OVCFs. However, the rigorous inclusion of only single-level thoracolumbar junction fractures allowed for a more focused observation of the procedure's specific impact on this biomechanically sensitive region. Future prospective randomized controlled trials comparing PVP with conservative management are necessary to further elucidate the isolated impact of cement augmentation on spinal kinematics. Third, radiologic analysis was based primarily on lateral WSXRs, and AP radiographic analysis was not performed. As a result, the lateral distribution of PMMA cement within the vertebral body could not be assessed, and potential associations between cement dispersion patterns and radiologic or clinical outcomes could not be analyzed. These limitations suggest that the findings should be interpreted with caution and underscore the need for future studies with longer follow-up periods, comparative study designs, and more comprehensive radiographic evaluation.

In conclusion, while PVP for single-level thoracolumbar OVCFs provides significant pain relief and immediate restoration of vertebral height, its impact on global sagittal alignment appears limited. Our findings suggest that PVP may contribute to local segmental stabilization rather than substantial correction of global sagittal balance. Further large-scale, prospective controlled trials are warranted to confirm these observations.

Author contributions

Conceptualization: KRK. Data curation: JO, KRK. Formal analysis: GJP, KRK. Investigation: JO, KRK. Funding acquisition: KRK. Methodology: GJP, KRK. Project administration: KRK. Resources: JO, KRK. Software: JO, GJP. Supervision: KRK. Validation: JO, KRK. Visualization: GJP, KRK. Writing – original draft: JO, KRK. Writing – review & editing: KRK.

Conflict of interest

Kwang-Ryeol Kim, an editor of the *Journal of Advanced Spine Surgery*, was not involved in the editorial evaluation or decision to publish this article. All remaining authors have declared no conflicts of interest.

Funding

This work was supported by research grants from Daegu Catholic University in 2023.

Acknowledgments

None.

ORCID

Junho Oh, https://orcid.org/0009-0004-5533-7310
Gi Jeong Park, https://orcid.org/0000-0001-7756-2632
Kwang-Ryeol Kim, https://orcid.org/0000-0001-8205-2987

References

1. Kim HJ, Park S, Park SH, et al. Prevalence of frailty in patients with osteoporotic vertebral compression fracture and its association with numbers of fractures. Yonsei Med J 2018;59:317-24.
2. Lee BG, Choi JH, Kim DY, Choi WR, Lee SG, Kang CN. Risk factors for newly developed osteoporotic vertebral compression fractures following treatment for osteoporotic vertebral compression fractures. Spine J 2019;19:301-5.
3. Wood KB, Li W, Lebl DR, Ploumis A. Management of thoracolumbar spine fractures. Spine J 2014;14:145-64.
4. Chen R, Lei S, Li G. The prevalence and multifactor analysis of thoracolumbar fasciitis in patients with osteoporotic vertebral compression fractures. Spine J 2025;25:1644-51.
5. Tu W, Niu Y, Su P, Liu D, Lin F, Sun Y. Establishment of a risk prediction model for residual low back pain in thoracolumbar osteoporotic vertebral compression fractures after percutaneous kyphoplasty. J Orthop Surg Res 2024;19:41.
6. Longo UG, Loppini M, Denaro L, Maffulli N, Denaro V. Conservative management of patients with an osteoporotic vertebral fracture: a review of the literature. J Bone Joint Surg Br 2012;94:152-7.
7. Longo UG, Loppini M, Denaro L, Maffulli N, Denaro V. Osteoporotic vertebral fractures: current concepts of conservative care. Br Med Bull 2012;102:171-89.
8. Anselmetti GC, Muto M, Guglielmi G, Masala S. Percutaneous vertebroplasty or kyphoplasty. Radiol Clin North Am 2010;48:641-9.
9. Korovessis P, Syrimpeis V, Korovesis A, Dimakopoulos G. Incidence of new osteoporotic adjacent vertebral body fractures: a comparison between conservative treatment and vertebral body augmentation (vertebroplasty, kyphoplasty): a systematic review and meta-analysis. Front Surg 2025;12:1594217.
10. Wang H, Sribastav SS, Ye F, et al. Comparison of percutaneous vertebroplasty and balloon kyphoplasty for the treatment of single level vertebral compression fractures: a meta-analysis of the literature. Pain Physician 2015;18:209-22.
11. Lainez Ramos-Bossini AJ, Lopez Zuniga D, Ruiz Santiago F. Percutaneous vertebroplasty versus conservative treatment and placebo in osteoporotic vertebral fractures: meta-analysis and critical review of the literature. Eur Radiol 2021;31:8542-53.

12. Sun Y, Zhang Y, Ma H, Tan M, Zhang Z. Therapeutic efficacy and safety of percutaneous curved vertebroplasty in osteoporotic vertebral compression fractures: a systematic review and meta-analysis. Orthop Surg 2023;15:2492-504.
13. Fisher CG, Vaccaro AR, Patel AA, et al. Evidence-based recommendations for spine surgery. Spine (Phila Pa 1976) 2020;45:851-9.
14. Firanescu CE, de Vries J, Lodder P, et al. Vertebroplasty versus sham procedure for painful acute osteoporotic vertebral compression fractures (VERTOS IV): randomised sham controlled clinical trial. BMJ 2018;361:k1551.
15. Buchbinder R, Johnston RV, Rischin KJ, et al. Percutaneous vertebroplasty for osteoporotic vertebral compression fracture. Cochrane Database Syst Rev 2018;4:CD006349.
16. Carli D, Venmans A, Lodder P, et al. Vertebroplasty versus active control intervention for chronic osteoporotic vertebral compression fractures: the VERTOS V randomized controlled trial. Radiology 2023;308:e222535.
17. Cazzato RL, Bellone T, Scardapane M, et al. Vertebral augmentation reduces the 12-month mortality and morbidity in patients with osteoporotic vertebral compression fractures. Eur Radiol 2021;31:8246-55.
18. Kawanishi M, Tanaka H, Ito Y, et al. Treatment for osteoporotic vertebral fracture: a short review of orthosis and percutaneous vertebroplasty and balloon kyphoplasty. Neurospine 2023;20:1124-31.
19. Beall DP, Phillips TR. Vertebral augmentation: an overview. Skeletal Radiol 2023;52:1911-20.
20. Yokoyama K, Ikeda N, Tanaka H, et al. The effectiveness of vertebral height restoration based on the vertebroplasty procedure used to treat osteoporotic vertebral fractures. Neurospine 2023;20:1159-65.
21. Kim AK, Jensen ME, Dion JE, Schweickert PA, Kaufmann TJ, Kallmes DF. Unilateral transpedicular percutaneous vertebroplasty: initial experience. Radiology 2002;222:737-41.
22. Yamada T, Yamato Y, Hasegawa T, et al. Influence of the sagittal vertical axis on the risk of falls in community-dwelling elderly people: a retrospective longitudinal study. Spine Surg Relat Res 2020;4:237-41.
23. Schwab FJ, Blondel B, Bess S, et al. Radiographical spinopelvic parameters and disability in the setting of adult spinal deformity: a prospective multicenter analysis. Spine (Phila Pa 1976) 2013;38:E803-12.
24. Marrs B, Andrews R, Rantell T, Pienkowski D. Augmentation of acrylic bone cement with multiwall carbon nanotubes. J Biomed Mater Res A 2006;77:269-76.
25. Feki F, Zairi F, Tamoud A, et al. Understanding the recovery of the intervertebral disc: a comprehensive review of in vivo and in vitro studies. J Bionic Eng 2024;21:1919-48.
26. Kim YC, Bok DH, Chang HG, et al. Increased sagittal vertical axis is associated with less effective control of acute pain following vertebroplasty. Bone Joint Res 2016;5:544-51.
27. McDonnell P, McHugh PE, O'Mahoney D. Vertebral osteoporosis and trabecular bone quality. Ann Biomed Eng 2007;35:170-89.
28. Patel SK, Khan S, Dasari V, Gupta S. Beyond pain relief: an in-depth review of vertebral height restoration after balloon kyphoplasty in vertebral compression fractures. Cureus 2023;15:e46124.
29. Mahato NK. Transitional dysmorphisms at the thoracolumbar and lumbosacral junctions: perspectives on biomechanical implications and etiological relationships. J Morphol Sci 2022;39:164-9.
30. Patwardhan AG, Khayatzadeh S, Havey RM, et al. Cervical sagittal balance: a biomechanical perspective can help clinical practice. Eur Spine J 2018;27(Suppl 1):25-38.
31. Yang H, Zou J. Minimally invasive vertebroplasty and kyphoplasty in treating osteoporotic vertebral compression fractures. In: Chen PQ, Lin RM, Tsai KS, editors. Osteoporosis of the spine: Asian perspectives. World Scientific Publishing; 2021. p. 333-9.

https://doi.org/10.63858/jass.26.0024

Original Article

J Adv Spine Surg 2026;16(1):9-16
https://doi.org/10.63858/jass.26.0026
pISSN 2234-0637 • eISSN 3140-0663

JASS
Journal of Advanced Spine Surgery

Should Lumbar Spinal Fixation Levels Be Extended in Case of Screw Loosening and Nonunion?: Allograft Bone Chip Could Avoid Fusion Extension

Minsuk Lee, M.D.[1], Jin Hoon Park, M.D., Ph.D.[1], Danbi Park[1,2], Chongman Kim, Ph.D.[3], Sun Woo Jang, M.D.[4], Chang Duk Yuk, M.D.[5]

[1]Department of Neurological Surgery, Asan Medical Center, University of Ulsan College of Medicine, Seoul, Korea
[2]College of Nursing, Korea University, Seoul, Korea
[3]Department of Industrial and Management Engineering, Myongji University, Seoul, Korea
[4]Department of Neurological Surgery, Gangneung Asan Hospital, University of Ulsan College of Medicine, Gangneung, Korea
[5]Department of Neurological Surgery, Spine Center, Jiwoo Hospital, Seongnam, Korea

Study Design: The study was designed as a retrospective clinical study.

Purpose: This study aimed to demonstrate that solid fusion and favorable outcomes can be achieved even without fusion extension through the application of an allograft bone chip insertion technique.

Overview of Literature: Screw loosening and nonunion are common complications following lumbar posterior fixation, often resulting from fusion failure. The optimal surgical strategy remains controversial, and most surgeons prefer extending fusion levels above or below the affected segment.

Methods: Twelve patients who underwent revision surgery for screw loosening and nonunion by a single surgeon were retrospectively analyzed. Allograft bone chips were inserted into loosened screw holes to enhance fixation and promote fusion. Radiologic outcomes were evaluated at 1 year using dynamic flexion–extension X-ray and computed tomography (CT). Solid fusion was defined as ≤3° of motion on X-ray and, in eight patients with CT, as a continuous trabecular bone bridge. Clinical outcomes were assessed using the numerical rating scale (NRS) for back and leg pain and the Oswestry Disability Index (ODI).

Results: From January 2020 to February 2022, 12 patients (7 men, 5 women; mean age, 65.8 years) underwent surgery. Eight were treated without fusion extension, three required one-level extension for adjacent segmental disease, and one for deformity correction. At 1 year, all patients achieved solid fusion with ≤3° motion, and CT confirmed a trabecular bone bridge in eight cases. Mean NRS scores for back and leg pain improved by 6.9 and 5.1 points, respectively, and ODI showed marked functional recovery.

Conclusion: The allograft bone chip insertion technique appears to be a practical revision option for managing screw loosening and nonunion in selected patients. It can achieve solid fusion and favorable outcomes without fusion extension, thereby minimizing surgical morbidity and preserving motion segments.

Keywords: Screw loosening, Nonunion, Short-segment fixation, Allograft bone chip, Solid fusion

Received: January 14, 2026; Revised: April 7, 2026; Accepted: May 13, 2026

Corresponding author: Sun Woo Jang, M.D.
Department of Neurological Surgery, Gangneung Asan Hospital, University of Ulsan College of Medicine, 38 Bangdong-gil, Gangneung 25440, Korea
TEL: +82-33-610-3260, FAX: +82-33-641-8130, E-mail: sunwoo0118@naver.com

Co-corresponding author: Chang Duk Yuk, M.D.
Department of Neurological Surgery, Spine Center, Jiwoo Hospital, 183 Sujeong-ro, Sujeong-gu, Seongnam 13295, Korea
TEL: +82-1544-6686, FAX: +82-31-756-5455, E-mail: ycdcd60@gmail.com

Introduction

Pedicle screw fixation provides three-column stability and strong pull-out strength for fusion in thoracolumbar surgery. It is widely used for fractures, degenerative disease, deformity, tumors, and infections.[1,2] Achieving solid fusion remains the primary goal, and efforts to improve fusion rates include the use of advanced biomechanical materials, optimization of bone quality, and refinement of surgical techniques.[3,4]

Despite these advances, screw loosening, pseudoarthrosis, and nonunion are still encountered in a fusion surgery.[5,6] Screw loosening typically results from mechanical stress, micromotion at the bone–screw interface, and poor bone quality, and it is also associated with cyclic loading and osteoporotic changes.[7,8] The reported incidence of screw loosening ranges from 1% to 15% in non-osteoporotic patients and up to 60% in osteoporotic cases.[4,9,10] When these complications lead to back pain, radiculopathy, or neurological decline, revision surgery is often required.

Currently, there is no standardized surgical strategy for managing screw loosening and nonunion.[11-14] Various revision techniques have been proposed, but long-segment fusion extension remains the most common approach.[12,15] However, this method inevitably sacrifices intact motion segments and increases the lever arm, which may lead to additional stress and a higher risk of adjacent segmental disease (ASD).[16,17] To overcome these drawbacks, our team has adopted short-segment revision using an allograft bone chip insertion technique to restore screw purchase and promote fusion. This study aimed to evaluate the fusion rate and clinical outcomes of this method in patients who underwent lumbar revision surgery with a minimum 1-year follow-up.

Methods

The study was designed and reported in accordance with the STROBE guidelines. We reviewed the electronic medical records, operative notes, and radiologic images of patients who underwent lumbar revision surgery for screw loosening and nonunion between January 2020 and February 2022. All procedures were performed by a single surgeon. Only cases in which revision was performed at the same fixation levels were included. One-level fusion extensions were analyzed only when required for unavoidable reasons, such as ASD or deformity correction.

1. Radiographic evaluation

Fusion status was evaluated at the 1-year follow-up using dynamic flexion–extension X-ray and computed tomography (CT). Solid fusion was defined as ≤3° of angular motion between the upper endplate of the most superior instrumented vertebra and the lower endplate of the most inferior vertebra on dynamic X-ray (Fig. 1A).[13,18-20] In eight patients who underwent postoperative CT, the presence of a continuous trabecular bone bridge across the fusion site was considered additional radiologic evidence of solid fusion (Fig. 1B).[21]

2. Surgical technique

All patients underwent lumbar revision surgery through a pos-

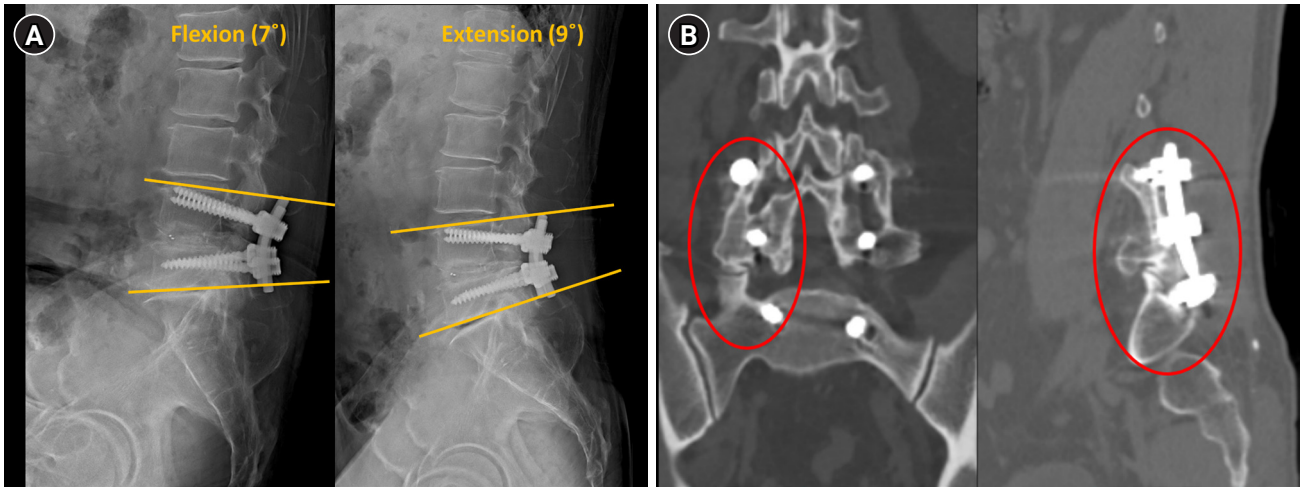

Fig. 1. Radiologic evaluation of fusion stability. (A) Lumbar flexion (7°) and extension (9°) lateral X-ray used to assess dynamic motion between the upper and lower instrumented vertebrae. (B) Postoperative computed tomography scans showing continuous trabecular bone bridging across the fusion site (red circles), confirming solid fusion.

https://doi.org/10.63858/jass.26.0026

terior approach along the previous incision. When additional decompression or deformity correction was required, fusion extension was performed by one level above or below the original construct. Patients were placed prone on a Jackson spinal table to maintain lumbar lordosis. After midline incision and careful dissection along the prior scar, all previous screws and rods were exposed and removed. To achieve stronger fixation, screws one size larger in diameter than the original were used (CD Horizon Solera Spinal System, Medtronic, Sofamor-Danek, Memphis, TN, USA). Allograft bone chips (Maxxeus, Kettering, OH, USA) were densely packed into loosened screw holes using an impactor and mallet—approximately 15 mL per hole when enlarged. New screws were then inserted along the original trajectory, requiring firm pressure due to the compacted graft material, thereby ensuring enhanced pull-out strength. For intact tracts without loosening, simple upsizing of the screw was performed (commonly from 6.5 mm to 7.5 mm) (Supplementary Video S1). After fixation, additional decompression or pedicle subtraction osteotomy (PSO) was carried out if indicated. Rods were applied and contour-matched to restore alignment. Finally, posterolateral fusion using autologous bone from decompression and supplemental allograft was performed, and screw position and alignment were confirmed with intraoperative anteroposterior and lateral X-ray.

3. Ethics statement

This retrospective study was conducted at a tertiary referral hospital and approved by the institutional review board, which waived the requirement for informed consent (IRB No. 2024-0113).

Results

1. Demographics

A total of 12 patients underwent revision lumbar surgery for screw loosening and nonunion (Fig. 2). The cohort included seven men and five women, with a mean age of 65.8 years, mean bone mineral density of –2.2 g/cm^2, mean hospital stay of 4.8 days, and mean follow-up duration of 13.3 months. Four patients were diagnosed with osteoporosis, and all completed at least 1 year of follow-up. Eight patients underwent revision without fusion extension, three required one-level extension for ASD, and one required one-level extension with PSO for deformity correction. Detailed demographic and operative characteristics are summarized in Table 1.

2. Radiologic and clinical outcomes

At the 1-year follow-up, all patients showed ≤3° of motion on dynamic flexion–extension X-ray, confirming the absence of instability. CT was performed in eight patients and demonstrated a continuous trabecular bone bridge at the fusion site in all cases. Consequently, solid fusion was achieved in all 12 patients, corresponding to a 100% fusion rate (Table 2).

Preoperative back and leg pain scores averaged 8.4±0.9 and 7.4±1.8, respectively, which improved to 1.5±0.7 and 2.3±1.2 at 1 year, representing mean reductions of 6.9 and 5.1 points on the numerical rating scale (NRS). Functional outcomes also improved markedly, with a mean Oswestry Disability Index reduction from 65.0% to 22.9% (Table 2, Fig. 3).

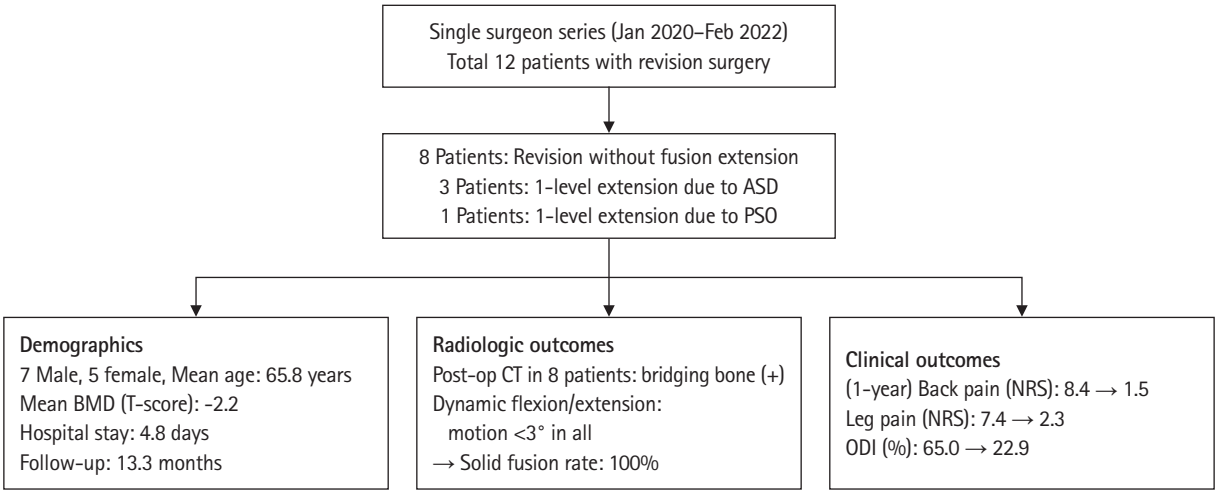

Fig. 2. Flowchart summarizing study enrollment and outcomes. Twelve patients underwent revision surgery for screw loosening and nonunion (eight without fusion extension, three with one-level extension for adjacent segmental disease (ASD), and one with pedicle subtraction osteotomy [PSO]). Radiologic and clinical results are summarized, showing 100% fusion rate and significant improvement in back/leg pain and Oswestry Disability Index (ODI). BMD: bone mineral density, CT: computed tomography, NRS: numerical rating scale.

Table 1. Demographics and characteristics of 12 patients

Patient No.	Age (years)	Sex	BMD	Diagnosis	Previous fusion level	Operative level	Hospital stay (days)	Follow-up period (months)
1	51	M	−1.5	Screw loosening (L5)	L3-5	L3–5	4	13
2	55	M	−1.8	Screw loosening (S1)+Rod fracture	L4–S1	L4–S1	5	14
3	64	M	−2.0	Screw loosening (L2, 3)	L2–S1	L2–S1	5	12
4	55	M	−1.6	Screw loosening (L5)	L3–5	L3–5	4	13
5	66	M	−2.3	Screw loosening (L5, S1)	L5–S1	L5–S1	5	15
6	71	M	−2.6	Screw loosening (S1)	L3–S1	L3–S1	5	14
7	83	F	−3.1	Screw loosening (S1)	L5–S1	L5–S1	6	12
8	80	F	−2.8	Screw loosening (L5)	L4–5	L4–5	5	13
9	71	F	−2.1	Screw loosening (L4)+ASD	L3–4	L3–4–5	4	15
10	59	F	−1.7	Screw loosening (L3)+ASD	L3–S1	L2–S1	4	12
11	67	M	−2.0	Screw loosening (L5, S1)+ASD	L4–S1	L3–S1	5	13
12	67	F	−2.5	Screw loosening (L3)+Flatback syndrome	L3–5	L3–S1 (L4 PSO)	6	14

BMD: bone mineral density, ASD: adjacent segment degeneration, PSO: pedicle subtraction osteotomy.

Table 2. Postoperative 1-year clinical and radiological outcomes of 12 patients

Patient No.	Δ Dynamic X-ray angle[a)]	Bone bridging on CT[b)]	Back pain (NRS)			Leg pain (NRS)			ODI (%)		
			Pre	1 Year	Δ (Pre–1 year)	Pre	1 Year	Δ (Pre–1 year)	Pre	1 Year	Δ (Pre–1 year)
1	2	+	9	0	9	8	3	5	71	18	53
2	1	+	5	2	3	5	2	3	45	25	20
3	0	+	8	4	4	4	4	0	56	39	17
4	2	–	10	4	6	7	4	3	73	40	33
5	2	–	7	4	3	7	4	3	59	38	21
6	1	+	10	0	10	9	1	8	78	13	65
7	0	+	7	1	6	7	2	5	59	22	37
8	1	+	7	0	7	10	2	8	67	15	52
9	0	+	10	1	9	8	2	6	55	14	41
10	2	–	9	0	9	9	1	8	73	13	60
11	0	–	9	2	7	9	2	7	74	25	49
12	2	+	10	0	10	6	1	5	70	13	57

NRS: numerical rating scale, ODI: Oswestry Disability Index, CT: computed tomography. [a)]Δ Dynamic x-ray angle, differences in flexion/extension X-ray of the upper endplate of the vertebral body at the highest level of the surgery and the lower endplate of the vertebral body at the lowest level. [b)]"+" indicates that postoperative CT was performed and bone bridging was confirmed; "-" indicates that CT was not performed (bridging not assessed).

3. Illustrative case

A 55-year-old man presented with persistent low back pain, bilateral leg pain, and numbness. He had previously undergone decompression at L4–5 in 2012 and posterior lumbar interbody fusion at L3–5 in 2019. Although symptoms improved temporarily, they gradually worsened, with severe back pain (NRS 9) and both leg pain (NRS 8) at presentation. Anteroposterior X-ray revealed a halo sign suggestive of L5 screw loosening, and CT confirmed bilateral L5 screw loosening with nonunion at L3–4–5 (Fig. 4A–C). Magnetic resonance imaging demonstrated preserved spinal canal dimension without significant stenosis (Fig. 4D, 4E), and neurological examination showed mild weakness (grade 4) of the left lower extremity.

Through a posterior approach, the previous instrumentation was removed. The L5 screw holes were markedly enlarged, and approximately 15 mL of allograft bone chips were densely impacted into each hole using an impactor and mallet. Larger (7.5 mm) screws were then reinserted along the original trajectory, requiring high insertional torque due to dense graft packing. An additional posterolateral fusion using autograft and allograft bone chips was also performed.

Postoperatively, the patient experienced marked relief of pain and numbness. At the 1-year follow-up, dynamic X-ray showed ≤3° of motion without instability, and anteroposterior X-ray

https://doi.org/10.63858/jass.26.0026

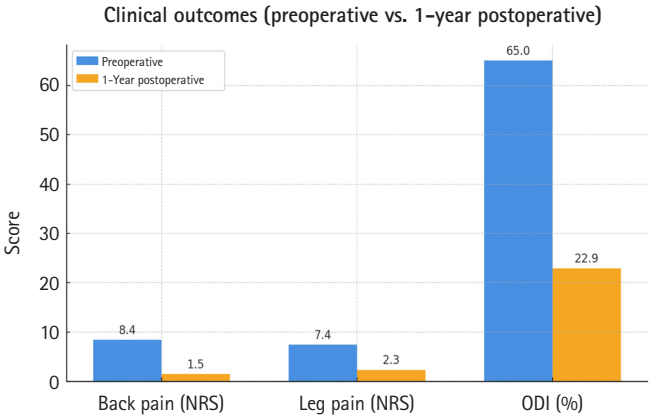

Fig. 3. Comparison of preoperative and 1-year postoperative clinical outcomes. Mean back pain (numerical rating scale [NRS]) improved from 8.4 to 1.5, leg pain (NRS) from 7.4 to 2.3, and Oswestry Disability Index (ODI) from 65.0% to 22.9%, indicating marked pain relief and functional recovery.

demonstrated a distinct bony bridge at the fusion site (Fig. 4F, 4G). Back pain resolved completely (NRS 0), and leg pain improved to 3, well controlled with medication.

Discussion

This study demonstrated that short-segment fusion using allograft bone chip insertion is an effective method for treating screw loosening and nonunion after lumbar posterior fixation. Solid fusion was achieved in all 12 patients without major complications during the 1-year follow-up. To our knowledge, this is the first report focusing on the use of allograft bone chips within screw holes for short-segment lumbar revision.

Traditionally, most surgeons have managed screw loosening and nonunion by extending the fusion construct to one or more adjacent levels.[14,22] However, this approach inevitably sacrifices intact motion segments and increases the lever arm, thereby raising the risk of ASD and implant failure.[9,23-25] Our results suggest that short-segment revision with bone chip augmentation can achieve comparable fusion rates while avoiding the disadvantages of long-segment fusion. The allograft bone chip insertion technique is simple yet effective, allowing shorter operative times and less blood loss. In addition, minimizing the fusion length reduces bending stress on the construct, which may lower the risk of screw loosening, as reported by Marie-Hardy et al.[22] These findings further support the biomechanical rationale for preserving motion segments whenever possible.

In osteoporotic patients, long-segment fusion is often associated with recurrent implant failure and proximal junctional kyphosis.[26] In our series, four osteoporotic patients achieved successful fusion with short-segment fixation, demonstrating the feasibility of this technique in compromised bone. Nevertheless, adjacent segment fractures may occur due to stress concentration similar to the "hammer effect" observed after vertebroplasty.[27] To mitigate these risks, our protocol includes bone-strengthening agents such as teriparatide or romosozumab and close postoperative monitoring.

In addition to fusion extension, bone cement augmentation has been considered another strategy to manage screw loosening by reinforcing fixation strength. Although this method can provide immediate mechanical stability, it carries inherent risks such as cement leakage into neural or vascular structures, potentially leading to serious complications including neurological injury or pulmonary embolism.[28,29] Moreover, cement obstructs cancellous channels and impedes biological fusion. In contrast, the allograft bone chip impaction technique preserves the trabecular architecture of the host bone, enabling osteoconduction and natural bone remodeling while achieving stable fixation within the same segment.[30]

Appropriate patient selection is essential when considering this technique. This technique may be most suitable for patients with localized screw loosening and nonunion, preserved overall spinal alignment, and no evidence of severe instability or progressive deformity. In such cases, reuse of the original screw trajectory with allograft bone chip insertion may provide sufficient mechanical stability and promote fusion while preserving motion segments. In contrast, patients with extensive bone loss, marked segmental instability, significant deformity, or multi-level involvement may be less suitable for this technique, as these conditions often require more robust stabilization through fusion extension. Therefore, careful preoperative assessment, including evaluation of alignment, stability, and bone quality, is crucial in determining the optimal surgical strategy for each patient.

When performing bone chip insertion, careful preoperative planning with CT is essential to confirm that the screw tract is isolated from neural structures. Because impacted bone chips can be densely compacted (up to 15 mL per hole), inadvertent communication with the spinal canal or nerve root may cause neurological injury. Intraoperative probing of each screw hole before impaction is strongly recommended.

In summary, the present study highlights a straightforward and biologically favorable approach for managing screw loosening and nonunion after lumbar fusion. By reusing existing screw trajectories and applying allograft bone chip impaction, surgeons can

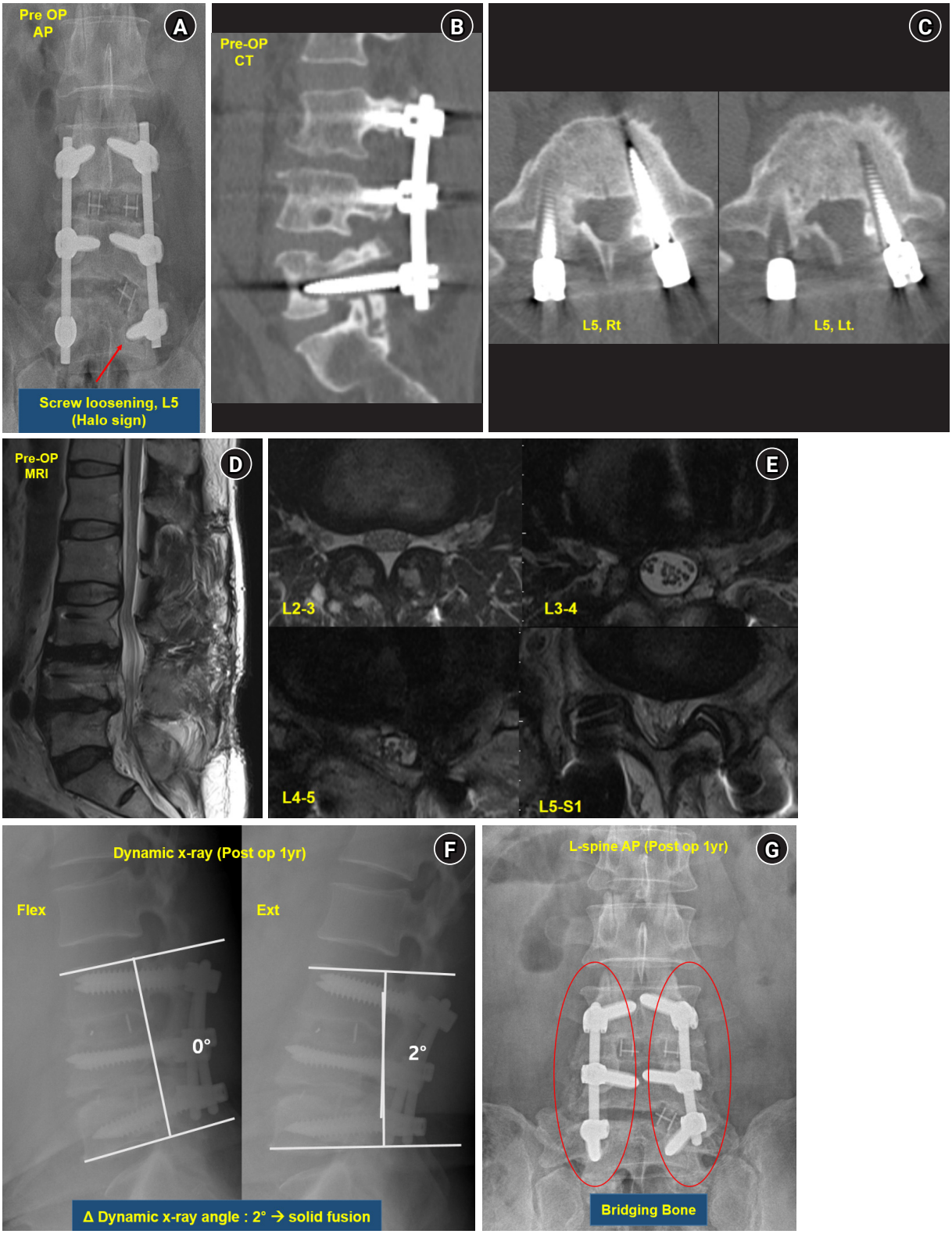

Fig. 4. Illustrative case of revision surgery for screw loosening and nonunion. (A) Preoperative X-ray showing L5 screw loosening (halo sign). (B) Preoperative sagittal computed tomography (CT) confirming bilateral L5 screw loosening. (C) Axial CT at L5 level demonstrating enlarged screw tracts bilaterally. (D) Sagittal T2-weighted magnetic resonance imaging (MRI) showing preserved spinal canal dimension without significant stenosis. (E) Axial MRI at L3–4 and L4–5 levels showing no significant stenosis. (F) One-year postoperative dynamic X-ray showing ≤2° of motion, consistent with solid fusion. (G) One-year postoperative X-ray demonstrating continuous bridging bone formation along the fusion site (red circles).

https://doi.org/10.63858/jass.26.0026

achieve stable fixation while minimizing surgical morbidity and preserving motion segments. This technique may serve as a practical alternative to long-segment fusion, particularly in elderly or osteoporotic patients in whom extensive instrumentation poses greater mechanical and physiological burdens.

This study has several limitations. Its retrospective design, small sample size, and single-surgeon experience may introduce selection bias and limit the generalizability of the findings. In addition, the absence of a control group precludes direct comparison with conventional revision strategies. Although fusion assessment was primarily based on flexion–extension radiographs, postoperative CT scans were performed in only a subset of patients (n = 8), allowing more precise confirmation of trabecular bone bridging. However, incomplete CT evaluation across all patients may have led to underestimation or overestimation of the true fusion rate. Furthermore, the relatively short follow-up period of 1 year may be insufficient to capture delayed implant failure or ASD. Nevertheless, the consistent fusion outcomes observed in this pilot series are encouraging. Future prospective studies with larger cohorts, inclusion of appropriate control groups, standardized CT-based fusion assessment for all patients, and longer follow-up are warranted to validate the long-term efficacy of this technique.

Short-segment fusion using an allograft bone chip insertion technique appears to be a practical and biologically favorable revision option for managing screw loosening and nonunion in selected patients. It may achieve solid fusion without extending the fusion level, thereby potentially reducing surgical morbidity and preserving motion segments. Although this approach cannot replace all fusion extension procedures, it can help avoid fusion extension in selected cases and serve as a practical alternative to long-segment fusion. Larger prospective studies with standardized fusion assessment and longer follow-up are needed to confirm its broader applicability.

Author contributions

Conceptualization: ML, SWJ, CDY. Data curation: ML. Formal analysis: ML. Investigation: ML. Methodology: ML, SWJ, CDY. Project administration: SWJ, CDY. Supervision: SWJ, CDY. Visualization: ML. Writing – original draft: ML. Writing – review & editing: ML, JHP, DP, CK, SWJ, CDY.

Conflict of interest

The authors have no conflicts of interest to declare.

Funding

None.

Acknowledgments

None.

ORCID

Minsuk Lee, https://orcid.org/0009-0005-2914-423X
Jin Hoon Park, https://orcid.org/0000-0002-0903-3146
Danbi Park, https://orcid.org/0000-0002-4055-9584
Chongman Kim, https://orcid.org/0000-0001-8620-3957
Sun Woo Jang, https://orcid.org/0000-0001-8425-4961
Chang Duk Yuk, https://orcid.org/0009-0008-7433-7315

Supplementary material

The supplementary data are available with this article at https://doi.org/10.63858/jass.26.0026.

References

1. Liljenqvist U, Hackenberg L, Link T, Halm H. Pullout strength of pedicle screws versus pedicle and laminar hooks in the thoracic spine. Acta Orthop Belg 2001;67:157-63.
2. Amirouche F, Solitro GF, Magnan BP. Stability and spine pedicle screws fixation strength: a comparative study of bone density and insertion angle. Spine Deform 2016;4:261-7.
3. Esses SI, Sachs BL, Dreyzin V. Complications associated with the technique of pedicle screw fixation: a selected survey of ABS members. Spine (Phila Pa 1976) 1993;18:2231-8.
4. Galbusera F, Volkheimer D, Reitmaier S, Berger-Roscher N, Kienle A, Wilke HJ. Pedicle screw loosening: a clinically relevant complication? Eur Spine J 2015;24:1005-16.
5. Sanden B, Olerud C, Petren-Mallmin M, Johansson C, Larsson S. The significance of radiolucent zones surrounding pedicle screws: definition of screw loosening in spinal instrumentation. J Bone Joint Surg Br 2004;86:457-61.
6. DeWald CJ, Stanley T. Instrumentation-related complications of multilevel fusions for adult spinal deformity patients over age 65: surgical considerations and treatment options in patients with poor bone quality. Spine (Phila Pa 1976) 2006;31(19 Suppl):S144-51.
7. Khalid SI, Nunna RS, Maasarani S, et al. Association of osteopenia and osteoporosis with higher rates of pseudarthrosis and revision surgery in adult patients undergoing single-level lumbar fusion. Neurosurg Focus 2020;49:E6.
8. Kim HJ, Kim SG, Lee HM, et al. Risk factors associated with the halo phenomenon after lumbar fusion surgery and its clinical significance. Asian Spine J 2008;2:22-6.
9. Yuan L, Zhang X, Zeng Y, Chen Z, Li W. Incidence, risk, and

outcome of pedicle screw loosening in degenerative lumbar scoliosis patients undergoing long-segment fusion. Global Spine J 2023;13:1064-71.
10. Jansen JU, Zengerle L, Hackenbroch C, Dreyhaupt J, Tao Y, Wilke HJ. Prediction of screw loosening by measuring the insertion torque in non-osteoporotic patients: an in vitro study. BMC Musculoskelet Disord 2025;26:415.
11. Dede O, Thuillier D, Pekmezci M, et al. Revision surgery for lumbar pseudarthrosis. Spine J 2015;15:977-82.
12. Ondra SL, Marzouk S. Revision strategies for lumbar pseudarthrosis. Neurosurg Focus 2003;15:E9.
13. Elgafy H, Vaccaro AR, Chapman JR, Dvorak MF. Rationale of revision lumbar spine surgery. Global Spine J 2012;2:7-14.
14. Sherif S, Arlet V. Revision surgery for non-union in adult spinal deformity. Eur Spine J 2020;29:103-15.
15. El Saman A, Meier S, Sander A, Kelm A, Marzi I, Laurer H. Reduced loosening rate and loss of correction following posterior stabilization with or without PMMA augmentation of pedicle screws in vertebral fractures in the elderly. Eur J Trauma Emerg Surg 2013;39:455-60.
16. Lee JC, Choi SW. Adjacent segment pathology after lumbar spinal fusion. Asian Spine J 2015;9:807-17.
17. Ebrahimkhani M, Arjmand N, Shirazi-Adl A. Biomechanical effects of lumbar fusion surgery on adjacent segments using musculoskeletal models of the intact, degenerated and fused spine. Sci Rep 2021;11:17892.
18. Bono CM, Bawa M, White KK, et al. Residual motion on flexion-extension radiographs after simulated lumbar arthrodesis in human cadavers. J Spinal Disord Tech 2008;21:364-71.
19. Frymoyer JW, Hanley EN Jr, Howe J, Kuhlmann D, Matteri RE. A comparison of radiographic findings in fusion and nonfusion patients ten or more years following lumbar disc surgery. Spine (Phila Pa 1976) 1979;4:435-40.
20. Kuslich SD, Ulstrom CL, Griffith SL, Ahern JW, Dowdle JD. The Bagby and Kuslich method of lumbar interbody fusion: history, techniques, and 2-year follow-up results of a United States prospective, multicenter trial. Spine (Phila Pa 1976) 1998;23:1267-78.
21. Park S, Jeong YH, Ha BJ, et al. Fusion rate of Escherichia coli-derived recombinant human bone morphogenetic protein-2 compared with local bone autograft in posterior lumbar interbody fusion for degenerative lumbar disorders. Spine J 2023;23:1877-85.
22. Marie-Hardy L, Pascal-Moussellard H, Barnaba A, Bonaccorsi R, Scemama C. Screw loosening in posterior spine fusion: prevalence and risk factors. Global Spine J 2020;10:598-602.
23. Lee SH, Lee S, Jang SW, et al. Unilateral pediculectomy and reduction with short-segment pedicle screw fixation for thoracolumbar burst fracture: a case series. World Neurosurg 2024;183:e116-26.
24. Seo DK, Kim CH, Jung SK, Kim MK, Choi SJ, Park JH. Analysis of the risk factors for unfavorable radiologic outcomes after fusion surgery in thoracolumbar burst fracture: what amount of postoperative thoracolumbar kyphosis correction is reasonable? J Korean Neurosurg Soc 2019;62:96-105.
25. Shin HK, Kim M, Lee S, et al. Surgical strategy for metastatic spinal tumor patients with surgically challenging situation. Medicine (Baltimore) 2022;101:e29560.
26. Kim DK, Kim JY, Kim DY, Rhim SC, Yoon SH. Risk factors of proximal junctional kyphosis after multilevel fusion surgery: more than 2 years follow-up data. J Korean Neurosurg Soc 2017;60:174-80.
27. Yoo CM, Park KB, Hwang SH, Kang DH, Jung JM, Park IS. The analysis of patterns and risk factors of newly developed vertebral compression fractures after percutaneous vertebroplasty. J Korean Neurosurg Soc 2012;52:339-45.
28. Kang SH, Kim KT, Park SW, Kim YB. A case of pedicle screw loosening treated by modified transpedicular screw augmentation with polymethylmethacrylate. J Korean Neurosurg Soc 2011;49:75-8.
29. Wu ZX, Gong FT, Liu L, et al. A comparative study on screw loosening in osteoporotic lumbar spine fusion between expandable and conventional pedicle screws. Arch Orthop Trauma Surg 2012;132:471-6.
30. Kim H, Lee CK, Yeom JS, Lee JH, Lee KH, Chang BS. The efficacy of porous hydroxyapatite bone chip as an extender of local bone graft in posterior lumbar interbody fusion. Eur Spine J 2012;21:1324-30.

https://doi.org/10.63858/jass.26.0026

Original Article

J Adv Spine Surg 2026;16(1):17-24
https://doi.org/10.63858/jass.26.0031
pISSN 2234-0637 • eISSN 3140-0663

JASS
Journal of Advanced Spine Surgery

Development and Validation of a Diagnostic Nomogram for Sarcopenia in Patients with Degenerative Lumbar Disease: A Retrospective Diagnostic Accuracy Study in Korea

Dae-Woong Ham, M.D.

Department of Orthopaedic Surgery, Chung-Ang University Hospital, Chung-Ang University College of Medicine, Seoul, Korea

Study Design: A retrospective diagnostic accuracy study was conducted using internal training and temporal validation cohorts.

Purpose: This study aimed to develop and validate sex-specific diagnostic nomograms for sarcopenia in patients with degenerative lumbar disease (DLD), based on body mass index (BMI), hand-grip strength (HGS), and computed tomography (CT)–derived lumbar muscle indices.

Overview of Literature: The Asian Working Group for Sarcopenia (AWGS) 2019 algorithm requires appendicular skeletal muscle mass (ASM) measurement by dual-energy X-ray absorptiometry or bioimpedance analysis together with HGS and a physical performance test. These measurements are not always feasible in spine clinics, although a preoperative lumbar CT is routinely available.

Methods: A training set of 196 patients scheduled for lumbar surgery and a temporal validation set of 150 patients with DLD were analyzed. Sarcopenia was diagnosed according to the AWGS 2019 criteria. Sex-specific multivariable logistic regression was performed using BMI, HGS, psoas muscle index, paraspinal muscle index (PaMI), and gluteal muscle index (GMI), and the resulting models were translated into nomograms. Discrimination was assessed by the area under the receiver operating characteristic curve (AUC), calibration by calibration plots and mean absolute error (MAE), and the optimal cut-off was identified using the Youden index.

Results: The prevalence of sarcopenia was 62.2% (122/196) in the training set and 58.0% (87/150) in the validation set. In the training set, sarcopenic patients had significantly lower BMI (23.7±3.7 vs. 27.0±3.3 kg/m^2), HGS (20.3±8.0 vs. 29.2±30.5 kg), PaMI (8.7±5.4 vs. 13.9±8.0), and GMI (26.1±5.7 vs. 30.9±6.2) than non-sarcopenic patients (all $p<0.05$). On validation, the male nomogram achieved an AUC of 0.958 with an MAE of 0.040, and the female nomogram achieved an AUC of 0.830 with an MAE of 0.021. The Youden index was 0.78 for males and 0.59 for females.

Conclusion: Sex-specific nomograms based on BMI, HGS, and CT-derived lumbar muscle indices provided accurate diagnosis of sarcopenia in patients with DLD without requiring whole-body ASM measurement or a physical performance test, offering a practical screening tool in the spine clinic.

Keywords: Lumbar vertebrae, Sarcopenia, Nomogram, Computed tomography, Paraspinal muscles

Received: May 8, 2026; Revised: May 29, 2026; Accepted: June 2, 2026

Corresponding author: Dae-Woong Ham, M.D.
Department of Orthopaedic Surgery, Chung-Ang University Hospital, Chung-Ang University College of Medicine, 102 Heukseok-ro, Dongjak-gu, Seoul 06973, Korea
TEL: +82-2-6299-2065, FAX: +82-2-6299-1575, E-mail: hamdgogo@gmail.com

Introduction

Sarcopenia is a progressive and generalized skeletal muscle disorder characterized by accelerated loss of muscle mass and function, and is associated with falls, fractures, functional decline, prolonged hospitalization, and mortality in older adults.[1,2] In patients with degenerative lumbar disease (DLD) who are candidates for spine surgery, coexisting sarcopenia has been reported to be associated with greater preoperative disability, higher rates of perioperative complications, slower postoperative recovery, and inferior patient-reported outcomes.[3-5] Identifying sarcopenia before surgery is therefore clinically meaningful and may inform preoperative optimization, prehabilitation, and shared decision-making.

The Asian Working Group for Sarcopenia (AWGS) 2019 algorithm requires the measurement of appendicular skeletal muscle mass (ASM) by dual-energy X-ray absorptiometry (DXA) or bioimpedance analysis (BIA), together with hand-grip strength (HGS) and a physical performance test such as a 6-meter gait speed or the 5-times sit-to-stand test.[1] Although this multi-component diagnostic algorithm is well validated, it is not always practical in busy spine outpatient clinics, where DXA or BIA equipment may not be readily available and where physical performance testing is often constrained by pain and limited mobility.[6,7] As a result, sarcopenia in surgical candidates is frequently undiagnosed and undertreated.

Lumbar computed tomography (CT) is routinely obtained as part of the preoperative workup for DLD, and provides a unique opportunity to quantify regional muscle mass at the lumbar level. CT-based indices of the psoas muscle, paraspinal muscle, and gluteal muscle have been shown to correlate with whole-body skeletal muscle mass and to predict adverse outcomes.[8-10] Combining these CT-derived indices with simple bedside measures such as body mass index (BMI) and HGS may therefore enable accurate diagnosis of sarcopenia without the need for whole-body ASM measurement or a formal physical performance test.

Nomograms are visual graphical scoring systems based on multivariable regression models that translate complex statistical predictions into clinically interpretable individual scores.[11] Although nomograms for sarcopenia have been proposed in community-dwelling older adults,[11] to our knowledge, no diagnostic nomogram has been developed and validated specifically for patients with DLD using only BMI, HGS, and CT-derived lumbar muscle indices. The objective of the present study was therefore to develop and validate sex-specific diagnostic nomograms for sarcopenia in patients with DLD.

Methods

1. Study design and participants

This was a single-center, retrospective diagnostic accuracy study using a training cohort and an independent temporal validation cohort, both enrolled at Chung-Ang University Hospital.

The training cohort consisted of 196 consecutive patients with DLD who were scheduled for elective lumbar spine surgery between January 2019 and December 2021 and who underwent preoperative evaluation including lumbar CT, BMI measurement, HGS testing, and the AWGS 2019–based sarcopenia work-up. Inclusion criteria were as follows: (1) age ≥ 50 years; (2) a clinical diagnosis of DLD, comprising lumbar spinal stenosis or lumbar disc herniation; and (3) availability of preoperative lumbar CT covering the L3 vertebral level. Exclusion criteria were as follows: (1) prior lumbar fusion or instrumented surgery; (2) spinal infection, primary or metastatic spinal tumor, or vertebral fracture; (3) any neuromuscular disorder potentially affecting muscle composition; and (4) incomplete preoperative data for any of the candidate variables. Of the 196 training patients, 173 had lumbar spinal stenosis (88.3%), and 23 had lumbar disc herniation (11.7%). The validation cohort consisted of 150 independent patients with DLD evaluated between January 2022 and June 2023 using the same inclusion and exclusion criteria.

2. Diagnosis of sarcopenia

Sarcopenia was diagnosed according to the AWGS 2019 criteria.[1] ASM was measured by BIA, and the appendicular skeletal muscle mass index (ASMI) was calculated as ASM divided by height squared (kg/m^2). Low muscle mass was defined as ASMI <7.0 kg/m^2 in men and <5.7 kg/m^2 in women. HGS was measured using a digital hand dynamometer with the dominant hand in the standing position with full elbow extension. Patients performed at least two trials, and the maximum value was recorded. Low muscle strength was defined as HGS <28.0 kg in men and <18.0 kg in women. Physical performance was assessed using a 6-meter gait speed test, and low physical performance was defined as a gait speed <1.0 m/s. Patients meeting the criterion for low ASMI together with either low HGS or low physical performance were classified as having sarcopenia.

3. CT-based muscle indices

All patients underwent preoperative lumbar CT as part of routine clinical care. The cross-sectional areas (CSAs, in cm^2) of the bilateral psoas muscles, paraspinal muscles (erector spinae and multifidus), and gluteal muscles were measured on a single axial

https://doi.org/10.63858/jass.26.0031

slice at the mid-level of the L3 vertebral body using a picture archiving and communication system. Muscle boundaries were manually delineated, and the area within a Hounsfield unit window of −29 to 150 was considered muscle tissue. To adjust for body size, three muscle indices were defined: the psoas muscle index (PMI) = (right+left psoas CSA)/height^2 (cm^2/m^2); the paraspinal muscle index (PaMI) = (right+left paraspinal CSA)/height^2 (cm^2/m^2); and the gluteal muscle index (GMI) = (right+left gluteal CSA)/height^2 (cm^2/m^2). Measurements were performed by a single trained investigator who was blinded to the AWGS-based sarcopenia status.

4. Candidate variables and model development

Five candidate predictors were prespecified based on clinical availability and biological plausibility: BMI, HGS, PaMI, PMI, and GMI. Because the diagnostic thresholds of the AWGS 2019 algorithm are sex-specific and because muscle morphology differs substantially between sexes, multivariable logistic regression models were fitted separately for male and female patients in the training set. All five predictors were entered into the model as continuous variables. Odds ratios with 95% confidence intervals (CIs) were estimated. The final regression equations were translated into sex-specific nomograms using the rms package in R, which assigned points to each predictor on a 0–100 scale and converted the total points into the predicted probability of sarcopenia (Fig. 1).

5. Model validation

The performance of each sex-specific nomogram was evaluated in the independent validation cohort. Discrimination was quantified using the area under the receiver operating characteristic curve (AUC) with 95% CIs (Fig. 2A, 2B). Calibration was evaluated using calibration plots based on 1,000 bootstrap resamples, and the mean absolute error (MAE) between predicted and observed probabilities was reported (Fig. 2C, 2D). The optimal cut-off probability for diagnosis of sarcopenia was determined by maximizing the Youden index (sensitivity+specificity−1), and the corresponding sensitivity, specificity, and accuracy were reported.

6. Statistical analysis

Continuous variables are presented as mean ± standard deviation, and categorical variables as frequencies and percentages. Between-group comparisons used the independent t-test or the Mann-Whitney U test for continuous variables, and the chi-square test or Fisher's exact test for categorical variables, as appropriate. A two-sided p-value of less than 0.05 was considered statistically significant. All analyses were performed using R version 4.2.2 (R Foundation for Statistical Computing, Vienna, Austria) with the rms, pROC, and ggplot2 packages.

7. Ethics statement

The study was approved by the Institutional Review Board of Chung-Ang University Hospital (IRB No. 2022-02-451) and was conducted in accordance with the Declaration of Helsinki. This study is reported in keeping with the relevant items of the TRIPOD (Transparent Reporting of a multivariable prediction model for Individual Prognosis Or Diagnosis) statement.[12] The requirement for written informed consent was waived owing to the retrospective nature of the analysis.

Results

1. Baseline characteristics of the training cohort

A total of 196 patients with DLD were included in the training cohort, of whom 122 (62.2%) were classified as having sarcopenia according to the AWGS 2019 criteria. The relatively high prevalence of sarcopenia is consistent with the advanced age and surgical candidacy of the study population. The proportion of women was higher in the sarcopenic group than in the non-sarcopenic group (68.9% vs. 52.7%, p = 0.034). Sarcopenic patients were significantly older (73.6 ± 6.5 vs. 70.6 ± 6.8 years, p = 0.002) and had significantly lower bone mineral density (0.613 ± 0.140 vs. 0.686 ± 0.122 g/cm^2, p < 0.001). BMI, HGS, PaMI, and GMI were all significantly lower in the sarcopenic group, whereas PMI did not differ significantly between the two groups (Table 1).

2. Baseline characteristics of the validation cohort

The validation cohort comprised 150 patients with DLD evaluated during a separate enrollment period (January 2022–June 2023), of whom 87 (58.0%) were classified as sarcopenic. Compared with non-sarcopenic patients, sarcopenic patients in the validation cohort were significantly older (70.7 ± 10.3 vs. 65.8 ± 11.9 years, p = 0.037) and had significantly lower BMI (24.5 ± 3.2 vs. 28.3 ± 2.6 kg/m^2, p < 0.001) and GMI (27.9 ± 4.3 vs. 32.1 ± 4.8, p < 0.001). The sex distribution and other variables were comparable between sarcopenic and non-sarcopenic patients (Table 2). When the training and validation cohorts were compared as a whole, the prevalence of sarcopenia was similar (62.2% vs. 58.0%, p = 0.491), although the validation cohort had a lower proportion of women, slightly younger age, and significantly higher PaMI and lower PMI, reflecting differences in case mix (Table 3).

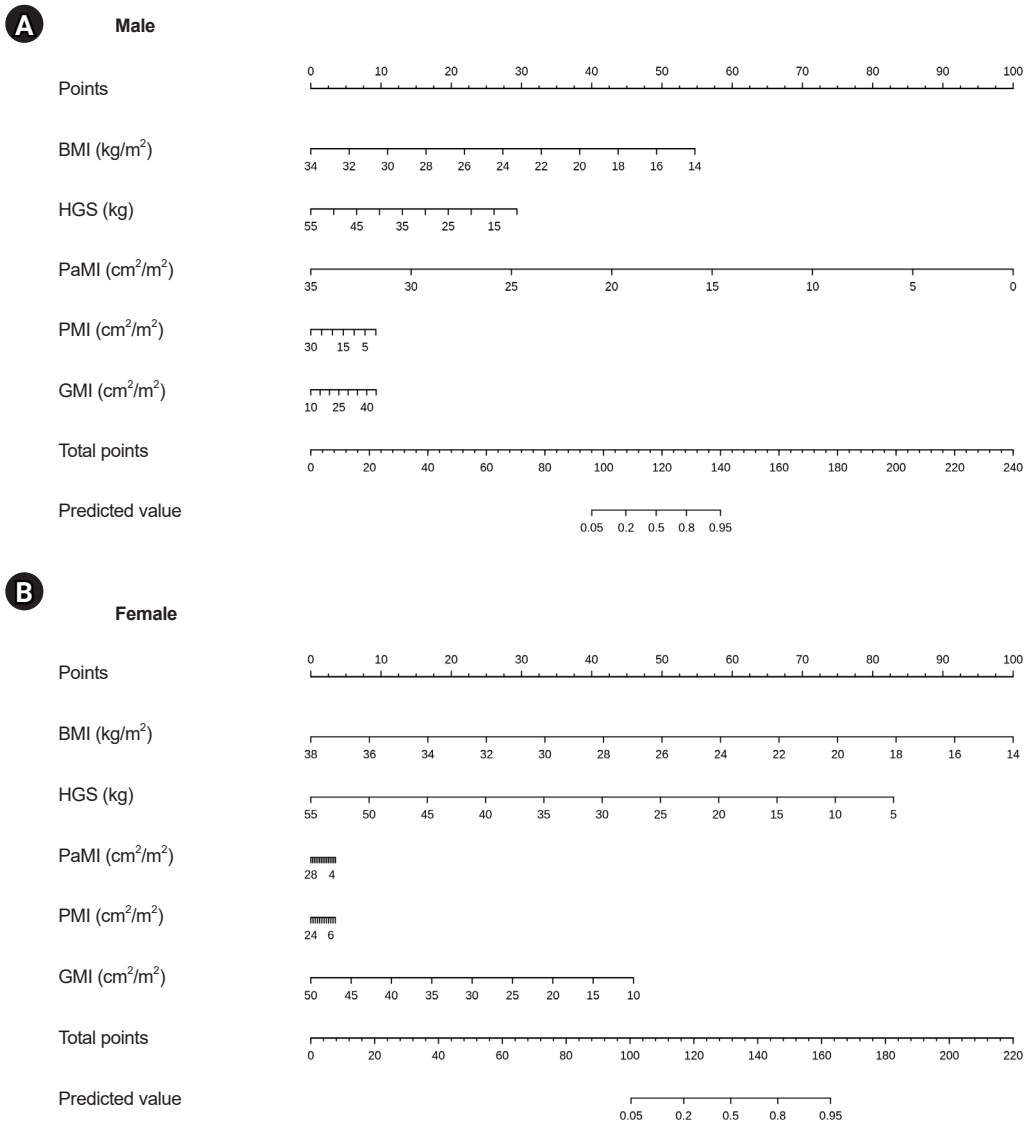

Fig. 1. Sex-specific diagnostic nomograms for sarcopenia in patients with degenerative lumbar disease. (A) Male nomogram. (B) Female nomogram. Each predictor (body mass index [BMI], hand-grip strength [HGS], paraspinal muscle index [PaMI], psoas muscle index [PMI], and gluteal muscle index [GMI]) is assigned a number of points on a 0–100 scale; the sum of the points across all predictors is converted into the predicted probability of sarcopenia.

3. Sex-specific diagnostic nomograms

Sex-specific multivariable logistic regression models were fitted in the training set using BMI, HGS, PaMI, PMI, and GMI as predictors. The regression coefficients were translated into nomograms in which each predictor contributed a number of points on a 0–100 scale; the sum of points across the five predictors was converted into the predicted probability of sarcopenia (Fig. 1).

4. Model performance in the validation cohort

In the independent validation cohort, the male nomogram achieved excellent discrimination, with an AUC of 0.958, while the female nomogram showed good discrimination, with an AUC of 0.830 (Fig. 2A, 2B). The calibration plots demonstrated good agreement between predicted and observed probabilities for both sexes, with an MAE of 0.040 for males (n = 73) and 0.021 for females (n = 122), indicating that the nomograms were well calibrated across the full range of risk (Fig. 2C, 2D). When the optimal cut-off was selected by maximizing the Youden index, the index was 0.78 for the male model and 0.59 for the female model, indicating high sensitivity and specificity for the diagnosis of sarcopenia in both sexes.

https://doi.org/10.63858/jass.26.0031

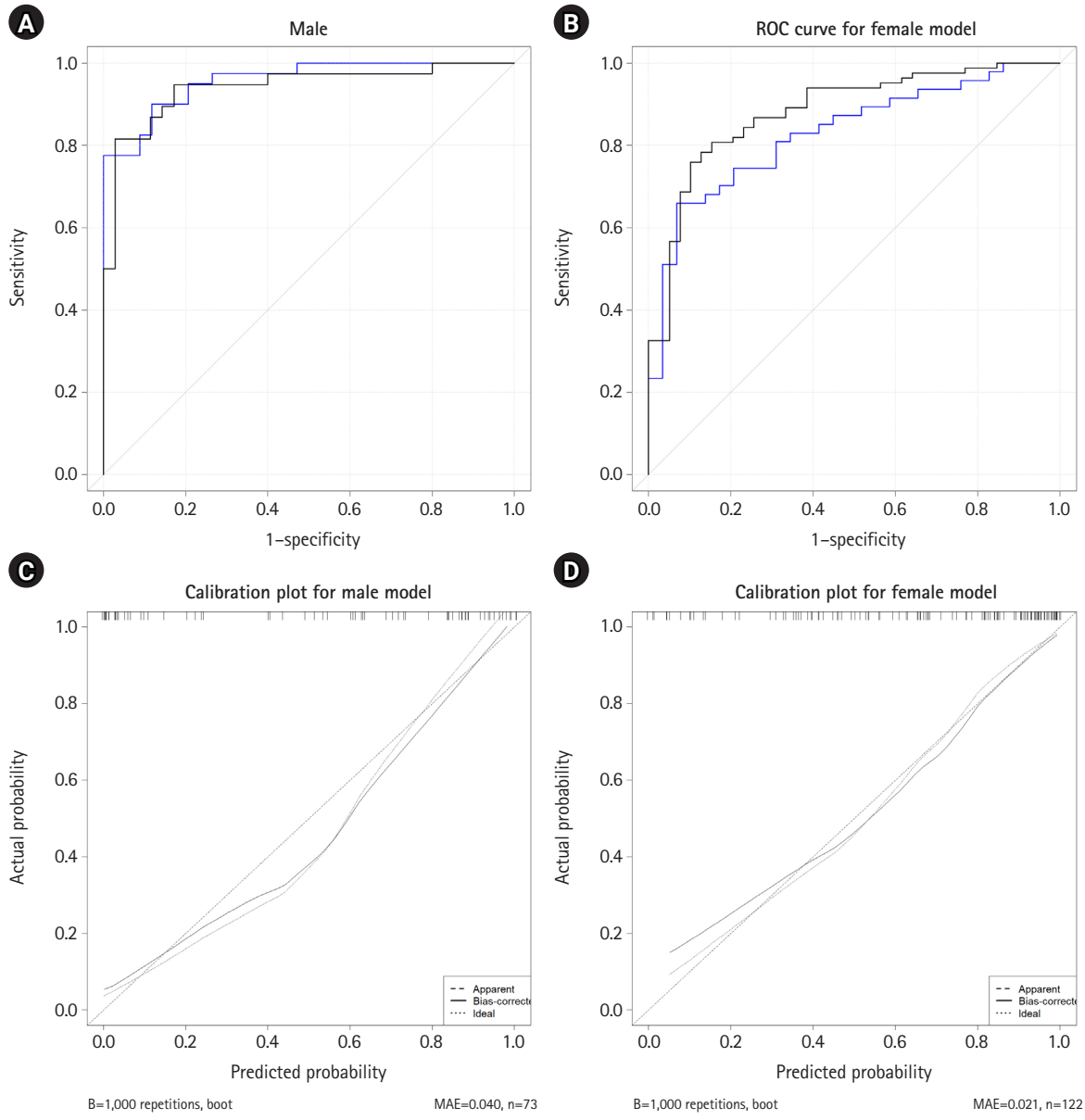

Fig. 2. Performance of the sex-specific nomograms in the independent validation cohort. (A) Receiver operating characteristic (ROC) curve for the male model. (B) ROC curve for the female model. (C) Calibration plot for the male model (mean absolute error [MAE]=0.040, n=73). (D) Calibration plot for the female model (MAE=0.021, n=122). In the calibration plots, the dashed line indicates ideal calibration; the solid line indicates the bias-corrected calibration based on 1,000 bootstrap resamples.

Discussion

The present study developed and validated sex-specific diagnostic nomograms for sarcopenia in patients with DLD using BMI, HGS, and three CT-derived lumbar muscle indices (PMI, PaMI, and GMI). In an independent temporal validation cohort, the male nomogram achieved excellent discrimination (AUC 0.958) and the female nomogram showed good discrimination (AUC 0.830), and both models were well calibrated, with MAEs of 0.040 and 0.021, respectively. These results suggest that the proposed nomograms allow accurate diagnosis of sarcopenia in patients with DLD without requiring whole-body ASM measurement or a formal physical performance test.

The clinical importance of identifying sarcopenia in patients with DLD has been increasingly recognized.[3,13] Sarcopenia has been associated with greater preoperative disability, longer hospital stay, higher complication rates, and inferior patient-reported outcomes after lumbar spine surgery.[3-5] Despite these implica-

Table 1. Baseline characteristics of the training cohort according to sarcopenia status

Variable	Non-sarcopenia (n = 74)	Sarcopenia (n = 122)	Total (n = 196)	p-value
Female sex	39 (52.7)	84 (68.9)	123 (62.8)	0.034
Age (years)	70.6 ± 6.8	73.6 ± 6.5	72.4 ± 6.8	0.002
BMD (g/cm^2)	0.686 ± 0.122	0.613 ± 0.140	0.640 ± 0.138	< 0.001
BMI (kg/m^2)	27.0 ± 3.3	23.7 ± 3.7	24.9 ± 3.9	< 0.001
HGS (kg)	29.2 ± 30.5	20.3 ± 8.0	23.7 ± 20.2	0.016
PaMI (cm^2/m^2)	13.9 ± 8.0	8.7 ± 5.4	10.6 ± 6.9	< 0.001
PMI (cm^2/m^2)	11.5 ± 17.4	10.2 ± 5.5	10.7 ± 11.6	0.525
GMI (cm^2/m^2)	30.9 ± 6.2	26.1 ± 5.7	27.9 ± 6.4	< 0.001

Values are presented as number (%) or mean ± standard deviation. BMD: bone mineral density, BMI: body mass index, HGS: hand-grip strength, PaMI: paraspinal muscle index, PMI: psoas muscle index, GMI: gluteal muscle index.

Table 2. Baseline characteristics of the validation cohort according to sarcopenia status

Variable	Non-sarcopenia (n = 63)	Sarcopenia (n = 87)	Total (n = 150)	p-value
Female sex	29 (46.0)	47 (54.0)	76 (50.7)	0.423
Age (years)	65.8 ± 11.9	70.7 ± 10.3	69.2 ± 11.0	0.037
BMD (g/cm^2)	0.681 ± 0.126	0.648 ± 0.167	0.658 ± 0.156	0.350
BMI (kg/m^2)	28.3 ± 2.6	24.5 ± 3.2	25.7 ± 3.5	< 0.001
HGS (kg)	26.5 ± 12.1	22.1 ± 10.3	23.5 ± 11.0	0.057
PaMI (cm^2/m^2)	14.9 ± 4.8	14.0 ± 3.4	14.3 ± 3.8	0.402
PMI (cm^2/m^2)	5.4 ± 1.9	4.8 ± 1.4	5.0 ± 1.6	0.153
GMI (cm^2/m^2)	32.1 ± 4.8	27.9 ± 4.3	29.2 ± 4.9	< 0.001

Values are presented as number (%) or mean ± standard deviation. BMD: bone mineral density, BMI: body mass index, HGS: hand-grip strength, PaMI: paraspinal muscle index, PMI: psoas muscle index, GMI: gluteal muscle index.

Table 3. Comparison of the training and validation cohorts

Variable	Training (n = 196)	Validation (n = 150)	Total (n = 346)	p-value
Sarcopenia	122 (62.2)	87 (58.0)	209 (60.4)	0.491
Female sex	123 (62.8)	76 (50.7)	199 (57.5)	0.032
Age (years)	72.4 ± 6.8	69.2 ± 11.0	71.3 ± 8.6	0.007
BMD (g/cm^2)	0.640 ± 0.138	0.658 ± 0.156	0.646 ± 0.144	0.330
BMI (kg/m^2)	24.9 ± 3.9	25.7 ± 3.5	25.2 ± 3.8	0.115
HGS (kg)	23.7 ± 20.2	23.5 ± 11.0	23.6 ± 17.5	0.894
PaMI (cm^2/m^2)	10.6 ± 6.9	14.3 ± 3.8	11.8 ± 6.3	< 0.001
PMI (cm^2/m^2)	10.7 ± 11.6	5.0 ± 1.6	8.8 ± 9.9	< 0.001
GMI (cm^2/m^2)	27.9 ± 6.4	29.2 ± 4.9	28.3 ± 6.0	0.069

Values are presented as number (%) or mean ± standard deviation. BMD: bone mineral density, BMI: body mass index, HGS: hand-grip strength, PaMI: paraspinal muscle index, PMI: psoas muscle index, GMI: gluteal muscle index.

tions, the routine application of the AWGS 2019 algorithm in spine outpatient clinics remains limited because DXA or BIA equipment is not always available and because physical performance testing is often constrained by pain and gait disturbance in surgical candidates.[6,7] A diagnostic tool that relies only on parameters routinely collected during the preoperative spine workup is therefore highly desirable. Lumbar CT, BMI, and HGS are typically obtained as part of routine care,[14] and repurposing these data to derive a sarcopenia probability minimizes additional patient burden and clinical resources.

Previous studies have shown that lumbar CT-based muscle indices correlate with whole-body skeletal muscle mass and predict adverse outcomes.[8,9,10,14] The psoas muscle has been the most widely studied marker, but isolated PMI has shown inconsistent associations with whole-body sarcopenia, particularly in women.[9,10] In the present training cohort, PMI alone did not differ sig-

https://doi.org/10.63858/jass.26.0031

nificantly between sarcopenic and non-sarcopenic patients, whereas PaMI and GMI showed strong univariate associations with sarcopenia. This finding is consistent with prior reports that paraspinal and gluteal muscles, which contain a larger proportion of postural type I fibers and a wider CSA, may better reflect global muscle mass than the psoas alone.[9] Combining the three muscle indices with BMI and HGS in a multivariable model, therefore, appears more informative than reliance on any single muscle measurement.

Yin et al.[11] previously developed a nomogram to predict sarcopenia in community-dwelling older adults using age, albumin, blood urea nitrogen, grip strength, and calf circumference, and reported a validation AUC of 0.92. Although their model demonstrated excellent performance, it was developed in a general medical examination cohort rather than in a spine surgical population, and it required laboratory tests and calf circumference measurement that are not part of the routine spine workup. The present nomograms are tailored to the DLD population and rely instead on data that are already available preoperatively, which enhances their applicability in the spine clinic.

The prevalence of sarcopenia in this study was 62.2% in the training cohort and 58.0% in the validation cohort, which is considerably higher than the 10%–30% typically reported in community-dwelling older adults.[1,13] This is likely attributable to the fact that the study population consisted exclusively of patients with DLD who were candidates for lumbar spine surgery, a group that tends to be older, more functionally impaired, and more likely to have reduced physical activity owing to chronic pain and limited mobility.

This study has several limitations that should be acknowledged. First, the analysis was retrospective and conducted at a single institution; the generalizability of the nomograms to other ethnicities, healthcare settings, and CT acquisition protocols requires confirmation in prospective multicenter cohorts. Second, the validation cohort, although collected during an independent enrollment period, was drawn from the same institutional source as the training cohort; external validation in a geographically separate population is warranted. Third, the case mix differed slightly between the training and validation cohorts in terms of sex distribution, age, and muscle index distributions; in particular, the PMI values were substantially higher in the training cohort than in the validation cohort, which may reflect differences in measurement technique or inter-observer variability between the two enrollment periods. Despite this discrepancy, both nomograms maintained good performance, suggesting reasonable robustness. Fourth, raw inspection of the training set identified a small number of extreme values for HGS and PMI that may reflect measurement or data-entry artifacts; these values were retained in the analysis to preserve the prespecified analytic plan, but the resulting wider variance is reflected in the standard deviations reported in Table 1 and should be interpreted with caution. Fifth, CT-based muscle indices were measured by a single observer; although this minimized inter-observer variability within each cohort, the inter- and intra-observer reproducibility of the measurements could not be quantified. Sixth, the nomograms are intended as a diagnostic screening tool rather than as a replacement for the AWGS 2019 algorithm, and patients with a high predicted probability should still undergo formal sarcopenia work-up whenever feasible.

In conclusion, sex-specific nomograms based on BMI, HGS, and CT-derived PMI, PaMI, and GMI provided accurate and well-calibrated diagnosis of sarcopenia in patients with DLD. These nomograms can serve as a practical screening tool in the spine clinic, leveraging data that are already collected during routine preoperative evaluation, and may facilitate earlier recognition and management of sarcopenia in surgical candidates with DLD.

Conflict of interest

The author has no conflicts of interest to declare.

Funding

None.

Acknowledgments

None.

ORCID

Dae-Woong Ham, https://orcid.org/0000-0003-4278-2701

References

1. Chen LK, Woo J, Assantachai P, et al. Asian Working Group for Sarcopenia: 2019 consensus update on sarcopenia diagnosis and treatment. J Am Med Dir Assoc 2020;21:300-7.
2. Cruz-Jentoft AJ, Bahat G, Bauer J, et al. Sarcopenia: revised European consensus on definition and diagnosis. Age Ageing 2019;48:16-31.
3. Cruz-Jentoft AJ, Sayer AA. Sarcopenia. Lancet 2019;393:2636-46.
4. Chen MJ, Lo YS, Lin CY, et al. Impact of sarcopenia on outcomes following lumbar spine surgery for degenerative disease: an updated systematic review and meta-analysis. Eur Spine J

2024;33:3369-80.
5. Bokshan SL, Han AL, DePasse JM, et al. Effect of sarcopenia on postoperative morbidity and mortality after thoracolumbar spine surgery. Orthopedics 2016;39:e1159-64.
6. Inose H, Yamada T, Hirai T, Yoshii T, Abe Y, Okawa A. The impact of sarcopenia on the results of lumbar spinal surgery. Osteoporos Sarcopenia 2018;4:33-6.
7. Beaudart C, McCloskey E, Bruyere O, et al. Sarcopenia in daily practice: assessment and management. BMC Geriatr 2016;16:170.
8. Hamaguchi Y, Kaido T, Okumura S, et al. Proposal for new diagnostic criteria for low skeletal muscle mass based on computed tomography imaging in Asian adults. Nutrition 2016;32:1200-5.
9. Ham DW, Lee J, Choi G, Kwon BT, Song KS. The cross-sectional area of gluteal muscle on multiaxial CT scan as a predictor for diagnosing sarcopenia in patients with degenerative lumbar disease. Eur Spine J 2024;33:3857-64.
10. Gibson DJ, Burden ST, Strauss BJ, Todd C, Lal S. The role of computed tomography in evaluating body composition and the influence of reduced muscle mass on clinical outcome in abdominal malignancy: a systematic review. Eur J Clin Nutr 2015;69:1079-86.
11. Yin G, Qin J, Wang Z, Lv F, Ye X. A nomogram to predict the risk of sarcopenia in older people. Medicine (Baltimore) 2023;102:e33581.
12. Collins GS, Reitsma JB, Altman DG, Moons KG. Transparent reporting of a multivariable prediction model for individual prognosis or diagnosis (TRIPOD): the TRIPOD statement. BMJ 2015;350:g7594.
13. Walston JD. Sarcopenia in older adults. Curr Opin Rheumatol 2012;24:623-7.
14. Zhuang CL, Zhang FM, Li W, et al. Associations of low handgrip strength with cancer mortality: a multicentre observational study. J Cachexia Sarcopenia Muscle 2020;11:1476-86.

https://doi.org/10.63858/jass.26.0031

Original Article

J Adv Spine Surg 2026;16(1):25-32
https://doi.org/10.63858/jass.26.0035
pISSN 2234-0637 • eISSN 3140-0663

JASS
Journal of Advanced Spine Surgery

Beyond Surgical Factors: Postoperative Thoracolumbar Alignment and L1–2 Disc Degeneration as Independent Drivers of Early-Onset Proximal Junctional Kyphosis

Woo-Sel Kim, M.D., Dal-Sung Ryu, M.D., Seung-Hwan Yoon, M.D., Ph.D.

Department of Neurosurgery, Inha University College of Medicine, Incheon, Korea

Purpose: This retrospective study investigated the distinct clinical and radiographic drivers of early- versus late-onset proximal junctional kyphosis (PJK) following multilevel thoracolumbar (TL) fusion.

Methods: After applying the exclusion criteria (spinal infection, neuromuscular disease, age <50 years), the analysis included 136 patients who underwent ≥4-level TL fusion and were followed up for a minimum of 2 years. PJK was classified as early (≤6 months) or late (>6 months) onset. Patient-related factors, surgical variables, sagittal spinopelvic parameters, and preoperative magnetic resonance imaging findings were analyzed using multivariate logistic regression to identify independent predictors of early PJK.

Results: Among 24 patients (17.6%) who developed PJK, the early and late-onset groups included 13 and 11 patients, respectively. The early PJK group exhibited significantly greater preoperative and postoperative TL angles compared with the late group (preoperative: 23.03±13.83° vs. 9.67±9.67°, p=0.024; postoperative: 19.6±6.95° vs. 6.95±6.35°, p<0.001). The Pfirrmann grade of the L1–2 intervertebral disc was significantly higher in the early PJK group (3.92±0.95 vs. 2.81±0.60, p=0.006). No surgical variables differed significantly between the groups. Multivariate analysis confirmed greater postoperative TL angle and more advanced L1–2 disc degeneration as independent predictors of early PJK.

Conclusion: Early-onset PJK following multilevel TL fusion is primarily driven by regional biomechanical vulnerabilities, specifically residual postoperative TL kyphosis and advanced adjacent L1–2 disc degeneration, rather than by surgical variables. Meticulous evaluation of regional TL alignment and adjacent disc health during surgical planning is critical for risk stratification and prevention of early junctional failure.

Keywords: Lumbar vertebrae, Thoracic vertebrae, Spinal fusion, Kyphosis, Intervertebral disc degeneration

Introduction

Multilevel thoracolumbar (TL) spinal fusion is increasingly performed for the management of advanced degenerative spinal disease, spinal deformity, and vertebral fractures, particularly in patients >60 years.[1)]

The complications of multilevel spinal fusion include adjacent segment disease, proximal junctional kyphosis (PJK), and proximal junctional failure (PJF). Among these, PJK is a postoperative radiographic phenomenon occurring after surgery for spinal de-

Received: May 29, 2026; Revised: June 2, 2026; Accepted: June 4, 2026
Corresponding author: Seung-Hwan Yoon, M.D., Ph.D.
Department of Neurosurgery, Inha University College of Medicine, 27 Inhang-ro, Jung-gu, Incheon, Korea
TEL: +82-32-890-2370, FAX: +82-32-890-2374, E-mail: nsyoon@gmail.com

formities in both adult and pediatric populations and is generally considered a form of adjacent segment pathology.[2] PJK is commonly defined as a proximal junctional angle (PJA) of >10° and at least 10° greater than the preoperative measurement between the upper instrumented vertebra (UIV) and the two supra-adjacent vertebrae.[3,4] PJF is a more severe condition within the spectrum of PJK and is characterized by structural failure, including vertebral body fracture or posterior ligamentous disruption, which may lead to pain or neurological deficits.[5]

Although many patients with radiographic PJK remain asymptomatic, some patients with progressive deformities or neurological deterioration may require revision surgery. The risk factors for PJK include advanced age, preoperative sagittal imbalance, excessive sagittal correction, combined anteroposterior approaches, sacral fusion, low bone mineral density (BMD), and a high body mass index (BMI).[2,4,6,7]

PJK is frequently identified during the early postoperative period, particularly within the first 6 months following multilevel spinal fusion, a threshold that has been widely employed to capture the early acute biomechanical phase of junctional failure and often presents a challenging clinical course. Despite this observation, most previous studies have analyzed PJK as a single entity without distinguishing between early- and late-onset patterns. Consequently, factors specifically associated with early-onset PJK remain insufficiently characterized.

The TL junction is a biomechanically vulnerable transition zone, in which altered sagittal alignment and adjacent disc degeneration may increase mechanical stress at the proximal junction following long-segment fusion.

Therefore, the present study compared early- and late-onset PJK following multilevel TL fusion and identified factors specifically associated with early PJK, with particular attention paid to sagittal alignment parameters and preoperative magnetic resonance imaging (MRI) findings.

Methods

1. Study design and patient population

We retrospectively reviewed the records of 141 patients who underwent TL fusion involving ≥4 vertebrae between April 2011 and August 2020. All surgeries were performed by a single spinal surgeon at a single institution. The minimum postoperative follow-up period was 2 years, and the mean follow-up duration was 3.6 years.

The inclusion criteria were as follows: (1) age >50 years at the time of surgery; (2) diagnosis of degenerative spinal disease, including spinal stenosis, spondylolisthesis, or osteoporotic vertebral compression fracture; and (3) multilevel TL fusion involving ≥4 levels. Patients were excluded if they had a spinal infection (n=2) or neuromuscular disease, including Parkinsonism (n=1), or were <50 years of age (n=2). After applying the exclusion criteria, 136 patients were eligible for inclusion in the final analysis.

The baseline patient characteristics included age, sex, height, weight, BMI, smoking status, and BMD. BMD was measured at the lumbar spine and femur using dual-energy X-ray absorptiometry (Prodigy, GE Healthcare, Madison, WI, USA).

Among these patients, 24 (17.6%) were diagnosed with PJK during follow-up. Patients who developed PJK were further classified according to the timing of the onset into early PJK (occurring ≤6 months postoperatively, n=13) and late PJK (occurring >6 months postoperatively, n=11), based on the 6-month cutoff commonly used in the literature to distinguish acute biomechanical failure from delayed degenerative junctional failure. Postoperative follow-up evaluations were routinely performed at 1 week; 1, 3, and 6 months after surgery, and at 6-month intervals thereafter.

2. Radiologic evaluation

1) Lumbar MRI

Preoperative lumbar MRI was performed using a 1.5-T system (Signa HDxt, GE Medical Systems, Milwaukee, WI, USA). Degenerative changes were evaluated using sagittal T1- and T2-weighted images. The presence of disc protrusion or extrusion, moderate-to-severe central canal stenosis, compression fracture (vertebral height loss was classified as mild, 20–25%; moderate, 25–40%; or severe, >40%), and spondylolisthesis (Meyerding grades I–II) was assessed.

Intervertebral disc degeneration at each lumbar level was graded using the Pfirrmann classification system.[8] To evaluate fatty infiltration of the paraspinal muscles, muscle quality was graded according to the Goutallier classification as follows: grade 0, normal muscle; grade 1, fatty streaks within the muscle; grade 2, less fat than muscle; grade 3, equal amounts of fat and muscle; and grade 4, more fat than muscle.[9]

2) Sagittal spinopelvic parameters

Sagittal spinopelvic parameters were measured using standing whole-spine lateral radiographs obtained preoperatively and 1 week postoperatively. The evaluated parameters included sagittal vertical axis, thoracic kyphosis, lumbar lordosis (LL), TL kyphosis, pelvic incidence (PI), pelvic tilt, sacral slope, and PI-LL mismatch.[10]

https://doi.org/10.63858/jass.26.0035

Thoracic kyphosis was defined as the Cobb angle between the upper endplate of T5 and the lower endplate of T12. Lumbar lordosis was measured between the lower end plate of T12 and the upper end plate of S1. TL kyphosis was defined as the Cobb angle between the upper endplate of T10 and the lower endplate of L2. Pelvic parameters were measured using standard definitions. Preoperative and postoperative values, as well as changes in each parameter, were compared between the early and late PJK groups.

3) PJK analysis

On each follow-up radiograph, the PJA was measured between the caudal endplate of the UIV and the cranial endplate of the second supra-adjacent vertebra. PJK was defined as an increase in the PJA of at least 10° compared with the preoperative measurement.[11] The presence of PJK and the time to its development were recorded for all patients (Fig. 1A–C).

3. Surgical factors

The surgical variables analyzed in this study included a history of previous spinal fusion, surgical approach (posterior-only or combined anterior-posterior), use of iliac screw fixation, level of the UIV above T9, level of the lowest instrumented vertebra (LIV at S1), number of fused levels, osteotomy performance (pedicle subtraction or Smith–Petersen osteotomy), UIV/LIV Cobb angle, and cement augmentation at the proximal junctional segments, including cement-augmented pedicle screws or percutaneous vertebroplasty.

4. Statistical analysis

Descriptive data are presented as means ± standard deviations for continuous variables and as frequencies and percentages for categorical variables. The normality of continuous variables was assessed using the Shapiro-Wilk test. The early and late PJK

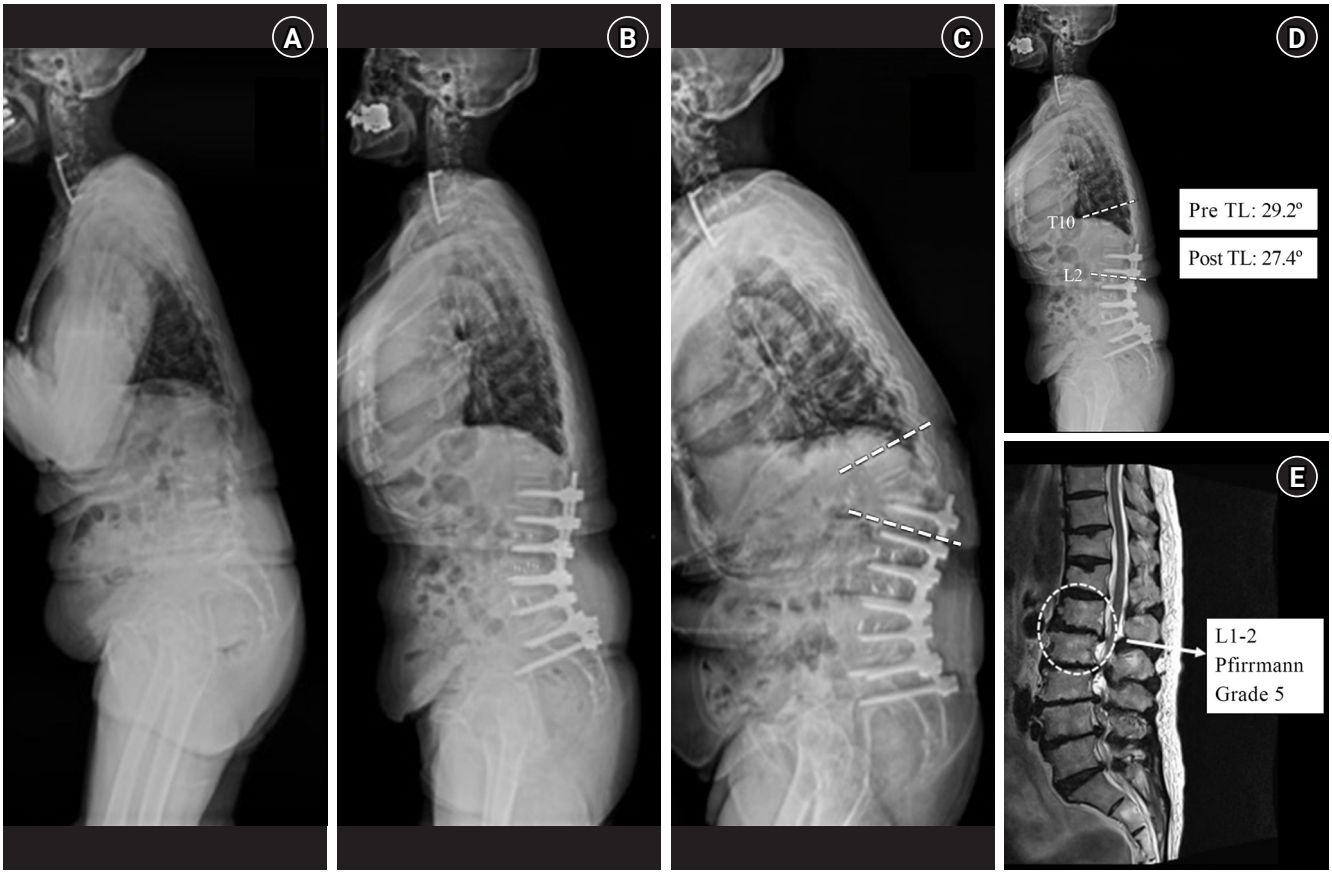

Fig. 1. Representative case of early proximal junctional kyphosis (PJK) in a 72-year-old woman with a stooping gait. (A) Preoperative standing lateral radiograph demonstrating degenerative flatback deformity. (B) Immediate postoperative radiograph following multi-level thoracolumbar fusion. (C) Follow-up radiograph obtained 3 months postoperatively demonstrating early PJK, with dashed lines indicating the increased proximal junctional angle. (D) Postoperative standing lateral radiograph with annotated T10–L2 Cobb angle measurement, demonstrating persistently elevated thoracolumbar kyphosis (preoperative TL angle: 29.2°; postoperative thoracolumbar [TL] angle: 27.4°). (E) Preoperative sagittal magnetic resonance imaging demonstrating advanced degeneration of the L1–2 intervertebral disc (Pfirrmann grade V, dashed circle).

groups were compared using the chi-square test, Student's t-test, or Mann-Whitney U test, as appropriate. Variables significant in the univariate analysis were entered into the multivariate logistic regression model to identify independent factors associated with early PJK. Statistical significance was set at $p < 0.05$. All statistical analyses were performed using SPSS version 26.0 (IBM Corp., Armonk, NY, USA).

5. Ethics statement

This retrospective cohort study was approved by the Institutional Review Board (IRB No. 2022-08-012-000). This type of study does not require informed consent.

Results

1. Baseline characteristics

The baseline characteristics of the patients with early and late PJK are summarized in Table 1. The mean age of patients did not differ significantly between the early and late PJK groups (68.92 ± 6.72 years vs. 69.0 ± 6.37 years, $p = 0.977$). Female patients were predominant in both groups, with no significant difference in sex distribution between the groups ($p = 0.202$).

Height, weight, BMI, smoking status, and BMD measured at the lumbar spine or femur did not differ significantly between the groups.

2. PJK characteristics and timing

The modes of PJK according to onset group are summarized in Table 1. The mean time to PJK onset in all patients was 18 months after surgery. In the early PJK group, PJK developed at a mean of 3 months postoperatively, whereas the mean onset time in the late PJK group was 35 months postoperatively.

Regarding the mode of PJK failure, vertebral fracture at the UIV or adjacent supra-adjacent vertebra was the most prevalent pattern in both groups. Fracture-related PJK was more frequently observed in the early PJK group than in the late PJK group, although the difference was not statistically significant.

3. Risk factor comparison

Comparisons of the surgical variables between the early and late PJK groups are summarized in Table 1. No statistically significant differences were observed between the two groups with respect to prior spinal surgery, surgical approach, use of iliac screw fixation, level of the UIV or LIV, number of fused levels, osteotomy performance, UIV/LIV Cobb angle, or use of cement augmentation.

Overall, none of the analyzed surgical variables were significantly associated with the timing of PJK onset.

4. Sagittal alignment and spinopelvic parameters

The pre- and postoperative sagittal alignment and spinopelvic parameters are summarized in Table 2. Preoperatively, the TL angle was significantly greater in the early PJK group compared with the late PJK group (23.03 ± 13.83° vs. 9.67 ± 9.67°, $p = 0.024$). No other preoperative sagittal parameters differed significantly between the groups.

Postoperatively, the TL angle remained significantly higher in the early PJK group than in the late PJK group (19.6 ± 6.95° vs. 6.95 ± 6.35°, $p < 0.001$). Other postoperative sagittal and pelvic parameters did not differ significantly between the two groups.

Comparison of the changes in sagittal parameters from the pre-

Table 1. Comparison of baseline characteristics, surgical variables, and mode of proximal junctional kyphosis between the early and late PJK groups

	Early PJK (n = 13)	Late PJK (n = 11)	p-value
Age (years)	68.92 ± 6.72	69 ± 6.37	0.977
Male:Female	4:9	1:10	0.202
Height (cm)	150.57 ± 8.39	151.48 ± 5.76	0.766
Weight (kg)	55.53 ± 6.94	54.43 ± 9.33	0.977
BMI	24.53 ± 2.61	23.61 ± 3.42	0.467
Current smoking	3 (23.1)	2 (18.2)	0.773
Lumbar BMD	−1.37 ± 0.94	−1.59 ± 1.85	0.718
Femoral BMD	−2.05 ± 0.95	−1.89 ± 1.24	0.772
PJK mode			
Fracture of UIV or UIV+1	12 (92.3)	8 (72.7)	0.300
Instrumented failure	1 (7.7)	3 (27.3)	
Surgical variables			
Previous surgery	9 (69.2)	10 (90.9)	0.202
Posterior only approach	12 (92.3)	10 (90.9)	0.904
Iliac screw fixation	3 (23.1)	3 (27.3)	0.817
UIV (above T9)	2 (15.4)	3 (27.3)	0.496
UIV (T10–L2)	11 (84.6)	8 (72.7)	
LIV (sacrum 1)	7 (53.8)	8 (72.7)	0.351
UIV/LIV cobb angle (°)	28.08 ± 14.14	25.78 ± 14.38	0.697
Posterior fusion levels	6.46 ± 1.76	6.54 ± 2.42	0.923
PSO	2 (15.4)	2 (18.2)	0.858
SPO	1 (7.7)	1 (9.1)	0.904
Cement screw or PVP	4 (30.8)	5 (45.5)	0.459

Values are presented as mean ± standard deviation or number (%). PJK: proximal junctional kyphosis, BMI: body mass index, BMD: bone mineral density, UIV: upper instrumented vertebra, LIV: lowest instrumented vertebra, PSO: pedicle subtraction osteotomy, SPO: Smith-Petersen osteotomy, PVP: percutaneous vertebroplasty.

https://doi.org/10.63858/jass.26.0035

Table 2. Comparison of sagittal alignment and pelvic parameters between the early PJK and late PJK groups

	Early PJK (n = 13)	Late PJK (n = 11)	p-value
Preoperative parameter			
SVA (mm)	56.86 ± 51.40	78.82 ± 65.49	0.367
LL (°)	25.93 ± 12.49	32.25 ± 24.84	0.428
TK (°)	20.52 ± 14.68	18.15 ± 13.73	0.689
TL (°)	23.03 ± 13.83	9.67 ± 9.67	0.024*
PI (°)	54.83 ± 13.53	56.68 ± 14.24	0.749
SS (°)	26.08 ± 7.10	26.23 ± 7.56	0.960
PT (°)	28.74 ± 10.75	30.40 ± 12.96	0.734
PI-LL (°)	28.90 ± 16.66	24.42 ± 27.06	0.624
Postoperative parameter			
SVA (mm)	48.75 ± 40.07	47.47 ± 42.39	0.940
LL (°)	34.33 ± 13.41	36.50 ± 15.99	0.722
TK (°)	20.86 ± 15.31	23.62 ± 14.22	0.654
TL (°)	19.6 ± 6.95	6.95 ± 6.35	< 0.001*
PI (°)	55.91 ± 12.89	57.60 ± 16.91	0.785
SS (°)	28.49 ± 12.05	27.96 ± 8.25	0.903
PT (°)	27.43 ± 12.30	28.91 ± 11.44	0.765
PI-LL (°)	21.57 ± 13.25	21.10 ± 18.91	0.944
Change in parameter			
SVA (mm)	8.11 ± 30.56	31.34 ± 77.33	0.329
LL (°)	8.40 ± 11.89	4.24 ± 16.24	0.477
TK (°)	0.34 ± 13.42	5.47 ± 6.74	0.264
TL (°)	3.43 ± 9.92	2.71 ± 5.17	0.830
PI (°)	1.07 ± 9.83	0.91 ± 7.10	0.965
SS (°)	2.40 ± 10.66	1.72 ± 7.06	0.858
PT (°)	1.30 ± 6.53	1.49 ± 5.59	0.942
PI-LL (°)	7.33 ± 11.05	3.32 ± 17.23	0.499

Values are presented as mean ± standard deviation. PJK: proximal junctional kyphosis, SVA: sagittal vertical axis, LL: lumbar lordosis, TK: thoracic kyphosis, TL: thoracolumbar angle, PI: pelvic incidence, SS: sacral slope, PT: pelvic tilt. *p < 0.05 was considered statistically significant.

operative to the postoperative period showed that although the change in sagittal vertical axis tended to be greater in the late PJK group (31.34 ± 77.33 mm vs. 8.11 ± 30.56 mm, p = 0.329), this difference was not statistically significant. No significant intergroup differences were observed in other alignment parameters.

5. MRI findings

Comparisons of preoperative lumbar MRI findings between the early and late PJK groups are shown in Table 3. The prevalence of disc protrusion or extrusion, central canal stenosis, spondylolisthesis, and compression fractures did not differ significantly between the groups. Fatty infiltration of the paraspinal muscles was also comparable.

Table 3. Comparison of lumbar spine magnetic resonance imaging between the early PJK and late PJK groups

	Early PJK (n = 13)	Late PJK (n = 11)	p-value
Disc protrusion/extrusion	10 (76.9)	7 (63.6)	0.485
Canal stenosis	8 (61.5)	8 (72.7)	0.885
Grade I	2	1	
Grade II	6	7	
Spondylolisthesis	7 (53.8)	5 (45.5)	0.688
Grade I	7 (53.8)	5 (45.5)	
Grade II	0 (0)	0 (0)	
Compression fracture	10 (76.9)	6 (54.5)	0.348
Mild (20%–25%)	3	4	
Moderate (25%–40%)	3	1	
Severe (> 40%)	4	1	
Fatty infiltration of paraspinal muscles			0.482
0: normal muscle	1 (7.7)	0 (0)	
1: fatty streak within muscle	2 (15.4)	5 (45.5)	
2: fat less than muscle	7 (53.8)	5 (45.5)	
3: fat and muscle equal	2 (15.4)	0 (0)	
4: fat greater than muscle	1 (7.7)	1 (9.1)	
Pfirrmann grade			
L1/2	3.92 ± 0.95	2.81 ± 0.60	0.006*
L2/3	4.30 ± 0.85	3.81 ± 0.87	0.173
L3/4	3.92 ± 0.86	3.54 ± 0.93	0.325
L4/5	3.76 ± 0.92	3.18 ± 0.75	0.100
L5/S1	3.50 ± 0.96	3.54 ± 0.93	0.925

Values are presented as number (%) or mean ± standard deviation. PJK: proximal junctional kyphosis. *p < 0.05 was considered statistically significant.

In contrast, the degree of intervertebral disc degeneration at the L1–2 level, as assessed using the Pfirrmann grading system, was significantly greater in the early PJK group than in the late PJK group (3.92 ± 0.95 vs. 2.81 ± 0.60, p = 0.006). Pfirrmann grades did not differ significantly at other lumbar levels.

6. Multivariate logistic regression analysis

The results of the multivariate logistic regression analysis are presented in Table 4. A representative case illustrating these findings is shown in Fig. 1D and 1E. The model included variables demonstrating potential associations in univariate analysis.

In the final multivariate model, a greater postoperative TL angle and a higher Pfirrmann grade of the L1–2 intervertebral disc were independently associated with early PJK. No surgical or other radiographic variables were significant predictors in the multivariate analysis.

Table 4. Results of multivariate logistic regression analysis for the presence of early PJK

Risk factors	Logistic regression		
	p-value	Odds ratio	95% CI
Postoperative TL (°)	0.030*	1.44	1.04–2.01
L1–2 Pfirrmann grade	0.019*	22.60	1.67–306.30

PJK: proximal junctional kyphosis, CI: confidence interval, TL: thoracolumbar angle. *$p < 0.05$ was considered statistically significant.

Discussion

PJK remains one of the most challenging complications of long-segment TL spinal fusion.[11] The reported incidence of PJK ranges from 20% to 35% in adult spinal deformity surgeries, with a pooled incidence of approximately 30%.[4] In the present study, PJK developed in 17.6% of patients after multilevel spinal fusion, within the lower range of previous reports. Among the patients who developed PJK, the temporal patterns and clinical characteristics differed between early- and late-onset PJK.

Early-onset PJK frequently develops within the first few months after surgery.[7,12] Yagi et al.[7] reported that approximately 76% of PJK cases occurred within 3 months. Consistent with this finding, early PJK in the present study occurred at a mean of 3 months postoperatively, whereas late PJK developed at a mean of 35 months. These temporal patterns support the clinical relevance of distinguishing early- from late-onset PJK, because early-onset PJK likely reflects acute biomechanical failure, whereas late-onset PJK may represent progressive degenerative changes.

The patient-related risk factors previously associated with PJK include advanced age, female sex, high BMI, and low BMD.[2,4,6,13,14] Osteopenia and osteoporosis have been suggested to contribute to junctional failure by reducing vertebral load-bearing capacity, particularly in older patients.[6,15-17] In the present study, the baseline demographic characteristics and BMD did not differ significantly between patients with early and late PJK. Although compression fractures were more frequently observed in the early PJK group, the difference was not statistically significant. These findings suggest that patient-related factors alone may not adequately explain the timing of PJK onset.

The surgical factors implicated in PJK development include surgical approach, UIV/LIV level selection, fusion length, osteotomy, rod stiffness, and cement augmentation.[3,7,14,18-21] In particular, fusion constructs extending to the sacrum are associated with higher rates of junctional complications.[22] However, in the present study, none of the analyzed surgical variables, including surgical approach, UIV and LIV levels, fusion length, osteotomy, iliac fixation, or cement augmentation, differed significantly between the early and late PJK groups. This finding suggests that surgical factors alone may not be the primary determinants of early PJK onset in this cohort.

In contrast, the results of sagittal alignment analysis demonstrated that TL kyphosis was significantly associated with early PJK. Both preoperative and postoperative TL angles were significantly greater in the early PJK group compared with the late PJK group, whereas other global sagittal and spinopelvic parameters did not differ significantly between the groups. Although the preoperative TL angle showed significance in univariate analysis, it did not remain significant in the multivariate model, suggesting that postoperative TL alignment, rather than baseline morphology alone, is more critical in the development of early PJK. Furthermore, the high collinearity between the pre- and postoperative TL angles likely contributed to the exclusion of the preoperative TL angle from the final multivariate model. Persistence of postoperative TL kyphosis likely increases mechanical stress at the proximal junction, thereby contributing to early structural failure. Moreover, the transition from a rigid thoracic spine to a more mobile lumbar segment can increase mechanical stress at the proximal junction after long-segment fusion, particularly in the presence of residual TL kyphosis or dynamic motion-related factors.[23] In the present study, the early PJK group showed significantly more advanced degeneration of the L1–2 intervertebral disc, as assessed by the Pfirrmann classification. This degeneration remained the strongest independent factor associated with early PJK in multivariate analysis (Table 4). Given the small subgroup size, however, the wide confidence interval (CI) for this estimate indicates that the magnitude of this association should be interpreted with caution. The L1–2 disc is located adjacent to the TL junction and is subjected to increased mechanical demand following long-segment fusion. Preexisting disc degeneration at this level may reduce resistance to kyphotic and compressive forces, thereby predisposing patients to early junctional failure. These findings are consistent with those reported previously, suggesting that adjacent segment degeneration near the TL junction increases the risk of junctional complications. Our results suggest that the health of the L1–2 intervertebral disc should be a primary consideration when selecting the UIV. In clinical practice, if preoperative MRI reveals advanced degeneration (Pfirrmann grade ≥ 4) at the L1–2 level, extending the fusion more cranially to a healthier segment may be considered to avoid placing the proximal junction at a biomechanically compromised level. However, because this suggestion is based on retrospective observations and was not directly tested in the present study, it should be regarded as hypothesis-generating

https://doi.org/10.63858/jass.26.0035

and requires confirmation in prospective studies. Collectively, increased postoperative TL angle and advanced L1–2 disc degeneration may predispose patients to proximal vertebral instability, thereby facilitating early-onset PJK.[3]

Several strategies have been proposed to reduce the risk of PJK and PJF, including cement augmentation, use of hooks at the UIV, and the use of transitional rods.[18,24] However, these surgical techniques were not associated with differences in the timing of PJK onset in the present study. Instead, the findings emphasized the importance of careful consideration of TL alignment and adjacent disc condition during preoperative planning and intraoperative correction. Thus, patients with excessive TL kyphosis or advanced L1–2 disc degeneration may represent a subgroup at higher risk for early PJK.

The biomechanical role of L1–2 disc degeneration likely differs depending on whether L1–2 is included in the fusion construct. Disc degeneration at this level is unlikely to directly drive early PJK. When unfused, preexisting degeneration may compromise load-sharing and resistance to kyphotic forces, particularly with residual postoperative TL kyphosis. The association between L1–2 disc degeneration and early PJK in this study likely reflects adjacent-segment vulnerability at the TL junction, rather than a single isolated mechanism.

This study had several limitations. First, the retrospective design and small sample size may have limited the generalizability of the results. In particular, the restricted number of patients in each subgroup (early PJK, n = 13; late PJK, n = 11) may have resulted in an underpowered multivariate model, and the wide CI observed for the L1–2 Pfirrmann grade (odds ratio, 22.6; 95% CI, 1.667 to 306.3) should be interpreted with caution, as it may reflect statistical instability rather than a true effect magnitude. Accordingly, the odds ratio for the L1–2 Pfirrmann grade should be regarded as imprecise and interpreted with particular caution, rather than as a precise estimate of effect size. Second, detailed bone quality assessments beyond BMD were unavailable. Third, the follow-up period may not have fully captured late-onset junctional complications.

Early-onset PJK after multilevel TL fusion is uniquely associated with greater postoperative TL kyphosis and more advanced degeneration of the adjacent L1–2 intervertebral discs. Conversely, surgical factors and global sagittal alignment parameters were not significantly associated with PJK onset. These findings indicate that early PJK is more closely associated with regional sagittal alignment at the biomechanically vulnerable TL junction and the preexisting structural integrity of the adjacent intervertebral disc, rather than to surgical techniques alone. Therefore, meticulous correction of regional TL alignment and thorough preoperative evaluation of the adjacent disc condition are important for identifying and managing patients at a high risk of early PJK.

Author contributions

Conceptualization: SHY. Methodology: DSR, SHY. Data curation: WSK. Formal analysis: WSK, DSR. Investigation: WSK, DSR. Supervision: SHY. Writing – original draft: WSK. Writing – review & editing: DSR, SHY. All authors read and approved the final manuscript.

Conflict of interest

The authors have no conflicts of interest to declare.

Funding

None.

Acknowledgments

None.

ORCID

Woo-Sel Kim, https://orcid.org/0009-0001-6066-4605
Dal-Sung Ryu, https://orcid.org/0000-0003-0895-3431
Seung-Hwan Yoon, https://orcid.org/0000-0003-0558-2313

References

1. Rajaee SS, Bae HW, Kanim LE, Delamarter RB. Spinal fusion in the United States: analysis of trends from 1998 to 2008. Spine (Phila Pa 1976) 2012;37:67-76.
2. Kim DK, Kim JY, Kim DY, Rhim SC, Yoon SH. Risk factors of proximal junctional kyphosis after multilevel fusion surgery: more than 2 years follow-up data. J Korean Neurosurg Soc 2017;60:174-80.
3. Glattes RC, Bridwell KH, Lenke LG, Kim YJ, Rinella A, Edwards C 2nd. Proximal junctional kyphosis in adult spinal deformity following long instrumented posterior spinal fusion: incidence, outcomes, and risk factor analysis. Spine (Phila Pa 1976) 2005;30:1643-9.
4. Kim YJ, Bridwell KH, Lenke LG, Glattes CR, Rhim S, Cheh G. Proximal junctional kyphosis in adult spinal deformity after segmental posterior spinal instrumentation and fusion: minimum five-year follow-up. Spine (Phila Pa 1976) 2008;33:2179-84.
5. Lau D, Clark AJ, Scheer JK, et al. Proximal junctional kyphosis and failure after spinal deformity surgery: a systematic review of the literature as a background to classification development.

Spine (Phila Pa 1976) 2014;39:2093-102.
6. Kim HJ, Bridwell KH, Lenke LG, et al. Proximal junctional kyphosis results in inferior SRS pain subscores in adult deformity patients. Spine (Phila Pa 1976) 2013;38:896-901.
7. Yagi M, King AB, Boachie-Adjei O. Incidence, risk factors, and natural course of proximal junctional kyphosis: surgical outcomes review of adult idiopathic scoliosis. Minimum 5 years of follow-up. Spine (Phila Pa 1976) 2012;37:1479-89.
8. Pfirrmann CW, Metzdorf A, Zanetti M, Hodler J, Boos N. Magnetic resonance classification of lumbar intervertebral disc degeneration. Spine (Phila Pa 1976) 2001;26:1873-8.
9. Goutallier D, Postel JM, Bernageau J, Lavau L, Voisin MC. Fatty muscle degeneration in cuff ruptures: pre- and postoperative evaluation by CT scan. Clin Orthop Relat Res 1994;304:78-83.
10. Makhni MC, Shillingford JN, Laratta JL, Hyun SJ, Kim YJ. Restoration of sagittal balance in spinal deformity surgery. J Korean Neurosurg Soc 2018;61:167-79.
11. Park SJ, Lee CS, Chung SS, Lee JY, Kang SS, Park SH. Different risk factors of proximal junctional kyphosis and proximal junctional failure following long instrumented fusion to the sacrum for adult spinal deformity: survivorship analysis of 160 patients. Neurosurgery 2017;80:279-86.
12. Annis P, Lawrence BD, Spiker WR, et al. Predictive factors for acute proximal junctional failure after adult deformity surgery with upper instrumented vertebrae in the thoracolumbar spine. Evid Based Spine Care J 2014;5:160-2.
13. Bridwell KH, Lenke LG, Cho SK, et al. Proximal junctional kyphosis in primary adult deformity surgery: evaluation of 20 degrees as a critical angle. Neurosurgery 2013;72:899-906.
14. Kim HJ, Lenke LG, Shaffrey CI, Van Alstyne EM, Skelly AC. Proximal junctional kyphosis as a distinct form of adjacent segment pathology after spinal deformity surgery: a systematic review. Spine (Phila Pa 1976) 2012;37(22 Suppl):S144-64.
15. Echt M, Ranson W, Steinberger J, Yassari R, Cho SK. A systematic review of treatment strategies for the prevention of junctional complications after long-segment fusions in the osteoporotic spine. Global Spine J 2021;11:792-801.
16. Hostin R, McCarthy I, O'Brien M, et al. Incidence, mode, and location of acute proximal junctional failures after surgical treatment of adult spinal deformity. Spine (Phila Pa 1976) 2013;38:1008-15.
17. Watanabe K, Lenke LG, Bridwell KH, Kim YJ, Koester L, Hensley M. Proximal junctional vertebral fracture in adults after spinal deformity surgery using pedicle screw constructs: analysis of morphological features. Spine (Phila Pa 1976) 2010;35:138-45.
18. Ghobrial GM, Eichberg DG, Kolcun JP, et al. Prophylactic vertebral cement augmentation at the uppermost instrumented vertebra and rostral adjacent vertebra for the prevention of proximal junctional kyphosis and failure following long-segment fusion for adult spinal deformity. Spine J 2017;17:1499-505.
19. Mendoza-Lattes S, Ries Z, Gao Y, Weinstein SL. Proximal junctional kyphosis in adult reconstructive spine surgery results from incomplete restoration of the lumbar lordosis relative to the magnitude of the thoracic kyphosis. Iowa Orthop J 2011;31:199-206.
20. O'Leary PT, Bridwell KH, Lenke LG, et al. Risk factors and outcomes for catastrophic failures at the top of long pedicle screw constructs: a matched cohort analysis performed at a single center. Spine (Phila Pa 1976) 2009;34:2134-9.
21. Yagi M, Fujita N, Tsuji O, et al. Low bone mineral density is a significant risk factor for proximal junctional failure after surgical correction of adult spinal deformity: a propensity score-matched analysis. Spine (Phila Pa 1976) 2018;43:485-91.
22. Maruo K, Ha Y, Inoue S, et al. Predictive factors for proximal junctional kyphosis in long fusions to the sacrum in adult spinal deformity. Spine (Phila Pa 1976) 2013;38:E1469-76.
23. Ham DW, Han H, Kim HJ, Park SM, Chang BS, Yeom JS. Risk factors for acute proximal junctional kyphosis after adult spinal deformity surgery in preoperative motion analysis. Eur Spine J 2021;30:1215-25.
24. Safaee MM, Osorio JA, Verma K, et al. Proximal junctional kyphosis prevention strategies: a video technique guide. Oper Neurosurg 2017;13:581-5.

https://doi.org/10.63858/jass.26.0035

Original Article

J Adv Spine Surg 2026;16(1):33-40
https://doi.org/10.63858/jass.26.0034
pISSN 2234-0637 • eISSN 3140-0663

JASS
JOURNAL OF ADVANCED SPINE SURGERY

Survival Analysis of Syringopleural, Syringoperitoneal, and Syringosubarachnoid Shunts for Syringomyelia: A Single-Center Retrospective Cohort Study

Hyung-Tae Kim, M.D., Dongkyu Kim, M.D., Ph.D., Bong-Ju Moon, M.D., Ph.D., Kyung-Hyun Kim, M.D., Ph.D., Jeong-Yoon Park, M.D., Ph.D., Sung-Uk Kuh, M.D., Ph.D., Dong-Kyu Chin, M.D., Ph.D., Keun-Su Kim, M.D., Ph.D., Hyun-Jun Jang, M.D.

Department of Neurosurgery, Spine and Spinal Cord Institute, Gangnam Severance Hospital, Yonsei University College of Medicine, Seoul, Korea

Study Design: This study was a retrospective single-center cohort study.

Purpose: This study aimed to compare long-term shunt patency by shunt type (syringo-subarachnoid [SS], syringo-pleural [SP], syringo-peritoneal [SPt]) and disease etiology (post-traumatic, post-infectious, idiopathic) in patients surgically treated for syringomyelia, using Kaplan-Meier survival methodology.

Overview of Literature: Syringomyelia shunting carries a well-documented revision burden, but direct comparative survival data across shunt modalities and etiologic subgroups are scarce, particularly from East Asian centers.

Methods: We retrospectively analyzed 42 patients (mean age, 47.6±11.8 years; 57.1% male) who underwent syringomyelia shunting at a tertiary neurosurgical center (January 2000–December 2020) with ≥12 months follow-up. Shunt type was classified as SS (n=12), SP (n=16), or SPt (n=14); etiology as post-traumatic (n=24), post-infectious (n=10), idiopathic (n=6), or hemorrhage/tumor-related (n=2). The primary endpoint was shunt revision surgery. Kaplan-Meier analysis, log-rank testing, and Cox proportional hazards regression were performed.

Results: Over a median follow-up of 15 months (range, 12 to 184 months), 16 patients (38.1%) underwent shunt revision. Overall 12- and 24-month patency rates were 79.6% and 72.5%, respectively (median shunt survival 72 months). By shunt type, 12-month patency was 75.0% (SS), 81.3% (SP), and 85.7% (SPt); 24-month patency declined to 48.2% for SS while SP and SPt remained at 81.3% and 85.7% (log-rank p=0.248). Post-infectious syringomyelia showed the shortest median shunt survival (36 months) compared with post-traumatic (not reached) and idiopathic (not reached) groups (log-rank p=0.232). No independent predictor of shunt failure was identified on multivariate Cox regression.

Conclusion: All three shunting techniques achieve approximately 80% one-year patency. SS may carry a higher long-term occlusion risk. Post-infectious syringomyelia requires closer postoperative surveillance. Larger prospective studies are needed to establish definitive shunt selection criteria.

Keywords: Syringomyelia, Shunting procedure, Shunt survival, Kaplan-Meier analysis, Shunt revision, Post-traumatic syringomyelia, Arachnoiditis

Received: May 19, 2026; Revised: June 9, 2026; Accepted: June 10, 2026

Corresponding author: Hyun-Jun Jang, M.D.
Department of Neurosurgery, Spine and Spinal Cord Institute, Gangnam Severance Hospital, Yonsei University College of Medicine, 211 Eonju-ro, Gangnam-gu, Seoul 06273, Korea
TEL: +82-2-2019-2114, FAX: +82-2-3461-9229, E-mail: janghj0@yuhs.ac

Introduction

Syringomyelia is characterized by a longitudinal fluid-filled cavity (syrinx) within the spinal cord parenchyma that progressively compresses and destroys adjacent neural tissue. The clinical syndrome typically comprises dissociated sensory loss, wasting and weakness of the upper limbs, and—in advanced cases—spastic paraparesis and autonomic dysfunction.[1,2] When conservative management fails or neurological deterioration progresses, surgical intervention is required.

The pathophysiology of syrinx formation differs substantially across etiologic categories. In post-traumatic syringomyelia, fibro-arachnoid scarring at the injury site generates abnormal intramedullary pressure gradients that drive fluid accumulation.[3-5] In post-infectious cases—commonly following tuberculous or bacterial meningitis—diffuse spinal arachnoiditis produces widespread subarachnoid adhesions that impair cerebrospinal fluid (CSF) circulation.[6-8] Idiopathic syringomyelia, by definition, lacks a clearly identified precipitant and often presents with a more indolent course.[1]

Current surgical options for syringomyelia include three principal shunting strategies: (1) syringo-subarachnoid shunting (SS), which creates a direct communication between the syrinx and the adjacent subarachnoid space; (2) syringo-pleural shunting (SP), which diverts syrinx contents into the ipsilateral pleural cavity; and (3) syringo-peritoneal shunting (SPt), which drains fluid into the peritoneal cavity.[9-12] Each technique exploits different pressure gradients and is subject to distinct failure mechanisms.

Published series on syringomyelia shunting are predominantly small and retrospective.[9-11,13-15] Formal survival analyses using Kaplan-Meier methodology—the statistical standard for time-to-event outcomes—are rarely reported in this disease context, and comparative data from East Asian centers remain sparse.

The objectives of the present study were as follows: (1) to characterize overall long-term shunt patency in a single-center cohort; (2) to compare shunt survival across SS, SP, and SPt using Kaplan-Meier analysis; and (3) to evaluate whether disease etiology independently influences the risk of shunt revision.

Methods

This is a single-center, retrospective cohort study. The institutional surgical database was queried for all patients who underwent syringomyelia shunting between January 2000 and December 2020. Inclusion criteria were as follows: (1) radiologically confirmed syringomyelia on magnetic resonance imaging (MRI); (2) primary syrinx shunting procedure performed at our institution; and (3) minimum postoperative follow-up of 12 months. Patients who underwent adhesiolysis alone without shunt insertion, or whose primary surgical objective was tumor resection or Chiari malformation decompression without concomitant shunting, were excluded. The study was approved by the Institutional Review Board of Gangnam Severance Hospital, Yonsei University Health System (IRB No. 3-2022-0461) and individual informed consent was waived given the retrospective design.

1. Surgical technique and shunt classification

All procedures were performed by attending neurosurgeons with spinal subspecialty training. Shunt type was selected at the surgeon's discretion based on the degree of subarachnoid space involvement, prior surgical history, and intraoperative findings. Syringo-subarachnoid shunts were placed via a posterior midline approach, with a T-bar silastic catheter tunneled from the syrinx lumen into the adjacent subarachnoid space. Syringo-pleural and syringo-peritoneal shunts employed a valveless silastic catheter system with the proximal limb positioned within the syrinx cavity and the distal limb tunneled subcutaneously to the ipsilateral pleural cavity or peritoneal cavity, respectively.

2. Variable definitions

Disease etiology was classified as (1) post-traumatic, defined by documented spinal cord injury antedating syrinx development by ≥6 months;[3,16,17] (2) post-infectious, defined by preceding meningitis, spinal cord infection, or tuberculous arachnoiditis confirmed by CSF analysis or imaging;[8,9,18] (3) hemorrhage/tumor-related; or (4) idiopathic, when no identifiable underlying cause was found after complete workup. Spinal level was dichotomized as cervical (C1–C7) or thoracic (T1–T12).

The primary endpoint was shunt revision surgery, defined as any return to the operating room for shunt revision, replacement, or externalization necessitated by clinical deterioration (new or worsening neurological symptoms), with or without radiological re-expansion of the syrinx on MRI. Patients who completed follow-up without revision were censored at the date of last clinical contact.

3. Statistical analysis

Continuous variables are presented as mean ± standard deviation or median with range; categorical variables as frequency and percentage. Shunt patency was estimated by the Kaplan-Meier product-limit method.[19] Between-group differences in survival were assessed by the log-rank test for two-group comparisons and

https://doi.org/10.63858/jass.26.0034

the multivariate log-rank test for three or more groups. Pairwise post-hoc comparisons were performed without adjustment for multiplicity given the exploratory nature of the analysis. Independent predictors of shunt failure were assessed using Cox proportional hazards regression[20] with age (continuous), shunt type (ordinal: SS = 1, SP = 2, SPt = 3), disease etiology (ordinal), and spinal level (binary) entered simultaneously. Proportional hazards assumptions were verified graphically using log-log plots. All analyses were performed in Python 3.10 (lifelines v0.27; scipy v1.11). Statistical significance was defined as $p < 0.05$ (two-tailed).

Results

1. Patient demographics and baseline characteristics

Of 149 patients who underwent syringomyelia surgery during the study period, 42 met the inclusion criteria. The remaining 107 patients were excluded due to incomplete follow-up (n = 82), adhesiolysis-only procedures (n = 12), concurrent tumor resection without shunting (n = 6), or combined shunting with adhesiolysis procedures (n = 7). Baseline characteristics are summarized in Table 1. The cohort comprised 24 men (57.1%) and 18 women, with a mean age of 47.6 ± 11.8 years (median, 51; range, 18 to 67 years). Disease involved the thoracic spine in 31 patients (73.8%) and the cervical spine in 11 (26.2%). The predominant etiology was post-traumatic (n = 24, 57.1%), followed by post-infectious (n = 10, 23.8%), idiopathic (n = 6, 14.3%), and hemorrhage/tumor-related (n = 2, 4.8%). Shunt type distribution was SP (n = 16, 38.1%), SPt (n = 14, 33.3%), and SS (n = 12, 28.6%). Baseline demographics were comparable across shunt type groups (all $p > 0.05$) (Table 1). Median follow-up was 15 months (mean, 36.7 ± 42.3 months; range, 12 to 184 months). During follow-up, 16 patients (38.1%) underwent revision surgery for shunt failure (Table 1).

2. Overall shunt survival

The overall 12- and 24-month Kaplan-Meier shunt patency rates were 79.6% and 72.5%, respectively. The estimated median shunt survival for the entire cohort was 72 months.

3. Shunt survival by shunt type

Kaplan-Meier survival estimates stratified by shunt type are presented in Table 2 and Fig. 1. The SS group demonstrated 12-month and 24-month patency rates of 75.0% and 48.2%, with a median shunt survival of only 18 months. The SP group achieved 12- and 24-month patency of 81.3% each, with an esti-

Table 1. Baseline characteristics by shunt type

Variable	Total (n = 42)	SS (n = 12)	SP (n = 16)	SPt (n = 14)	p-value
Age (years)	47.6 ± 11.8	46.3 ± 14.2	48.9 ± 11.1	47.1 ± 10.8	0.838
Male sex	24 (57.1)	7 (58.3)	9 (56.3)	8 (57.1)	> 0.99
Thoracic level	31 (73.8)	8 (66.7)	12 (75.0)	11 (78.6)	0.824
Etiology					
Post-traumatic	24 (57.1)	6 (50.0)	10 (62.5)	8 (57.1)	0.976
Post-infectious	10 (23.8)	4 (33.3)	3 (18.8)	3 (21.4)	-
Hemorrhage/tumor-related	2 (4.8)	0 (0)	1 (6.3)	1 (7.1)	-
Idiopathic	6 (14.3)	2 (16.7)	2 (12.5)	2 (14.3)	-
Shunt revision	16 (38.1)	6 (50.0)	5 (31.3)	5 (35.7)	0.667
Follow-up (months)	15 (12–184)	16 (12–80)	16 (12–144)	32 (12–184)	0.180

Values are presented as mean±standard deviation, number (%), or median (range). p-values by one-way ANOVA (continuous) or Fisher exact test (categorical). SS: syringo-subarachnoid shunt, SP: syringo-pleural shunt, SPt: syringo-peritoneal shunt.

Table 2. Kaplan-Meier shunt survival estimates by shunt type

Outcome	SS (n = 12)	SP (n = 16)	SPt (n = 14)	p-value (log-rank)
Shunt revisions, n (%)	6 (50.0)	5 (31.3)	5 (35.7)	0.471
12-Month patency (%)	75	81.3	85.7	0.248
24-Month patency (%)	48.2	81.3	85.7	
Shunt survival (months), median	18	144	72	
Follow-up (months), median (range)	16 (12–80)	16 (12–144)	32 (12–184)	

Patency rates are Kaplan-Meier estimates. Overall p-value by three-group log-rank test. SS: syringo-subarachnoid shunt, SP: syringo-pleural shunt, SPt: syringo-peritoneal shunt.

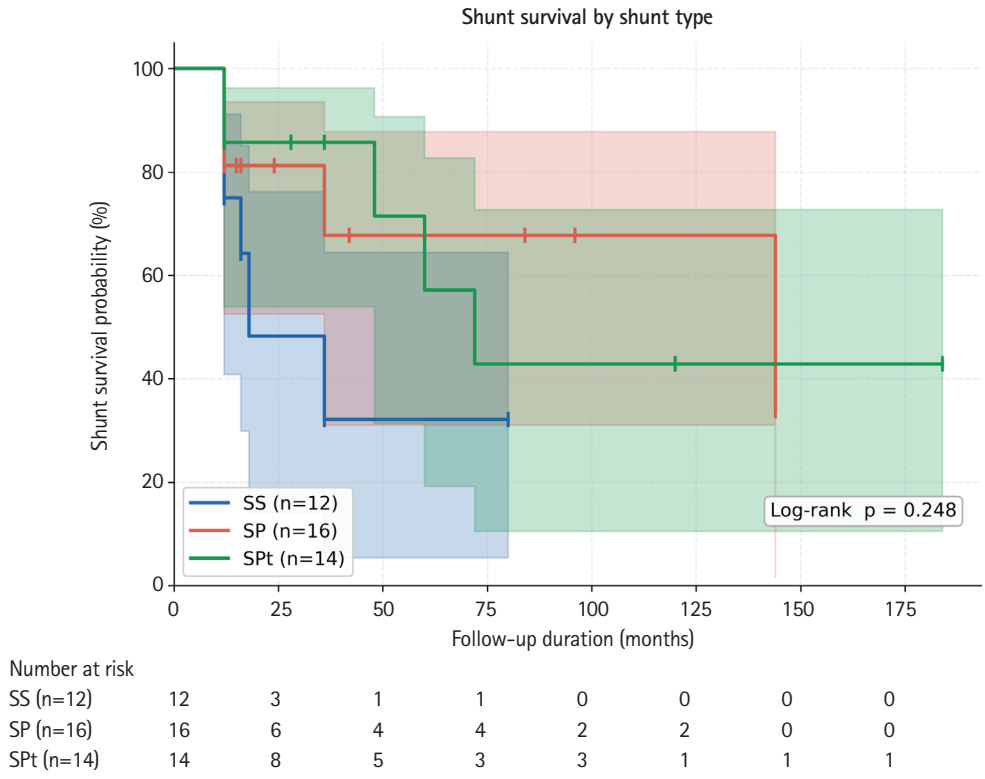

Fig. 1. Kaplan-Meier shunt survival curves stratified by shunt type. Tick marks indicate censored observations. Numbers at risk at each time point are shown below the x-axis. SS: syringo-subarachnoid shunt, SP: syringo-pleural shunt, SPt: syringo-peritoneal shunt.

mated median survival of 144 months. The SPt group showed 12- and 24-month patency rates of 85.7% each and a median shunt survival of 72 months. Although SS demonstrated a numerically inferior trajectory beyond 12 months, the overall difference across the three groups did not reach statistical significance (log-rank p = 0.248) (Fig. 1). Pairwise comparisons also failed to achieve significance: SS vs. SP (p = 0.179), SS vs. SPt (p = 0.155), and SP vs. SPt (p = 0.927) (Table 2, Fig. 1).

4. Shunt survival by disease etiology

Kaplan-Meier survival curves stratified by etiology are shown in Fig. 2. Post-infectious syringomyelia demonstrated the shortest median shunt survival (36 months) and the highest revision burden (n = 10; 12-month patency, 72.7%). Post-traumatic and idiopathic groups both had median survivals that were not reached within the observation period (12-month patency, 82.1% and 83.3%, respectively). The hemorrhage/tumor-related group (n = 2) was too small for meaningful survival estimation. No statistically significant difference across etiologic groups was detected (log-rank p = 0.232) (Fig. 2). Direct pairwise comparison of post-traumatic versus post-infectious cases showed a consistent trend favoring the post-traumatic group but did not achieve significance (log-rank p = 0.236) (Fig. 3), likely reflecting inadequate statistical power (Figs. 2, 3).

5. Multivariable Cox proportional hazards analysis

Multivariable Cox regression results are presented in Table 3. None of the preoperative variables entered—age, shunt type, disease etiology, or spinal level—were independently associated with shunt failure at the $p < 0.05$ threshold. The hazard ratio (HR) for shunt type was 0.714 (95% confidence interval [CI], 0.420 to 1.215; p = 0.214), suggesting a trend toward lower failure risk with SP and SPt that did not reach significance. The HR for disease etiology was 0.863 (95% CI, 0.533 to 1.399; p = 0.551). Age and spinal level were similarly non-significant (Table 3).

Discussion

This retrospective cohort study provides survival analysis data for syringomyelia shunting across three surgical modalities and four etiologic subgroups from a single tertiary East Asian neurosurgical center. The overall 12-month shunt patency of 79.6% and revision rate of 38.1% are consistent with the range of 60%–85% reported in historical series.[9-11,13,14]

https://doi.org/10.63858/jass.26.0034

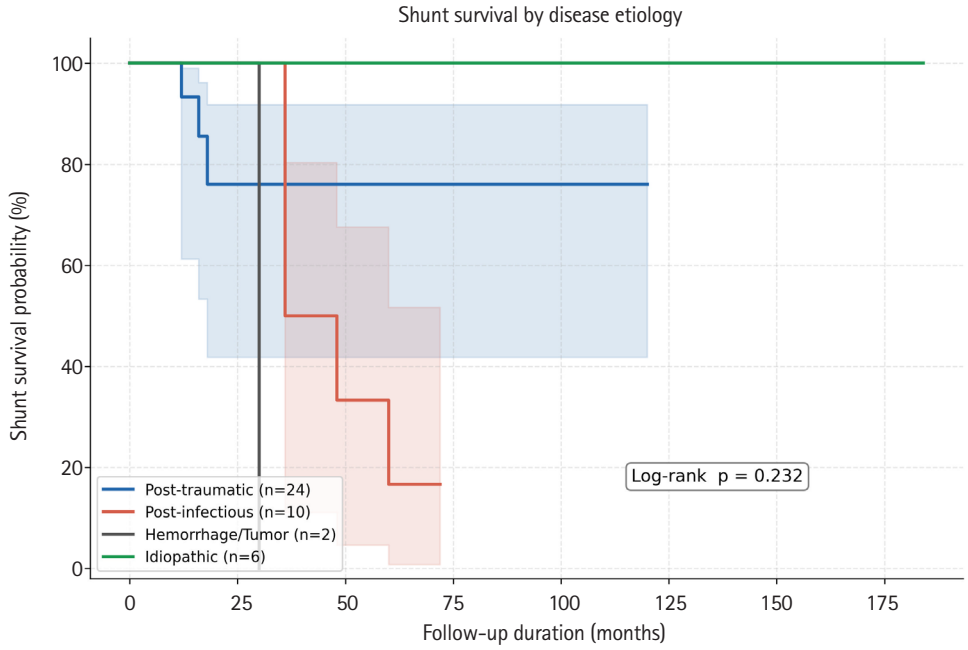

Number at risk								
Post-traumatic (n=24)	24	5	3	3	2	1	0	0
Post-infectious (n=10)	10	5	2	1	1	1	0	0
Hemorrhage/tumor (n=2)	2	1	0	0	0	0	0	0
Idiopathic (n=6)	6	3	3	2	2	1	1	1

Fig. 2. Kaplan-Meier shunt survival curves by disease etiology. Tick marks on the curves indicate censored observations. Numbers at risk at each time point are shown below the x-axis.

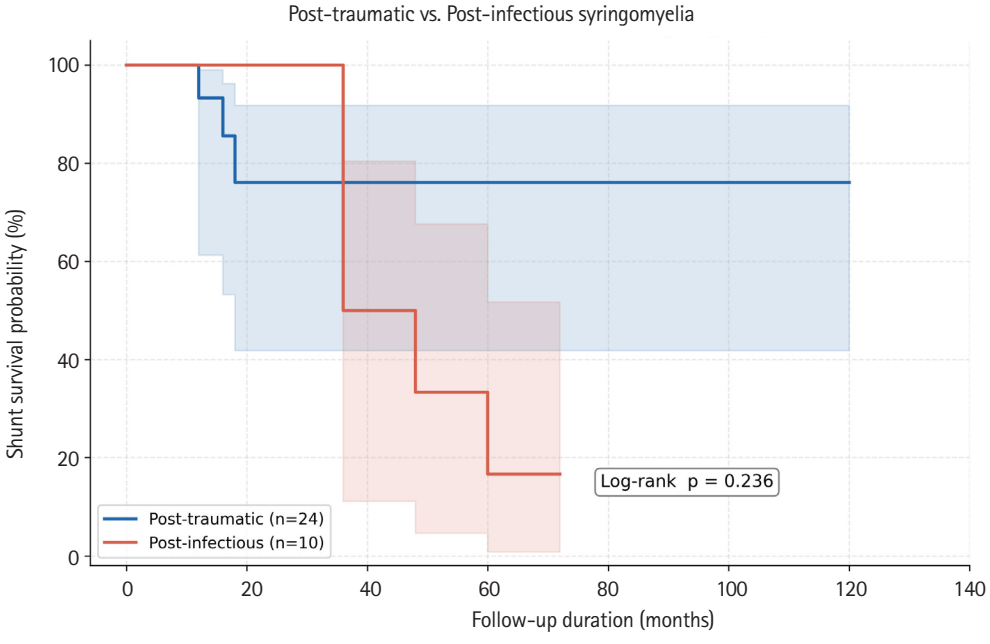

Number at risk								
Post-traumatic (n=24)	24	6	4	4	4	2	1	1
Post-infectious (n=10)	10	5	3	1	1	1	1	1

Fig. 3. Head-to-head Kaplan-Meier comparison: post-traumatic vs. post-infectious syringomyelia (log-rank p=0.236). Tick marks on the curves indicate censored observations. Numbers at risk at each time point are shown below the x-axis.

Table 3. Multivariable Cox proportional hazards analysis for shunt failure

Variable	Hazard ratio	95% Confidence interval	p-value
Age (per year increase)	1.035	0.988–1.084	0.146
Shunt type (SS→SP→SPt)	0.714	0.420–1.215	0.214
Disease etiology	0.863	0.533–1.399	0.551
Spinal level (thoracic vs. cervical)	0.955	0.327–2.786	0.933

Hazard ratio <1 indicates lower hazard of revision (longer patency) for higher-coded category. SS=1, SP=2, SPt=3 for shunt type coding. SS: syringo-subarachnoid shunt, SP: syringo-pleural shunt, SPt: syringo-peritoneal shunt.

Our data suggest that SS may carry an inferior long-term patency profile. The 24-month patency of SS declined markedly to 48.2%, compared with 81.3% for SP and 85.7% for SPt, and the median shunt survival of SS (18 months) was substantially shorter. The physiological rationale for this observation relates to the pressure dynamics exploited by each technique. SS shunts rely on the pressure differential between the high-pressure syrinx and the adjacent subarachnoid space; in patients with ongoing arachnoid fibrosis or subarachnoid adhesions—conditions inherent to post-traumatic and post-infectious disease—this gradient may be insufficient or unstable.[8,15,18,21] SP and SPt shunts, conversely, drain into large-capacity body cavities with consistently lower pressure (pleural cavity, −5 to 0 cmH_2O; peritoneum, ≈0 cmH_2O), providing theoretically more reliable sustained drainage.[13,14,22] These findings align with the series by Tator et al.,[12] who reported early occlusion as the primary limitation of the syringosubarachnoid technique, and with the comparative data of Batzdorf et al.[10]

Nonetheless, the log-rank test did not detect a statistically significant difference across shunt types (p = 0.248). This should not be interpreted as equivalence; the sample sizes in each arm (n = 12–16) are substantially underpowered to detect the magnitude of difference observed between SS and SP at 24 months (48.2% vs. 81.3%). A sample of > 80 patients per arm would be required for 80% power at α = 0.05 under these effect assumptions, underscoring the need for multicenter collaboration.

The etiology-stratified analysis yielded a clinically meaningful finding: post-infectious syringomyelia was associated with the highest revision burden (n = 10) and the shortest median shunt survival, markedly inferior to post-traumatic (not reached) and idiopathic (not reached) groups. Post-infectious cases in our cohort predominantly involved a history of tuberculous meningitis or bacterial meningitis resulting in spinal arachnoiditis. The dense fibroinflammatory adhesions in this setting impair CSF circulation bidirectionally: proximally, generating the pressure that drives syrinx formation, and distally, by progressively encasing and obstructing the shunt catheter following implantation.[6,8,9,18] These findings are consistent with the series by Klekamp et al.,[9] who similarly reported higher revision rates in arachnoiditis-related syringomyelia compared with other etiologies. Clinically, this mandates a lower threshold for MRI surveillance and symptom reassessment in post-infectious patients.

Post-traumatic syringomyelia demonstrated the most durable shunt longevity in our cohort, with a median survival not reached over a maximum follow-up of 184 months. The predominantly focal nature of the pathological process in post-traumatic syringomyelia—centered on the injury-level fibro-arachnoid scar rather than diffuse spinal arachnoiditis—likely explains the relatively favorable shunt durability observed.[5-7,16,17] This is consistent with earlier series by Klekamp et al.,[21] who noted better outcomes after shunting in post-traumatic compared with post-infectious arachnoiditis.

The absence of significant independent predictors on Cox regression is likely attributable to the small sample size rather than a genuine absence of effect. Unmeasured confounders—including intraoperative extent of arachnoid adhesions (graded by some authors as Klekamp grade I–IV),[8] catheter type and gauge, CSF pressure measurement, and surgeon volume—may also have diluted true associations. The ordinal coding of shunt type and etiology additionally imposes linearity assumptions that may not reflect the underlying biology.

Several limitations of this study merit acknowledgment. First, the retrospective single-center design introduces selection and confounding biases, particularly because shunt type was non-randomly assigned. Second, data collection spanning two decades introduces temporal heterogeneity in surgical technique, catheter materials, and postoperative imaging protocols. Third, only 42 of 149 patients in the database met full inclusion criteria, reducing representativeness. Fourth, our primary endpoint of revision surgery may underestimate true shunt failure if subclinical dysfunction was not systematically investigated by surveillance imaging. Fifth, the hemorrhage/tumor-related subgroup (n = 2) was too small for meaningful subgroup analysis. Future prospective multicenter registries with standardized outcome definitions, mandatory surveillance MRI protocols, and intraoperative arachnoid adhesion grading are needed to overcome these limitations.

https://doi.org/10.63858/jass.26.0034

Syringomyelia shunting with SS, SP, or SPt achieves approximately 80% 1-year shunt patency. Syringo-subarachnoid shunts appear to carry a higher long-term occlusion risk, with a 24-month patency of only 48.2% compared with 81%–86% for SP and SPt, though this finding requires confirmation in larger series. Post-infectious syringomyelia is associated with the highest revision burden and shortest median shunt survival, warranting heightened postoperative surveillance. Multicenter prospective studies with standardized protocols are required to definitively guide shunt type selection and postoperative management in syringomyelia.

Author contributions

Conceptualization: HJJ. Data curation: HTK, DK. Formal analysis: HTK, HJJ. Investigation: HTK, DK, KHK, JYP, SUK, DKC, KSK. Methodology: HJJ, BJM. Project administration: HJJ. Supervision: DK, BJM, KHK, JYP, SUK, DKC, KSK. Validation: DK, HJJ. Visualization: HTK, HJJ. Writing – original draft: HTK, HJJ. Writing – review & editing: all authors.

Conflict of interest

Bong Ju Moon, a contributing editor of the *Journal of Advanced Spine Surgery*, was not involved in the editorial evaluation or decision to publish this article. All remaining authors have declared no conflicts of interest.

Funding

None.

Acknowledgments

None.

ORCID

Hyung-Tae Kim, https://orcid.org/0009-0004-3890-2146
Dongkyu Kim, https://orcid.org/0000-0001-6509-1167
Bong-Ju Moon, https://orcid.org/0000-0003-1681-9734
Kyung-Hyun Kim, https://orcid.org/0000-0002-1338-5523
Jeong-Yoon Park, https://orcid.org/0000-0002-3728-7784
Sung-Uk Kuh, https://orcid.org/0000-0003-2566-3209
Dong-Kyu Chin, https://orcid.org/0000-0002-9835-9294
Keun-Su Kim, https://orcid.org/0000-0002-3384-5638
Hyun-Jun Jang, https://orcid.org/0000-0001-6063-3510

References

1. Milhorat TH. Classification of syringomyelia. Neurosurg Focus 2000;8:E1.
2. Barnett HJ, Jousse AT. Nature, prognosis and management of posttraumatic syringomyelia. Vol. 1. Major problems in neurology. In: Walton JN, editor. Syringomyelia. WB Saunders; 1973. p. 145-64.
3. Williams B. On the pathogenesis of syringomyelia: a review. J R Soc Med 1980;73:798-806.
4. Greitz D. Unraveling the riddle of syringomyelia. Neurosurg Rev 2006;29:251-63.
5. Schurch B, Wichmann W, Rossier AB. Post-traumatic syringomyelia (cystic myelopathy): a prospective study of 449 patients with spinal cord injury. J Neurol Neurosurg Psychiatry 1996;60:61-7.
6. Brodbelt AR, Stoodley MA. Post-traumatic syringomyelia: a review. J Clin Neurosci 2003;10:401-8.
7. Edgar R, Quail P. Progressive post-traumatic cystic and non-cystic myelopathy. Br J Neurosurg 1994;8:7-22.
8. Klekamp J. Treatment of syringomyelia related to nontraumatic arachnoid pathologies of the spinal canal. Neurosurgery 2013;72:376-89.
9. Klekamp J, Iaconetta G, Batzdorf U, Samii M. Syringomyelia associated with foramen magnum arachnoiditis. J Neurosurg 2002;97(3 Suppl):317-22.
10. Batzdorf U, Klekamp J, Johnson JP. A critical appraisal of syrinx cavity shunting procedures. J Neurosurg 1998;89:382-8.
11. Sgouros S, Williams B. A critical appraisal of drainage in syringomyelia. J Neurosurg 1995;82:1-10.
12. Tator CH, Meguro K, Rowed DW. Favorable results with syringosubarachnoid shunts for treatment of syringomyelia. J Neurosurg 1982;56:517-23.
13. Barbaro NM, Wilson CB, Gutin PH, Edwards MS. Surgical treatment of syringomyelia: favorable results with syringoperitoneal shunting. J Neurosurg 1984;61:531-8.
14. Padovani R, Cavallo M, Gaist G. Surgical treatment of syringomyelia: favorable results with syringosubarachnoid shunting. Surg Neurol 1989;32:173-80.
15. Leschke JM, Mumert ML, Kurpad SN. Syringosubarachnoid shunting using a myringotomy tube. Surg Neurol Int 2016;7(Suppl 1):S8-11.
16. Vernon JD, Silver JR, Symon L. Post-traumatic syringomyelia: the results of surgery. Paraplegia 1983;21:37-46.
17. Carroll AM, Brackenridge P. Post-traumatic syringomyelia: a review of the cases presenting in a regional spinal injuries unit in the north east of England over a 5-year period. Spine (Phila Pa 1976) 2005;30:1206-10.
18. Davidoff CL, Liu S, Wong JH, Koustais S, Rogers JM, Stoodley

MA. Treatment of syringomyelia in patients with arachnoiditis at the craniocervical junction. World Neurosurg 2017;107:565-73.
19. Kaplan EL, Meier P. Nonparametric estimation from incomplete observations. J Am Stat Assoc 1958;53:457-81.
20. Cox DR. Regression models and life-tables. J R Stat Soc Ser B Methodol 1972;34:187-220.
21. Klekamp J, Batzdorf U, Samii M, Bothe HW. Treatment of syringomyelia associated with arachnoid scarring caused by arachnoiditis or trauma. J Neurosurg 1997;86:233-40.
22. Isik N, Elmaci I, Isik N, et al. Long-term results and complications of the syringopleural shunting for treatment of syringomyelia: a clinical study. Br J Neurosurg 2013;27:91-9.

https://doi.org/10.63858/jass.26.0034

Technical Note

J Adv Spine Surg 2026;16(1):41-45
https://doi.org/10.63858/jass.26.0028
pISSN 2234-0637 • eISSN 3140-0663

JASS
Journal of Advanced Spine Surgery

External Femoral Traction for Reduction of Traumatic Lumbar Spondyloptosis: A Technical Note

Christina Gerges Castro, M.D.[1], Isaac Lapite, M.D.[2], Jonathan Kark, M.D.[2], James M. Wright III, M.D.[1]

[1]Department of Neurological Surgery, Oregon Health & Science University, Portland, OR, USA
[2]Department of Orthopaedics and Rehabilitation, Oregon Health & Science University, Portland, OR, USA

Traumatic lumbar spondyloptosis is a rare entity associated with high-velocity mechanisms and is the most severe form of lumbar spondylolisthesis. Operative management is often required; however, the relative merits of reduction versus in situ fusion remain debated, largely owing to the technical difficulty of attaining satisfactory fracture reduction. In this report, we describe external femoral traction as a novel technique for closed reduction of traumatic lumbar spondyloptosis. A 27-year-old man presented after a tree he was cutting fell on him and was found to have T3–7 AO Spine (AOS) A1 fracture, L3 AOS B2 fracture, and L5 AOS C fracture. Neurologic exam was consistent with multilevel nerve root injury. Definitive treatment included bilateral femoral traction, open reduction, and combined anterior/posterior fixation. A multidisciplinary team including orthopedic surgery, plastic surgery, vascular surgery, and neurosurgery were involved. Complete reduction was obtained, and the patient experienced near-complete resolution of neurologic symptoms. This technique offers a unique solution to the challenge of traumatic lumbar spondyloptosis. Further study and follow-up are needed to confirm the utility and durability of this technique and the cranial extent of injury for which this technique might be applied.

Keywords: Spinal injuries/surgery, Spondylolisthesis/surgery, Lumbar vertebrae/injuries, Spinal fusion/methods

Introduction

Traumatic lumbar spondyloptosis is a rare entity associated with high velocity mechanisms and is the most severe form of lumbar spondylolisthesis (Meyerding Grade V).[1-3] Patients often present with significant polytrauma and may experience back pain, spinal deformity, or neurologic deficits of variable severity. Operative management is required for reduction and stabilization. The primary operative technique previously described in the literature included open reduction with osteotomies and internal fixation.[1,4-7] A single 2013 study reported closed reduction of traumatic spondyloptosis using lumbar hyperextension and full torso longitudinal traction followed immediately by open internal fixation.[3] To date, no other reports regarding external reduction of traumatic lumbar spondyloptosis exist. In this report, we describe an external femoral traction as a novel technique for closed reduction of traumatic lumbar spondyloptosis.

A 27-year-old man presented to the emergency room as a trauma activation after a tree he was cutting fell on him. On initial neurosurgical evaluation, he was found to have bilateral hip flexion weakness (motor score 3/5 bilaterally), minimal movement in ankle dorsiflexion and plantar flexion (motor score 1/5 bilaterally), and diminished sensation to light touch in bilateral S1 dermatomes. Foley catheterization was required for urinary reten-

Received: February 27, 2026; Revised: April 29, 2026; Accepted: May 15, 2026
Corresponding author: Christina Gerges Castro, M.D.
Department of Neurological Surgery, Oregon Health & Science University, 3181 SW Sam Jackson Park Rd., Portland, OR 97239, USA
TEL: +1-503-494-4314, FAX: +1-503-346-6810, E-mail: Gerges@ohsu.edu

tion. Rectal tone was spared. Computed tomography (CT) of the spine demonstrated T3–7 AO Spine (AOS)[8] A1 fracture, L3 AOS B2 fracture, and L5 AOS C fracture (Fig. 1). Vascular imaging of the abdomen was obtained due to significant risk of large vessel injury with this pathology, although no vascular injury was noted. Magnetic resonance imaging (MRI) of the spine was subsequently obtained (Fig. 2). A waiver of informed consent was granted due to the absence of patient identifiers.

Technical Note

1. Initial approach

An initial attempt at standard open reduction was performed, including facetectomies, discectomies, and the use of reduction towers with posterior segmental instrumentation extending from T12 to the pelvis. This upper instrumented vertebra was selected to bypass the thoracolumbar junction and provide a stable proximal anchor in the setting of a high-grade L5 AOS C-type fracture with a long lever arm and multilevel injury. Unfortunately, the reduction could not be maintained. Traumatic durotomies sustained at the time of injury were repaired primarily, followed by a muscle graft and dural sealant. Postoperative CT imaging demonstrated persistent L5–S1 spondyloptosis, with the L5 vertebral body remaining ventral to the sacrum (Fig. 3). The patient was subsequently returned to the operating room for a reduction attempt using femoral traction.

2. Distal femoral traction

The patient was positioned supine on the operating room table and was sterilely prepared and draped. A sterile 2.0-mm Kirschner wire was selected from the skeletal traction tray and advanced percutaneously through the distal femoral metaphysis from lateral to medial using a motorized wire driver. Care was taken to ensure a tension-free skin exit site. The sharp ends were protected, the Kirschner traction bow was attached to the wire, and 40 pounds of longitudinal traction was placed on each extremity using rope, sandbags, and a pulley system.

3. Revision fusion and spondyloptosis reduction

The previous incision was opened. The previous rods were temporarily removed. The L5 level was identified, and the facet and disrupted pedicle remnant were removed with Leksell rongeurs with care to protect the traversing and exiting roots. A Cobb elevator was inserted to distract across the disc space; however, reduc-

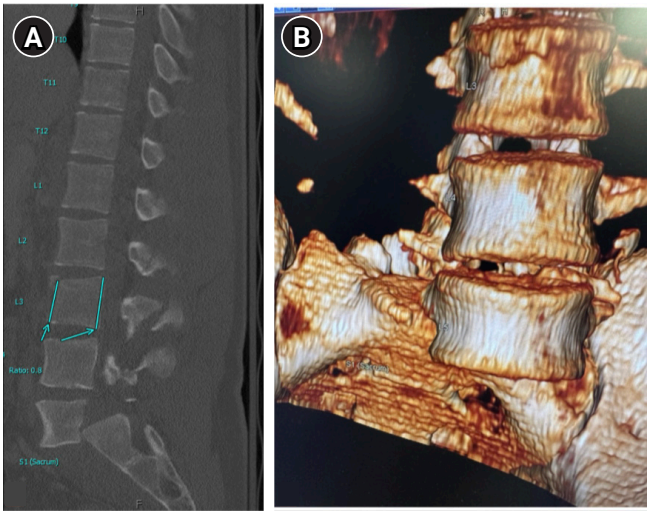

Fig. 1. (A) Sagittal computed tomography (CT) image at the time of presentation demonstrating L3 AO Spine B2 fracture, and L5 spondyloptosis. (B) 3-D reconstruction of CT imaging demonstrating anterior inferior displacement of the L5 vertebral body over the sacrum.

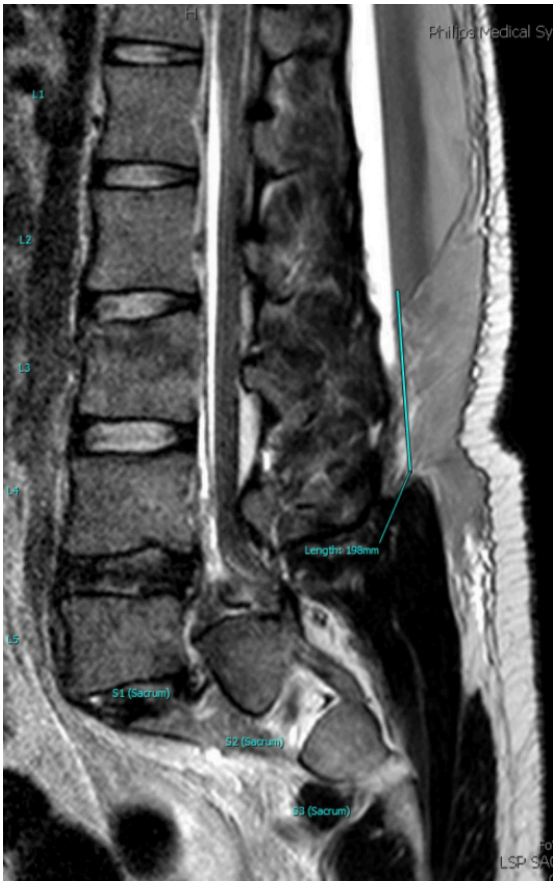

Fig. 2. Sagittal T2 sequence magnetic resonance imaging redemonstrating L3 AO Spine (AOS) B2 fracture and L5 AOS C fracture.

https://doi.org/10.63858/jass.26.0028

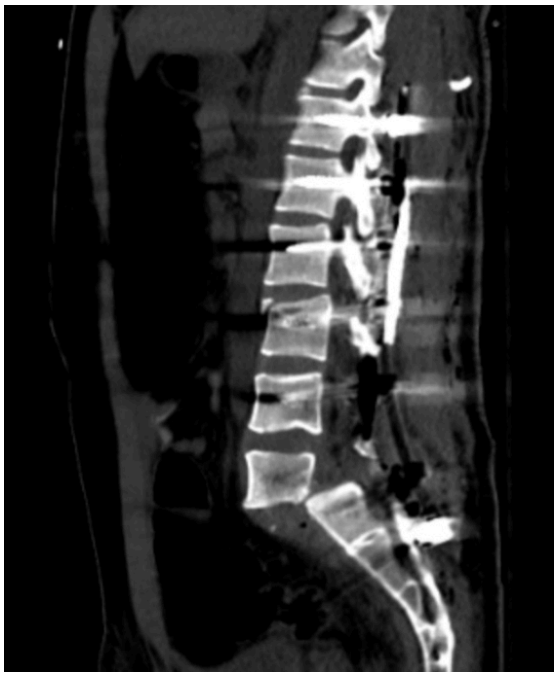

Fig. 3. Sagittal computed tomography demonstrating initial unsuccessful attempt at open reduction.

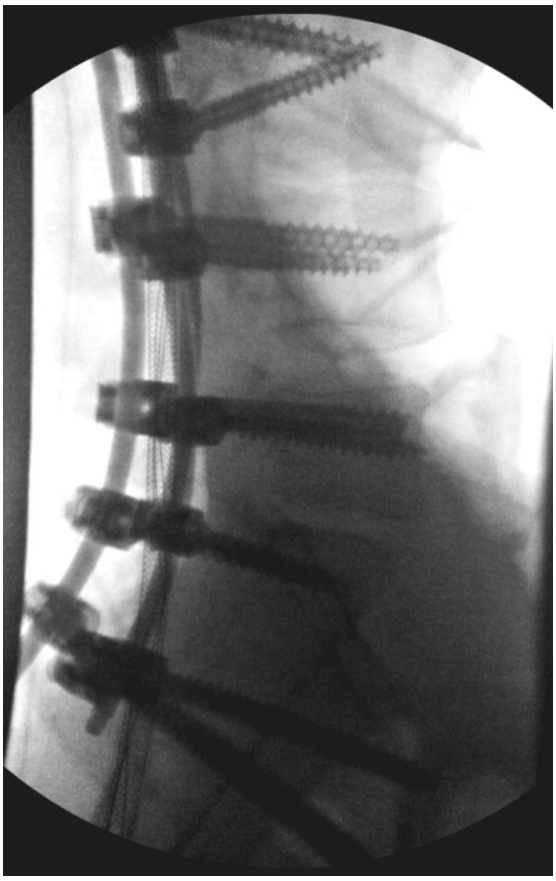

Fig. 4. Intraoperative X-ray taken after spondyloptosis reduction and posterior instrumentation.

tion was achieved almost entirely through the application of longitudinal traction rather than manual manipulation. A temporary rod was placed from L4–S1 on the right. An appropriately contoured rod was positioned on the left side to span the entirety of the construct, and set caps were applied and sequentially tightened to preserve the achieved reduction. The temporary right-sided rod was subsequently removed and replaced with an appropriately sized and contoured rod, after which the set caps were placed and fully tightened. Upon completion of posterior fixation, the 40-pound sandbags were removed from the traction pulley system.

A lumbar drain was placed at the L3–4 interspace under direct visualization and secured. Fusion allograft and autograft material were placed over the lamina, facets, and transverse processes of the instrumented levels. Complex spine closure was performed by a plastic surgeon. Hardware disposition following this portion of the procedure is available in Fig. 4.

4. Anterior lumbar interbody fusion

Following closure, the patient was rotisserie-flipped for an anterior approach. A vascular surgeon exposed the anterior lumbar spine from L4–S1. Discectomy was completed at L5/S1 using standard techniques. A trial was sized. Using fluoroscopic guidance, an anterior lumbar interbody fusion cage was placed and secured. This process was repeated at L4–5 to augment the adjacent segment, improve load sharing, and enhance construct stability across the lumbosacral junction. The anterior incision was then closed. Final hardware disposition is available in Fig. 5.

5. Removal of traction pin

The pin was cut with the skin on one end. It was cleaned with chlorhexidine and pulled through the contralateral end carefully.

6. Postoperative course

A pseudomeningocele was appreciated on MRI (Fig. 6). The lumbar drain was weaned and eventually removed. Following an uneventful postoperative course, the patient was discharged to an inpatient rehabilitation facility with residual bilateral foot drop and urinary retention requiring regular straight catheterization. At the 6-week postoperative visit, all urinary symptoms had resolved. By the 1-year postoperative visit, his foot drop had resolved bilaterally. He was ambulatory without ankle-foot orthotics with no bladder or bowel symptoms. His only residual symptoms currently are minimal back pain and bilateral foot numbness.

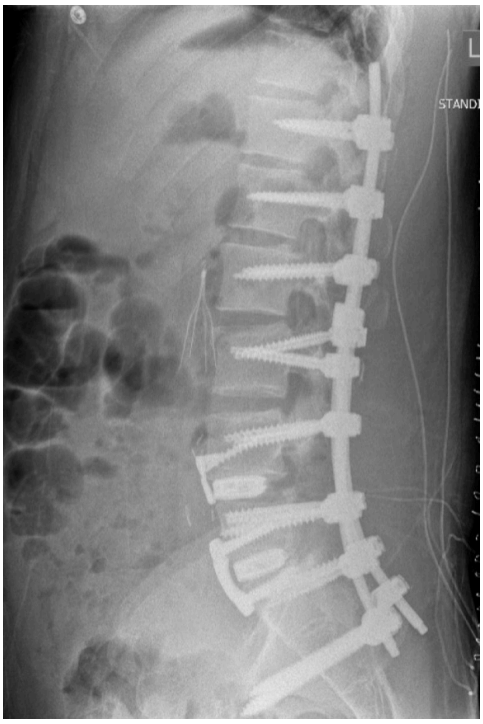

Fig. 5. Postoperative X-ray demonstrating final hardware disposition (L4/5, L5/S1 anterior lumbar interbody fusion and T12-pelvis posterior segmental fusion).

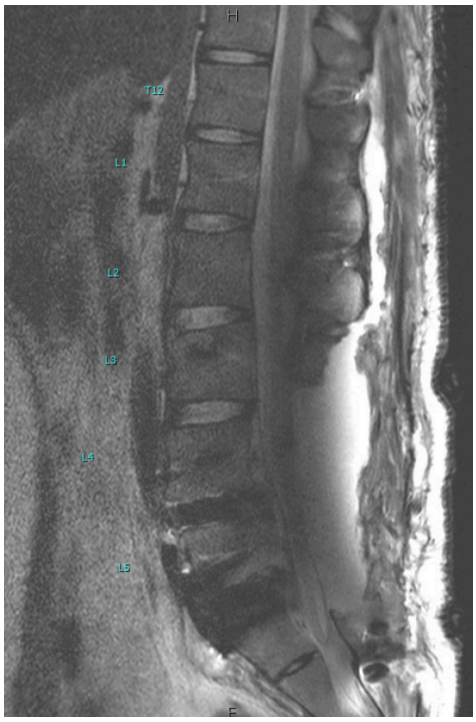

Fig. 6. Postoperative sagittal T2 orthopedic-metal artifact reduction sequence magnetic resonance imaging demonstrating pseudomeningocele secondary to durotomies sustained at the time of injury.

Discussion

Lumbar spondyloptosis represents one of the most extreme forms of translational spinal instability. Given the scarcity of high-quality evidence, there remains no consensus for optimal surgical management. Reduction is technically demanding and includes restoration of alignment, decompression of neural elements, and fixation across a severely destabilized segment. In traumatic cases of spondyloptosis, early reduction and fusion have been associated with significant improvements in patient-reported pain, disability scores, and radiographic alignment. Xu et al.[4] and Zhou et al.[9] reported complete reduction and fusion in traumatic lumbar spondyloptosis, with patients achieving pain relief, neurologic improvement, restored alignment, and solid bony fusion.

In situ fusion has been proposed as an alternative when in chronic spondyloptosis or when reduction is not feasible or deemed unsafe. No reports of in situ fusion with or without decompression for acute traumatic spondyloptosis were identified. Wangtaphan et al.[10] and Emel et al.[11] described cases of delayed presentation of traumatic lumbosacral spondyloptosis wherein in situ fusion was performed, resulting in improved back pain and bony fusion at the level of injury. While in situ fusion avoids risks associated with reduction maneuvers, it has several drawbacks, including persistent deformity and potential for chronic pain related to malalignment. Additionally, fusion without reduction may compromise the ability to achieve robust biomechanical fixation, increasing the risk of pseudarthrosis, although this has not been reported for this pathology.

In this technical note, we describe the novel application of bilateral femoral traction as an adjunctive method for achieving controlled reduction of lumbar spondyloptosis prior to posterior fixation. The biomechanical rationale for femoral traction lies in the ability to generate longitudinal distraction across the lumbosacral junction, counteracting the anterior shearing vector that is characteristic of the pathology. By applying traction through bilateral femoral pins, realignment may be achieved through ligamentotaxis and soft-tissue tensioning. This can decrease the need for forceful intraoperative manipulation, restore relative anatomical orientation, and facilitate subsequent instrumentation.

While skeletal traction has been described for cervical and thoracic spondyloptosis and spinopelvic dissociation, its use in the lumbosacral spine remains rarely reported.[3,12-14] To our knowledge, the use of femoral traction as a reduction maneuver for this pathology has not been described in the literature.

This technique offers several practical advantages. It allows

https://doi.org/10.63858/jass.26.0028

controlled, titratable traction using readily available equipment. It can be performed with the patient in the supine or prone position, depending on the planned surgical approach. It enables continuous radiographic monitoring to gauge reduction progress and tissue response. Furthermore, by restoring partial alignment prior to exposure, traction can facilitate localization, instrumentation, and reduction maneuvers during definitive fixation.

However, several precautions and limitations should be emphasized. Excessive or rapid traction may risk neurovascular injury, particularly stretch injury to the lumbosacral plexus or compromise of iliac and femoral vessels. Importantly, traction is not a substitute for definitive stabilization; rather, it is an adjunct to facilitate safer and more controlled alignment restoration.

In summary, femoral traction provides a simple and reproducible adjunct for the reduction of traumatic lumbar spondyloptosis. When applied judiciously under imaging guidance, it may enhance the safety and efficiency of subsequent open reduction and fixation. Future studies and accumulation of technical experience are needed to better define patient selection criteria, optimal traction parameters, and long-term outcomes associated with this approach.

This technique offers a unique solution to the challenge of traumatic lumbar spondyloptosis. Further study and follow-up are needed to confirm the utility and durability of this technique and the cranial extent of injury for which this technique might be applied.

Author contributions

Conceptualization: CGC, JK, JMW. Methodology: CGC, IL. Supervision: JK, JMW. Writing – original draft: CGC. Writing – review & editing: IL, JK, JMW.

Conflict of interest

The authors have no conflicts of interest to declare.

Funding

None.

Acknowledgments

None.

ORCID

Christina Gerges Castro, https://orcid.org/0000-0001-6858-0636
Isaac Lapite, https://orcid.org/0000-0002-4706-1076
Jonathan Kark, https://orcid.org/0000-0003-0363-401X
James M. Wright III, https://orcid.org/0000-0002-4482-7582

References

1. Braithwaite J, Gruber J, Fakhoury J, Katsigiorigis G, Grewal K. Acute traumatic spondyloptosis: a case report. Cureus 2023;15:e36457.
2. Meyerding HW. Spondylolisthesis. Surg Gynecol Obstet 1932;54:371-7.
3. Francis T, Steinmetz M, Moore T. Traumatic spondyloptosis of the lumbar spine: closed reduction and internal fixation. Spine (Phila Pa 1976) 2013;38:E1636-40.
4. Gautam S, Tamang RS, Joshi K, Bhusal S, Shrestha R. Surgical management of traumatic spondyloptosis: a case series. J Med Case Rep 2024;18:468.
5. Xu F, Tian Z, Fu C, et al. Mid-lumbar traumatic spondyloptosis without neurological deficit: a case report and literature review. Medicine (Baltimore) 2020;99:e19578.
6. Amesiya R, Orwotho N, Nyati M, Mugarura R, Mwaka ES. Traumatic spondyloptosis of the lumbar spine: a case report. J Med Case Rep 2014;8:453.
7. Akesen B, Mutlu M, Kara K, Aydinli U. Traumatic lumbosacral spondyloptosis: a case report and review of the literature. Global Spine J 2014;4:59-62.
8. Vaccaro AR, Oner C, Kepler CK, et al. AO Spine thoracolumbar spine injury classification system: fracture description, neurological status, and key modifiers. Spine (Phila Pa 1976) 2013;38:2028-37.
9. Zhou TH, Tang X, Xu YQ, Zhu YL. Traumatic spondyloptosis of L4. Spine (Phila Pa 1976) 2010;35:E855-9.
10. Wangtaphan W, Oo M, Paholpak P, Wang Z, Sakakibara T, Kasai Y. Traumatic lumbosacral spondyloptosis treated five months after injury occurrence: a case report. Spine (Phila Pa 1976) 2012;37:E1410-4.
11. Emel E, Ozer F, Karagoz Guzey F, Alatas I, Guzey D. Lumbosacral spondyloptosis treated by two-staged fusion in situ operation: a case report. Turk Neurosurg 2006;16:145-9.
12. Ramieri A, Domenicucci M, Cellocco P, Lenzi J, Dugoni DE, Costanzo G. Traumatic spondylolisthesis and spondyloptosis of the subaxial cervical spine without neurological deficits: closed re-alignment, surgical options and literature review. Eur Spine J 2014;23 Suppl 6:658-63.
13. Anokwute MC, House H, Huh A, Ordaz J, McVeigh L, Stockwell DW. Systematic review of traumatic thoracic spondyloptosis and presentation of a novel approach for management with quad rod construct. Oper Neurosurg 2022;23:e237-44.
14. Williams SK, Quinnan SM. Percutaneous lumbopelvic fixation for reduction and stabilization of sacral fractures with spinopelvic dissociation patterns. J Orthop Trauma 2016;30:e318-24.

Case Report

J Adv Spine Surg 2026;16(1):46-50
https://doi.org/10.63858/jass.26.0023
pISSN 2234-0637 • eISSN 3140-0663

JASS
JOURNAL OF ADVANCED SPINE SURGERY

Chondroma in Lumbar Region Misdiagnosed as Herniated Disc: A Case Report

Hyoung Bin Kim, M.D., Byung Kwan Choi, M.D., In Ho Han, M.D., Dong Hwan Kim, M.D.

Department of Neurosurgery and Medical Research Institute, Pusan National University Hospital, Pusan National University School of Medicine, Busan, Korea

Chondroma is a benign cartilaginous neoplasm, rarely encountered in the lumbar spine. We report a case involving a 70-year-old female who presented with lower limb radiating pain that started four years ago. Although no pronounced muscle weakness was noted, the patient experienced progressively worsening radiating pain in the L4 dermatome. Initial evaluation, including magnetic resonance imaging (MRI) performed at another medical facility, suggested a potential lesion associated with left L4–5 lumbar disc herniation. Despite non-surgical interventions, the patient experienced limited symptomatic relief, prompting her to seek further care at our clinic. Subsequent contrast-enhanced MRI conducted at our facility revealed a mass exhibiting peripheral rim enhancement surrounding the L4 nerve root. Suspecting a neurogenic tumor, we decided to perform surgical excision of the mass. Postsurgery, histopathological analysis confirmed the presence of hyaline cartilage with lobular architecture and chondrocytes in lacunae, leading to the conclusive diagnosis of chondroma. Following the surgical procedure, the previously reported radiating pain exhibited notable improvement.

Keywords: Lumbar vertebrae, Intervertebral disc displacement, Chondroma, Magnetic resonance imaging

Introduction

Chondroma, a benign tumor originating in cartilaginous structures, presents a distinctive challenge in medical diagnosis. Although it can potentially manifest in any bone structure, its primary occurrence is observed in the long bones of the hands and feet.[1] The incidence rate is exceptionally low, making the diagnosis of chondroma in the lumbar spine particularly challenging. This challenge is exacerbated by the infrequent utilization of contrast-enhanced gadolinium imaging, especially in patients presenting with symptoms such as back pain and radiating discomfort in the lower extremities. This report describes a case of chondroma in the lumbar region of a 70-year-old female who presented with radiating pain in her lower extremities.

Case Report

A 70-year-old female with osteoporosis presented with a history of low back pain accompanied by numbness in her left lower extremities persisting for the past 4 years. The patient reported severe radiating pain localized to the left L4 sensory dermatome, exacerbated by walking. Notably, there was no observed motor weakness upon neurological examination. A magnetic resonance imaging (MRI) obtained at another medical facility approximately

Received: December 18, 2025; Revised: February 24, 2026; Accepted: March 17, 2026
Corresponding author: Dong Hwan Kim, M.D.
Department of Neurosurgery and Medical Research Institute, Pusan National University Hospital, Pusan National University School of Medicine, 179 Gudeok-ro, Seo-gu, Busan 49241, Korea
TEL: +82-51-240-7257, FAX: +82-51-244-0282, E-mail: smile0402@hanmail.net

eight months before admission indicated a suspected far lateral disc on the left side of the lumbar 4/5 region.

The patient underwent a left L4–5 transforaminal epidural block, which resulted in only 10 days of temporary relief. Subsequent contrast-enhanced MRI conducted at our hospital revealed a benign neurogenic tumor with cystic degeneration. The tumor demonstrated high signal intensity on T2-weighted imaging, low signal intensity on T1-weighted imaging, and peripheral enhancement on gadolinium-enhanced MRI. Measuring approximately 8 mm in size, the mass displayed a well-defined round shape and was located at the left neural foramen of the L4–5 level, causing severe compression of the left exiting L4 nerve root or potentially arising from the L4 nerve root (Fig. 1).

Subsequently, a surgical intervention involving L4–5 left facetectomy and complete gross resection of the extradural mass was performed, suspecting a neurogenic tumor. In the surgical field, a well-marginated yellowish mass was discovered beneath the L4 root (Fig. 2). Histopathological examination confirmed the diagnosis of chondroma (Fig. 3).

Immediately postoperation, the radiating pain in the L4 dermatome exhibited improvement, and the patient was discharged without any complications.

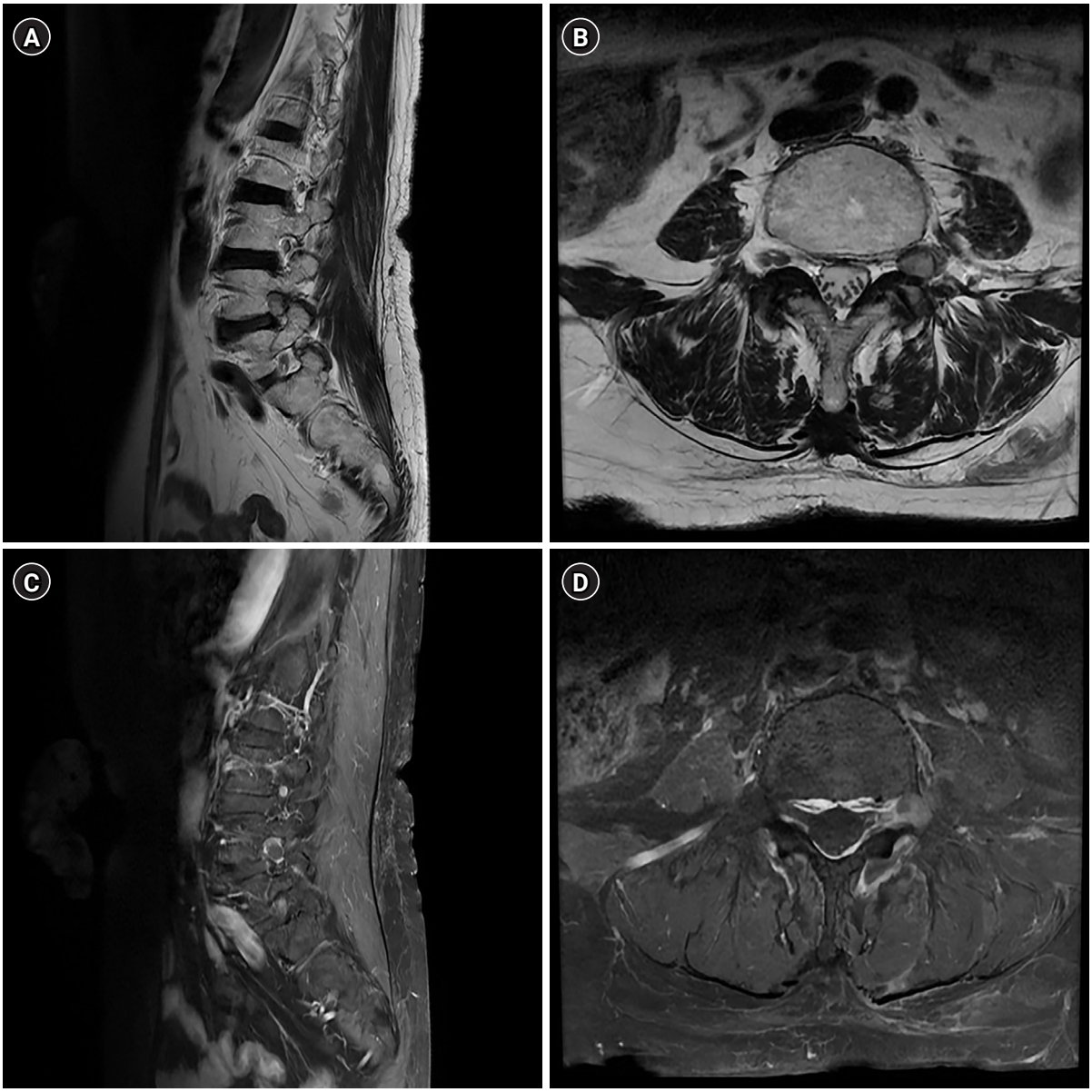

Fig. 1. Magnetic resonance finding of the tumor. (A) The tumor-like lesion demonstrated high signal intensity on T2-weighted imaging. (B) Low signal intensity on T1-weighted imaging. (C, D) Peripheral enhancement on T1-enhancement imaging.

Discussion

Chondroma, constituting 5% of all bone tumors, is the most prevalent cartilaginous tumor.[1,2] While its typical occurrence is in the long bones of the hands and feet, it can manifest in uncommon sites such as the ribs, pelvis, and spine. Notably, spinal chondromas are exceptionally rare, accounting for approximately 3% of all chondromas.[1] Symptomatic chondromas within the lumbar spine are particularly scarce, with only 22 reported cases (Table 1).[1-16]

Chondroma can be categorized based on their location into enchondromas (within the medullary cavity), periosteal chondromas (developing within and beneath periosteal connective tissue), and soft tissue chondromas, also referred to as synovial chondromas (found in extra-osseous and extra-synovial soft tissue regions).[3,17]

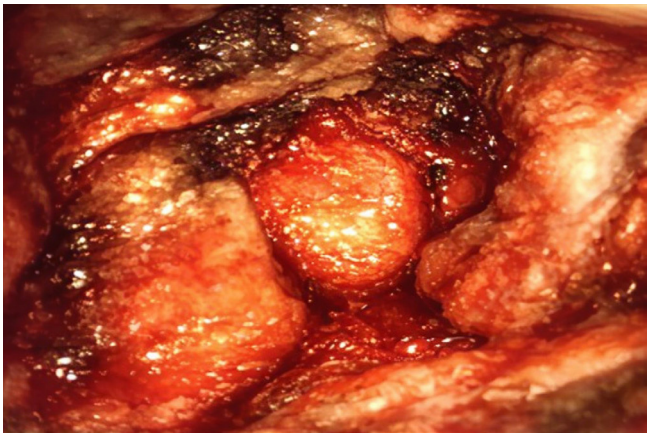

Fig. 2. In the surgical field, a well-marginated yellowish mass beneath the L4 root.

Therefore, distinguishing between periosteal and soft tissue chondromas becomes challenging when a chondroma is located extradural in the spinal canal. In our case, the mass is identified as a soft tissue chondroma due to its extra-osseous location.

Depending on the tumor's location, various neurological signs and symptoms may arise. Spinal chondromas can invade the vertebral body, pedicle, lamina, and transverse/spinous processes, leading to radiculopathy, as observed in this case, or myelopathy if cord compression occurs.[4] In our literature review, the neural arch was the most commonly affected location, with back pain and radiculopathy being the predominant associated symptoms in the lumbar spine.

The duration of symptoms before chondroma diagnosis varied, ranging from days to years, attributed to its slow-growing pattern and frequent misdiagnosis. The clinical characteristics, such as an acute onset of back pain with leg pain, closely mimic those of lumbar disc herniation, as demonstrated in our case. The absence of routine use of gadolinium in cases of lumbar radiculopathy contributes to the exclusion of spinal chondroma from diagnostic considerations in these patients. Even with contrast-enhanced MRI, the lesion is often initially misinterpreted as a neurogenic or dumbbell tumor extending into the foramen and extraforaminal area rather than a rare chondroma. Therefore, spinal chondroma is unlikely to be considered initially. Nonetheless, the aforementioned findings suggest the value of administering contrast to rule out this pathology in patients with lumbar disc herniation exhibiting unusual characteristics, such as inadequate response to treatment or foraminal-extraforaminal location.

Although these findings were not observed on computed tomography (CT) in the present study, in some reported cases CT

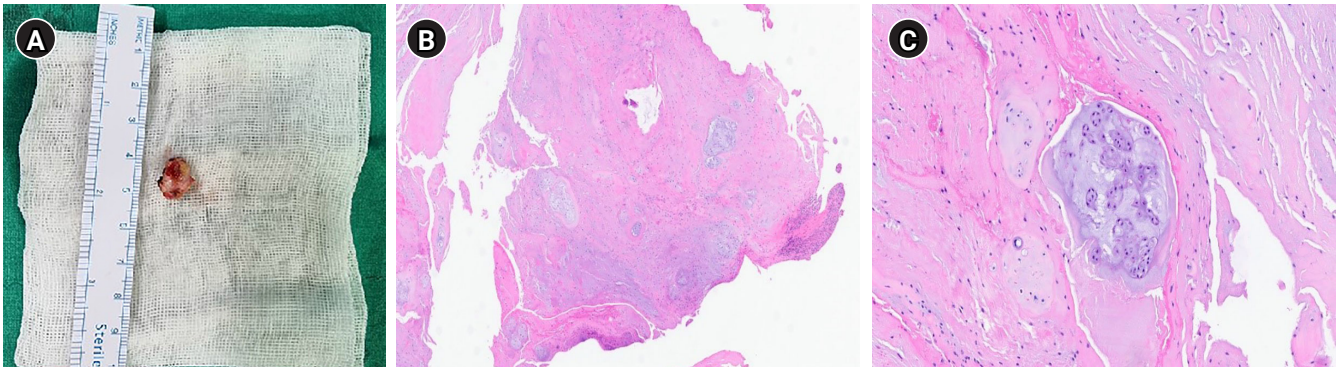

Fig. 3. Biopsy finding. (A) Hyaline cartilage with lobular architecture, separated by fibrous bands (foci of calcification). (B, C) Histopathological examination with hematoxylin and eosin (H&E) staining revealed chondrocytes within lacunae showing uniform nuclei without atypia, with focal binucleation (B: ×40, C: ×200).

https://doi.org/10.63858/jass.26.0023

Table 1. Reported cases of symptomatic lumbar spine chondromas

Study	Age (years)	Sex	Clinical presentation	Symptoms duration	Site	Origin
Pittoni et al.[6] (1928)[a]	25	M	Swelling	8 months	L1	Not reported
Peycelon et al.[6] (1936)[a]	12	M	Swelling	6 months	L1	Spinous processes
Godlewski et al.[6] (1960)[a]	56	F	Cord compression	8 months	L1	Vertebral body
Paillas et al.[6] (1963)[a]	40	M	Swelling	Not reported	L5	Neural arch
	12	M	Pain	24 months	L1	Neural arch
De Mourgues et al.[6] (1964)[a]	34	M	Swelling	Not reported	L2	Neural arch
Nag and Falconer[7] (1966)	50	M	Sciatica	30 months	L4	Vertebral body
Herndon and Cohen[8] (1970)	10	F	Sciatica	24 months	L4	Vertebral body
Bell[6] (1971)	25	M	Pain, swelling	5 days	L1–L2	Neural arch
Bland and McDonald[5] (1990)	36	M	Sciatica	5 months	L3–L4	Neural arch
Gaetani et al.[9] (1996)	44	M	Sciatica	18 months	L4	Neural arch
Erten et al.[10] (1999)	35	M	Sciatica	2 years	L5–S1	Neural arch
Motooka et al.[11] (2002)	66	M	Sciatica	Not reported	L5	Neural arch
Ogata et al.[12] (2007)	77	M	Cord compression	1 month	L3	Neural arch
Cetinkal et al.[13] (2008)	54	F	Cord compression	3 years	L2	Neural arch
Cho et al.[3] (2009)	49	F	Sciatica	2 weeks	L2	Neural arch
Kim et al.[1] (2013)	47	F	Cord compression	1 week	L2	Neural arch
Pace et al.[14] (2014)	46	F	Cord compression	3 weeks	L3	Neural arch
Thien et al.[4] (2014)	56	F	Cord compression	2 months	L3	Neural arch
Esteves et al.[15] (2018)	52	M	Cord compression	1 week	L2–L3	Neural arch
Kim et al.[16] (2020)	74	F	Sciatica	1 year	L2–L3	Neural arch
Robles and Mundis[2] (2021)	57	M	Cord compression	2 weeks	L4	Neural arch
Present case	70	F	Sciatica	4 years	L4	Neural arch

Modified from Kim et al. Korean J Spine 2013;10:252-4[1], according to Creative Commons license. [a]Cited by Bell (1971)[6].

has demonstrated calcification or focal bony destruction, thereby aiding in the assessment of the relationship between the tumor and adjacent osseous structures. MRI is valuable for evaluating soft tissue extension and confirming the diagnosis.[18] Chondromas typically exhibit low signal intensity in T1-weighted images, high signal intensity in T2-weighted images, and peripheral enhancement with gadolinium contrast in MRI.[4,19] Without contrast enhancement, differentiation from disc herniation based solely on symptoms and imaging findings can be challenging. Furthermore, even with contrast-enhanced imaging, distinguishing it from nerve sheath tumors can be difficult if the findings are non-specific, and the mass shows enhancement along the neural foramen.[3,4] According to previous reports, sequestrated disc fragments may demonstrate varying degrees of peripheral rim enhancement, depending on the extent of adjacent angiogenesis and granulation tissue formation resulting from the associated inflammatory response.[20] Therefore, biopsy remains indispensable for an accurate diagnosis. Histopathological findings of chondroma typically reveal chondrocytes arranged in a pseudolobular fashion and may be associated with ossified regions.[5]

Despite the scarcity of reported cases and the absence of known malignant transformations, surgical resection is recommended for patients with uncontrolled pain, neurological deficit, or accelerated growth.

Spinal chondroma is an exceedingly uncommon condition characterized by a paucity of symptoms. However, when symptoms manifest, differentiating it from nerve sheath tumors and disc herniation can be challenging. Consequently, it is imperative to consider chondroma as a potential differential diagnosis, especially when contrast-enhanced MRI reveals peripheral rim enhancement, characteristic of this lesion.

Author contributions

Project administration: DHK. Supervision: DHK. Visualization: IHH. Resources: BKC. Writing – original draft: HBK, DHK. Writing – review & editing: HBK, DHK.

Conflict of interest

The authors have no conflicts of interest to declare.

Funding

None.

Acknowledgments

This work was supported by clinical research grant in 2022.

ORCID

Hyoung Bin Kim, https://orcid.org/0009-0005-1398-9764
Byung Kwan Choi, https://orcid.org/0000-0001-5244-4592
In Ho Han, https://orcid.org/0000-0001-7193-6533
Dong Hwan Kim, https://orcid.org/0000-0001-8982-7917

References

1. Kim DH, Nam KH, Choi BK, Han I. Lumbar spinal chondroma presenting with acute sciatica. Korean J Spine 2013;10:252-4.
2. Robles LA, Mundis GM. Chondromas of the lumbar spine: a systematic review. Global Spine J 2021;11:232-9.
3. Cho HJ, Shim JC, Kim HK, et al. A soft tissue chondroma originating from the dura mater of the lumbar spinal canal and it mimicked a nerve sheath tumor: a case report with the MR imaging. J Korean Soc Radiol 2009;60:221-5.
4. Thien A, Teo CH, Lim CC, Karandikar A, Dinesh SK. Soft tissue chondroma mimicking "dumbbell" neurogenic tumour: a rare cause of lumbar radiculopathy. J Clin Neurosci 2014;21:1073-4.
5. Bland LI, McDonald JV. Chondroma of the lumbar spine, a rare cause of sciatica: case report. Neurosurgery 1990;26:685-7.
6. Bell MS. Benign cartilaginous tumours of the spine: a report of one case together with a review of the literature. Br J Surg 1971;58:707-11.
7. Nag TK, Falconer MA. Enchondroma of the vertebral body: report of a case causing bilateral sciatica. Br J Surg 1966;53:1067-71.
8. Herndon JH, Cohen J. Chondroma of a lumbar vertebral body in a child: an unusual tumor resembling a chordoma. J Bone Joint Surg Am 1970;52:1241-7.
9. Gaetani P, Tancioni F, Merlo P, Villani L, Spanu G, Baena RR. Spinal chondroma of the lumbar tract: case report. Surg Neurol 1996;46:534-9.
10. Erten SF, Kocak A, Mizrak B, Kutlu R, Colak A. An end-plate chondroma mimicking calcified lumbar disc herniation: a case report and review of the literature. Neurosurg Rev 1999;22:145-8.
11. Motooka Y, Kondoh T, Kurihara E, Tamaki N. Chondroma of the lumbar spinal canal: a case report. No To Shinkei 2002;54:347-51.
12. Ogata T, Miyazaki T, Morino T, Nose M, Yamamoto H. A periosteal chondroma in the lumbar spinal canal: case report. J Neurosurg Spine 2007;7:454-8.
13. Cetinkal A, Guven G, Topuz AK, Colak A, Demircan MN, Haholu A. Lumbar spinal chondroma presenting with radiculopathy: case report. Turk Neurosurg 2008;18:397-9.
14. Pace J, Lozen AM, Wang MC, Cochran EJ. Extradural chondroma presenting as lumbar mass with compressive neuropathy. J Craniovertebr Junction Spine 2014;5:131-3.
15. Esteves S, Catarino I, Quesado M, Lopes D, Sousa C. Acute paraparesis due to a lumbar spinal chondroma: case report and review of the literature. SciFed J Bone Spine 2018;1:1.
16. Kim YG, Kim TW, Kim EJ, Park KH. Extradural chondroma on the lumbar spine: a case report. Nerve 2020;6:86-8.
17. Fletcher CD, Unni KK, Martens F. Pathology and genetics of tumours of soft tissue and bone. IARC Press; 2002.
18. Walden MJ, Murphey MD, Vidal JA. Incidental enchondromas of the knee. AJR Am J Roentgenol 2008;190:1611-5.
19. Ropper AE, Cahill KS, Hanna JW, McCarthy EF, Gokaslan ZL, Chi JH. Primary vertebral tumors: a review of epidemiologic, histological, and imaging findings, part I: benign tumors. Neurosurgery 2011;69:1171-80.
20. Jeong G, Park H, Lee SJ, Park DH, Paeng SH, Lee E. Imaging of sequestered lumbar discs. J Korean Soc Radiol 2024;85:3-23.

https://doi.org/10.63858/jass.26.0023

Case Report

J Adv Spine Surg 2026;16(1):51-55
https://doi.org/10.63858/jass.26.0025
pISSN 2234-0637 • eISSN 3140-0663

JASS
JOURNAL OF ADVANCED SPINE SURGERY

Unresolved Chronic Epidural Hematoma with Burst Fracture Mimicking Malignancy in a Patient with Paraplegia: A Case Report

Geon-Hwee Jeon, M.D., Seung-Hwan Yoon, M.D., Ph.D., Dal-Sung Ryu, M.D.

Department of Neurosurgery, Inha University College of Medicine, Incheon, Korea

The incidence of compression fractures is increasing in aging populations. Differentiating pathological fracture types is complex and requires careful consideration during diagnosis. This case report describes the clinical course of a 54-year-old female patient presenting with progressive paraplegia after a back injury sustained while lifting a heavy object. Initial imaging revealed a burst fracture at T12 and severe spinal cord compression due to an epidural mass extending from T12 to L2. Clinical assessment raised suspicions of a hematologic malignancy or pathological fractures. Laminectomy and spinal fusion, along with mass removal, resulted in partial improvement in motor function and patient-reported pain levels. However, further evaluation and biopsy revealed chronic inflammation with fibrosis consistent with an unresolved hematoma. This case underscores the importance of a comprehensive differential diagnosis and multidisciplinary collaboration, integrating radiologic, surgical, and pathologic correlation, in the management of complex spinal pathologies.

Keywords: Hematoma, Arachnoiditis, Compression fractures, Neoplasm metastasis, Paraplegia

Introduction

Compression fractures of the spine can have various etiologies, including trauma, osteoporosis, and malignancy.[1,2] The incidence of compression fractures is increasing with rapidly aging populations.[1] Although high-energy impacts can lead to traumatic fractures, even minor trauma causes fractures in individuals with osteoporosis.[1] Additionally, spinal column metastasis can lead to compression fractures.[2] Previous studies have reported that approximately 5.5% of vertebral compression fractures (VCFs) are related to malignancy, as identified by routine biopsy, including both metastatic spinal lesions and primary spinal malignancy.[3] Consequently, differentiating pathological fracture types is more complex than it initially appears and requires careful consideration during diagnosis.[2,4,5] This case highlights the diagnostic challenges and treatment approach for a patient initially suspected of having a spinal malignancy.

Case Report

A 54-year-old woman presented to the emergency department with severe lower back pain, weakness in both legs, and difficulty ambulating after a fall. Her symptoms began a month earlier after lifting a heavy object, initially presenting with incomplete paraplegia that progressively worsened. Another fall injury 1 week prior to her visit exacerbated her symptoms. She had a history of

Received: December 31, 2025; Revised: March 13, 2026; Accepted: April 7, 2026
Corresponding author: Dal-Sung Ryu, M.D.
Department of Neurosurgery, Inha University College of Medicine, 27 Inhang-ro, Jung-gu, Incheon 22332, Korea
TEL: +82-32-890-3596, FAX: +82-32-890-2374, E-mail: dalsung.ryu@gmail.com

complex psychiatric disorders, including depression and schizophrenia, but no other notable medical or neoplastic conditions. On physical examination, the patient's right leg strength was graded as I, left leg strength as II across all joints, and low back pain was 7 on a numerical rating scale. She had voiding difficulty requiring urinary catheterization, whereas bowel function was intact. Thoracic and lumbar spine radiographs revealed a T12 burst fracture. Whole-spine computed tomography (CT) showed compression fractures at both T7 and T12 (Fig. 1A). The T12 lesion demonstrated features of a subacute or chronic burst fracture with retropulsion of the posterior vertebral body, and a mass in the posterior epidural space extending from T12 to L2 with severe central canal narrowing. Additionally, an ill-defined radiopacity was noted in the intradural and left anterior epidural spaces extending from T12 to L2. Although an iatrogenic cement leakage was initially suspected, the patient had no history of any spinal procedures. Among the differential diagnoses for epidural calcification - namely metastatic disease with epidural extension and arachnoiditis ossificans (AO)—the metastatic etiology appeared more likely (Fig. 1B, 1C).[6] Initial magnetic resonance imaging (MRI) revealed compression fractures at T7 and T12 (Fig. 1D, 1E). The T12 fracture showed convex bowing of the posterior cortex with associated cord compression and an epidural mass. T1-weighted MRI revealed loss of normal marrow signal within the T12 vertebral body and an epidural mass causing cord compression. The mass appeared hyperintense, with a central area that was isointense to hypointense, resulting in central canal narrowing. T2-weighted imaging revealed that the T12 compression fracture was hyperintense and the epidural mass was heterogeneous but generally hyperintense with associated cord compression (Fig. 1E, 1F). Although contrast-enhanced MRI was recommended for further evaluation, it was not performed because the patient declined additional imaging studies. The patient's laboratory results revealed thrombocytosis with a platelet count of 551

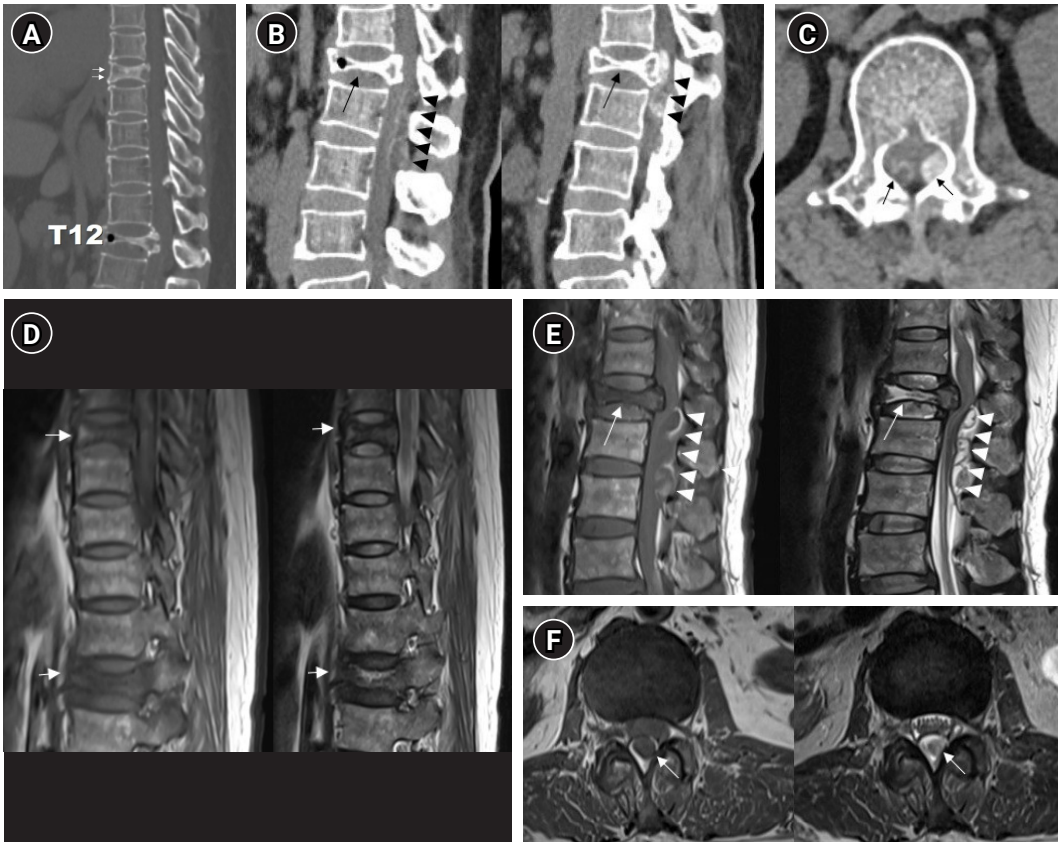

Fig. 1. Preoperative imaging. (A) Whole-spine computed tomography (CT) sagittal image demonstrating compression fracture at T7 (arrows) and T12. (B) Whole-spine CT sagittal image showing a compression fracture at T12 (arrows) and an epidural mass (arrowheads). (C) Whole-spine CT axial image at the T12 level. The mass (arrows) consisted of a hyperdense component on the left and a hyperdense capsule with an isodense to slightly hypodense interior on the right. (D) The magnetic resonance imaging (MRI) T1, T2-weighted sagittal sequences demonstrating compression fractures at T7 and T12 (arrows). (E) The MRI T1, T2-weighted sagittal sequences demonstrating T12 compression fractures (arrows) and an epidural mass (arrowheads). (F) The MRI T1, T2-weighted axial sequences at the L1 level showing an epidural mass (arrows).

https://doi.org/10.63858/jass.26.0025

K/μL. Bone mineral density measurements indicated osteopenia, with a lumbar T-score of −1.6 and femoral neck T-score of −1.8. Further evaluations to rule out malignancy, including chest CT, abdominopelvic CT, positron emission tomography–CT, and tumor marker laboratory tests, showed no significant findings; however, a tissue biopsy was deemed necessary.[3] The patient underwent a laminectomy, spinal fusion, and mass removal. The surgical procedures included total laminectomy of T12 and L1, subtotal laminectomy of the upper L2, pedicle screw fixation from T10 to L2, and posterolateral fusion. The epidural mass was carefully removed, and the fibrous tissue adherent to the dura was excised (Fig. 2). The surgery was completed after ensuring adequate decompression of the spinal cord. The pathological results of the laminectomized bone showed no evidence of malignancy. The epidural mass showed chronic inflammation with nodular fibrosis and bony detritus, indicating a chronic unresolved hematoma. On postoperative day 5, the patient's right leg strength was graded I, while left leg strength improved to grade III for hip flexion and knee extension but decreased to grade I for ankle dorsiflexion. The patient had improved neurological status 1 month after discharge. Her left leg strength improved further to grade III for both ankles and great toe dorsiflexion, while the right leg remained at grade I. Postoperative imaging confirmed a well-decompressed state (Fig. 3).

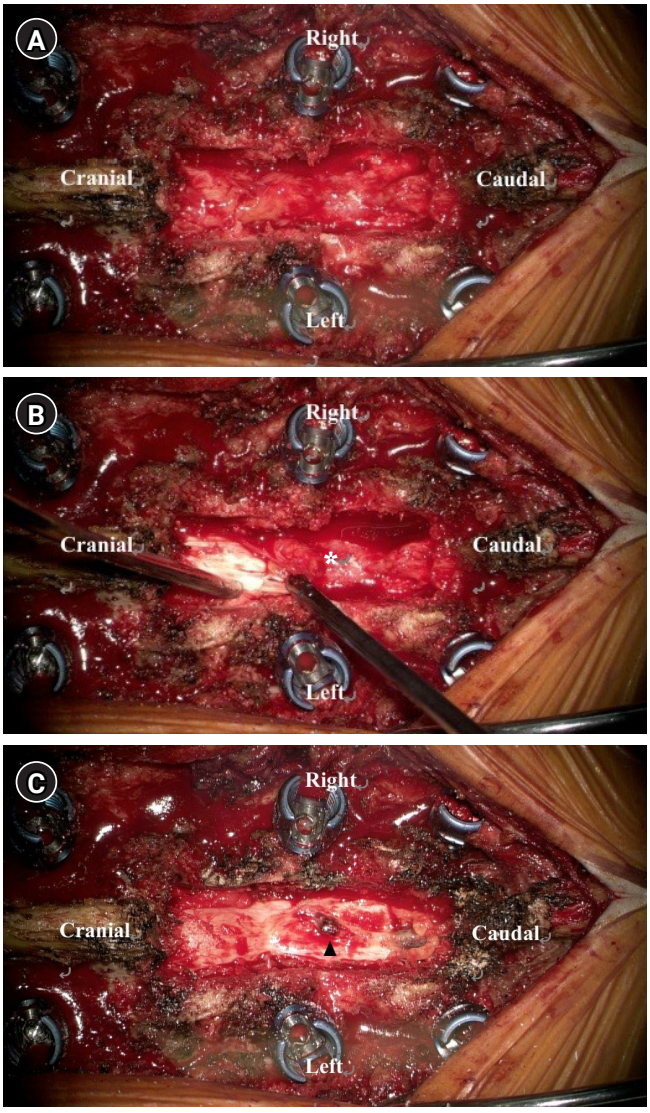

Fig. 2. Intraoperative images. (A) Post-laminectomy image showing the decompressed spinal canal with fibrous tissue adherent to the dura. (B) Image showing the removal of fibrous tissue (asterisk) adherent to the dura mater, which appears elongated and torn. (C) The image shows the spinal region after extending the laminectomy to the upper L2 level. Complete decompression was achieved with the removal of all fibrous tissue. Areas of old hemorrhage (arrowhead) are visible, appearing as clumped regions.

This case report was conducted in accordance with the ethical standards of the institutional and national research committee and with the Helsinki Declaration. Institutional Review Board approval was not required for this case report. All patient information was fully anonymized, and no identifiable personal data were included in this manuscript.

Discussion

In this case, we initially suspected a pathologic spinal fracture with a malignant epidural tumor at admission; however, surgical histopathological examination revealed that the remaining mass was an unabsorbed hematoma. VCFs pose considerable diagnostic challenges, particularly when distinguishing benign and malignant osteoporotic fractures, which require vastly different management strategies and have different prognostic outcomes.[1-5] In previous imaging studies, the characteristic imaging features observed on CT and MRI, including specific morphological changes, enhancement patterns, and MRI signal intensities, helped differentiate these fracture types.[4,5] Benign osteoporotic VCFs typically show normal signals in the posterior elements, retropulsed bone fragments and are accompanied by additional benign fractures on MRI.[4,5] These fractures also have preserved normal marrow signal with regular margins, and exhibit a linear horizontal hypointense T1/T2 band, fluid signs, and normal enhancement relative to adjacent vertebrae and after 3-month follow-up. On CT, benign fractures often display retropulsed bones, sharp fracture lines, puzzle signs, and an intravertebral vacuum.[1,4,5] However, malignant VCFs show abnormal signals in the posterior elements, the presence of an epidural or paravertebral soft tissue

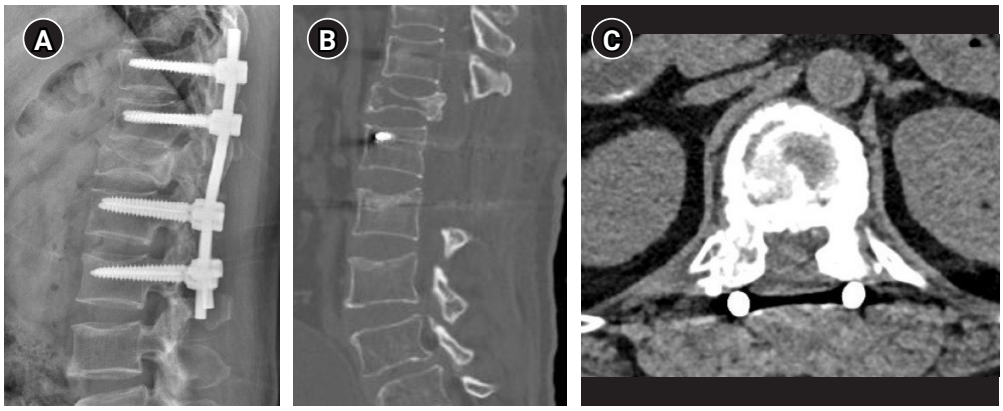

Fig. 3. Postoperative imaging. (A) Postoperative X-ray indicating spinal fusion from T10 to L2, demonstrating successful instrumentation and alignment post-surgery. (B) Postoperative computed tomography (CT) sagittal scan showing a well-decompressed state at the T12, L1, and upper L2 levels. The previously noted calcified lesions are no longer visible. (C) Postoperative CT axial scan at the T12 level, confirming the absence of the calcified lesion on the central canal and effective decompressive laminectomy.

mass, and an expanded posterior vertebral contour, often with metastasis to other vertebrae, on MRI.[1,2,4,5] These fractures exhibit geographic replacement of the normal marrow signal, irregular margins, and increased enhancement relative to the adjacent vertebrae at 3-month follow-up.[1,4,5] On CT, malignant fractures typically involve bone destruction and the presence of an epidural or focal paravertebral soft-tissue mass.[1,2,4,5]

In this case, the initial imaging suggested a malignant process owing to the presence of T12 and T7 compression fractures, an epidural mass, and thrombocytosis. Whole-spine CT findings indicated calcifications and a posterior epidural mass extending from T12 to L1, which caused severe central canal narrowing. Additionally, an ill-defined radiopacity was noted in the intradural space and left anterior epidural space extending from T12 to the L2 level central canal. These findings initially suggested malignancy, given the abnormal posterior element signal, the presence of a mass with irregular margins, and bone destruction on CT.[1,2,4,5] However, the biopsy results revealed chronic inflammation with fibrosis, consistent with an organized hematoma. Imaging findings suggested AO in the intradural space, which was not biopsied. This divergence from typical imaging features of malignancy highlights the complexities and potential pitfalls in VCF diagnosis. The patient presented with features common to both benign and malignant VCFs, including severe back pain and paraplegia. The presence of calcification within the epidural mass, which is not typically observed in benign osteoporotic fractures, initially suggested a malignancy. Conversely, the organized hematoma and chronic inflammation observed on biopsy indicate a benign process secondary to trauma. Subacute hematomas can be difficult to detect by CT imaging, and gradually appear isodense over time.[7,8] However, MRI can provide a clearer view, revealing the form of the hematoma and enabling a precise assessment of the affected cord levels.[7,8] MRI results can also indicate bleeding duration; acute hematomas typically appear hypointense on T1-weighted images and hyperintense on T2-weighted images.[7-9] As the hematoma progresses to the early subacute stage, it becomes hyperintense on T1-weighted MRI and hypointense on T2-weighted MRI.[7-9] Over time, the hematoma becomes increasingly hyperintense on T1-weighted sequences and hypointense on T2-weighted sequences, often exhibiting a mosaic pattern.[7-9]

In the present case, the posterior epidural mass was identified as an organized hematoma consistent with traumatic spinal epidural hematoma (TSEH). TSEH involves bleeding primarily from the posterior epidural venous plexus, which is susceptible to rupture due to its lack of valves and proximity to pressure fluctuations.[7-10] This network is particularly vulnerable at cervicothoracic and thoracolumbar junctions.[7,9,11,12] Clinical cases have linked TSEH to activities such as heavy lifting, straining, and hypertension.[7-9,11,12] However, some researchers, such as Beatty and Winston[13], have suggested that arterial sources may be responsible for the bleeding, arguing that venous hemorrhage would not generate sufficient pressure to compress the spinal cord. Both TSEH and non-TSEH can present with acute pain followed by rapidly progressive neurologic deficits, and timely decompression is critical for favorable outcomes.[7,8,10,11,14]

The presence of AO added further complexity to this case, owing to its rarity and difficulty in accurately diagnosing it. AO involves ossification within the subarachnoid space, potentially leading to the obstruction of cerebrospinal fluid flow and spinal cord compression.[6] Non-contrast CT is particularly effective in

https://doi.org/10.63858/jass.26.0025

demonstrating the extent of ossification and complements MRI findings.[6] Although the diagnosis of AO was based on imaging rather than biopsy, the presence of ossified lesions complicated the clinical picture.

This case highlights the importance of integrating radiologic, surgical, and pathologic findings in diagnostic evaluation. Although advanced imaging techniques provide valuable insights, they must be interpreted cautiously and correlated with clinical and histopathological findings to avoid misdiagnosis.[1-5] Distinguishing benign and malignant VCFs remains challenging and requires careful consideration of all diagnostic modalities.[1-5] Furthermore, maintaining a high index of suspicion and utilizing a multidisciplinary approach is essential to achieve an accurate diagnosis and appropriate management.

In conclusion, this case report underscores the importance of distinguishing an unresolved epidural hematoma from a malignancy via surgical resection. Suspicion of malignancy considerably influences the decision-making processes of both the medical team and the patient's caregivers, impacting the overall treatment plan. Although mass formation with compression fractures is rare, it can occur as a result of trauma. Hence, careful attention must be paid to the diagnosis to avoid misinterpretation and ensure appropriate management.

Author contributions

Conceptualization: GHJ. Data curation: GHJ. Investigation: GHJ, SHY. Validation: SHY, DSR. Supervision: DSR. Writing – original draft: GHJ. Writing – review & editing: DSR.

Conflict of interest

The authors have no conflicts of interest to declare.

Funding

None.

Acknowledgments

None.

ORCID

Geon-Hwee Jeon, https://orcid.org/0009-0004-4382-6846
Seung-Hwan Yoon, https://orcid.org/0000-0003-0558-2313
Dal-Sung Ryu, https://orcid.org/0000-0003-0895-3431

References

1. Gutierrez-Gonzalez R, Royuela A, Zamarron A. Survival following vertebral compression fractures in population over 65 years old. Aging Clin Exp Res 2023;35:1609-17.
2. Taylor TN, Bridges CS, Pupa LE, Morrow BA, Smith BG, Montgomery NI. Retrospective review of 181 patients with pathologic vertebral compression fractures. J Pediatr Soc North Am 2023;5:697.
3. Mukherjee S, Thakur B, Bhagawati D, et al. Utility of routine biopsy at vertebroplasty in the management of vertebral compression fractures: a tertiary center experience. J Neurosurg Spine 2014;21:687-97.
4. Mauch JT, Carr CM, Cloft H, Diehn FE. Review of the imaging features of benign osteoporotic and malignant vertebral compression fractures. AJNR Am J Neuroradiol 2018;39:1584-92.
5. Abdel-Wanis ME, Solyman MT, Hasan NM. Sensitivity, specificity and accuracy of magnetic resonance imaging for differentiating vertebral compression fractures caused by malignancy, osteoporosis, and infections. J Orthop Surg (Hong Kong) 2011;19:145-50.
6. Nagashima Y, Nishimura Y, Ito H, Nishii T, Oyama T, Saito R. Diagnosis and treatment strategies for arachnoiditis ossificans following subarachnoid hemorrhage: a case report. NMC Case Rep J 2022;9:295-9.
7. Al-Mutair A, Bednar DA. Spinal epidural hematoma. J Am Acad Orthop Surg 2010;18:494-502.
8. Fedor M, Kim ES, Ding K, Muizelaar JP, Kim KD. Spontaneous spinal epidural hematoma: a retrospective study on prognostic factors and review of the literature. Korean J Spine 2011;8:272-82.
9. Tamburrelli FC, Meluzio MC, Masci G, Perna A, Burrofato A, Proietti L. Etiopathogenesis of traumatic spinal epidural hematoma. Neurospine 2018;15:101-7.
10. Cho YW, Moon JG. Acute nontraumatic spinal epidural hematoma at cervical spine. J Korean Neurosurg Soc 2003;34:268-70.
11. Agrawal A, Reddy UM, Brinda K, Moscote-Salazar LR. Posttraumatic acute spinal epidural hematoma of the dorsolumbar region. Indian J Neurotrauma 2020;17:50-2.
12. Alrazooqi MK, Skikic E, Iqbal SS, Sulaiman L, Muhammed Noori OQ. Traumatic spinal epidural hematoma with significant neurologic findings: a case report. Cureus 2023;15:e38869.
13. Beatty RM, Winston KR. Spontaneous cervical epidural hematoma: a consideration of etiology. J Neurosurg 1984;61:143-8.
14. Kahraman MA, Senturk S. The necessity of extensive decompression for spinal epidural hematoma: a case report and literature review. Cureus 2023;15:e44192.

Case Report

J Adv Spine Surg 2026;16(1):56-61
https://doi.org/10.63858/jass.26.0029
pISSN 2234-0637 • eISSN 3140-0663

JASS
JOURNAL OF ADVANCED SPINE SURGERY

Clinical Application of Combined Pulsed Radiofrequency and Low-Temperature Thermal Radiofrequency for Postoperative Radicular Pain: A Case Report

Cheol Sik Kim, M.D., Jong Hun Seo, M.D., Ph.D., Pius Kim, M.D., Ph.D., Sang Woo Ha, M.D., Ph.D., Chang Il Ju, M.D., Ph.D., Chi Ho Kim, M.D., Ph.D.

Department of Neurosurgery, Chosun University College of Medicine, Gwangju, Korea

Postoperative radicular pain may persist after lumbar spine surgery despite adequate decompression and the absence of a definite compressive lesion on imaging. Management of such cases remains challenging. This study aimed to report the clinical outcomes of combined pulsed radiofrequency (PRF) and low-temperature thermal radiofrequency. We retrospectively reviewed two patients with postoperative radicular pain without evidence of a high-grade compressive lesion. Both patients showed temporary relief after selective nerve root block. PRF (42°C, 120 seconds), followed by low-temperature thermal radiofrequency (55°C, 60 seconds), was applied under fluoroscopic guidance. Both patients demonstrated significant pain reduction without neurological complications, and symptom improvement was maintained for at least 12 months. The combination of PRF and low-temperature thermal radiofrequency may represent a feasible minimally invasive treatment option. Further studies are required to clarify its effectiveness and indications.

Keywords: Radicular pain, Pulsed radiofrequency treatment, Radiofrequency ablation, Neuromodulation, Spinal ganglion

Introduction

Postoperative radicular pain may persist after lumbar spine surgery despite adequate decompression and the absence of a definite compressive lesion on imaging. This condition is thought to be associated with neuropathic mechanisms and neural sensitization.[1-4]

Pulsed radiofrequency (PRF) is a neuromodulation technique widely used for radicular pain; however, its clinical efficacy remains variable and the exact mechanism of PRF is not fully understood.[5] Conventional thermal radiofrequency is typically applied at high temperatures (80°C–90°C) and carries a risk of irreversible neural injury.[6,7] In contrast, low-temperature thermal radiofrequency may provide a more controlled thermal effect at lower temperatures.

In this study, we report our clinical experience with the combined use of PRF and low-temperature thermal radiofrequency in patients with postoperative radicular pain.

Case Report

1. Case 1

A 76-year-old male presented with progressive left lower extremity weakness and radicular pain. Imaging revealed a left-sid-

Received: April 18, 2026; Revised: May 15, 2026; Accepted: May 21, 2026
Corresponding author: Chi Ho Kim, M.D., Ph.D.
Department of Neurosurgery, Chosun University College of Medicine, 309 Pilmun-daero, Dong-gu, Gwangju 61452, Korea
TEL: +82-62-220-3126, FAX: +82-62-227-4575, E-mail: chiho13@naver.com

ed ruptured disc with inferior migration at the L2–3 level, causing compression of the left L3 nerve root (Fig. 1A, 1B). The patient underwent transforaminal endoscopic lumbar discectomy (TELD) at L2–3. Postoperatively, motor weakness improved; however, radicular pain along the L3 dermatome persisted despite adequate decompression and the absence of a definite residual compressive lesion on follow-up imaging (Fig. 2A, 2B).

A selective nerve root block (SNRB) targeting the left L3 nerve root resulted in temporary symptom relief. Based on this response, PRF followed by low-temperature thermal radiofrequency was performed. After the procedure, the patient reported significant pain reduction (visual analog scale [VAS] score decreased from 7 to 2), with mild transient numbness that resolved spontaneously. Symptom improvement was maintained for over 12 months without recurrence or complications.

2. Case 2

A 79-year-old male presented with left lower extremity radicu-

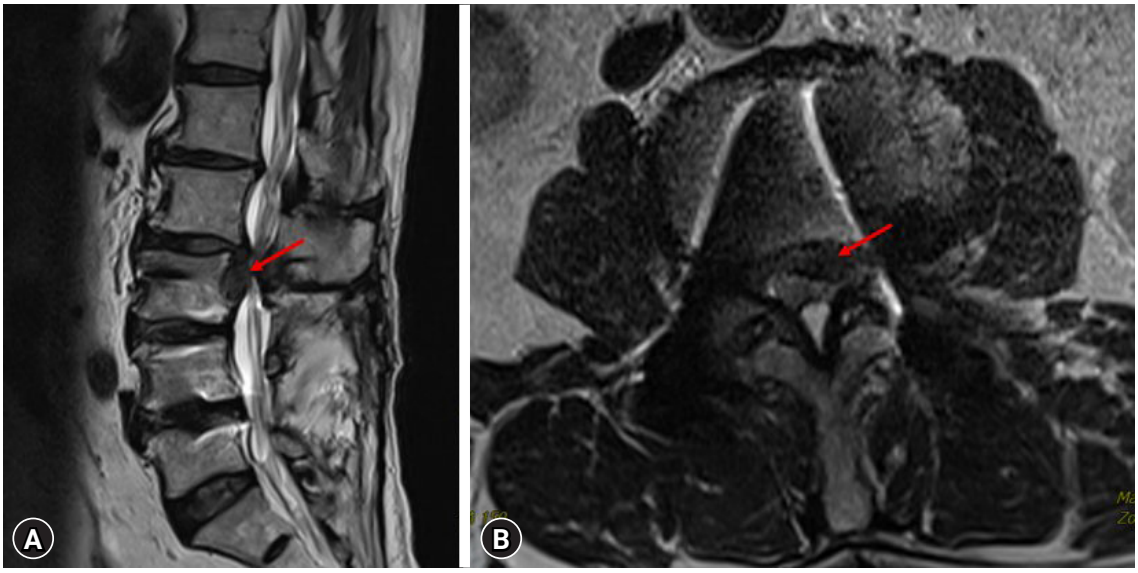

Fig. 1. Preoperative magnetic resonance imaging sagittal view (A) and axial view (B) showing a left-sided disc herniation with inferior migration at the L2–3 level (arrows).

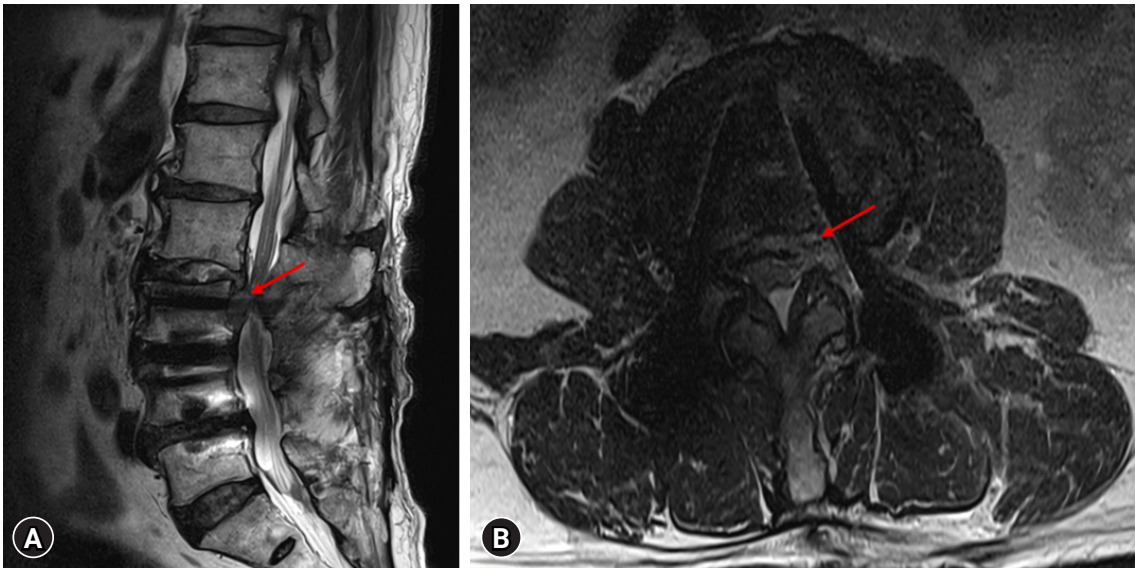

Fig. 2. Postoperative magnetic resonance imaging sagittal view (A) and axial view (B) showing adequate decompression at the L2–3 level after endoscopic discectomy (arrows).

lar pain and motor weakness. Imaging revealed a ruptured disc at the L4–5 level causing compression of the left L4 nerve root (Fig. 3A, 3B). The patient underwent TELD at L4–5. Postoperatively, motor weakness improved; however, radicular pain along the L4 dermatome persisted despite adequate decompression and the absence of a definite residual compressive lesion on follow-up imaging (Fig. 4A, 4B).

A left L4 SNRB provided temporary symptom relief, but the pain recurred. After 3 months of conservative management, combined PRF and low-temperature thermal radiofrequency was performed. The patient reported significant pain reduction (VAS score decreased from 6 to 3), with transient numbness along the L4 distribution. At 2-year follow-up, symptom improvement was maintained without recurrence or complications.

3. Intervention technique

All instruments used for the procedure, including the radiofrequency (RF) needle and electrode, are shown in Fig. 5A. After

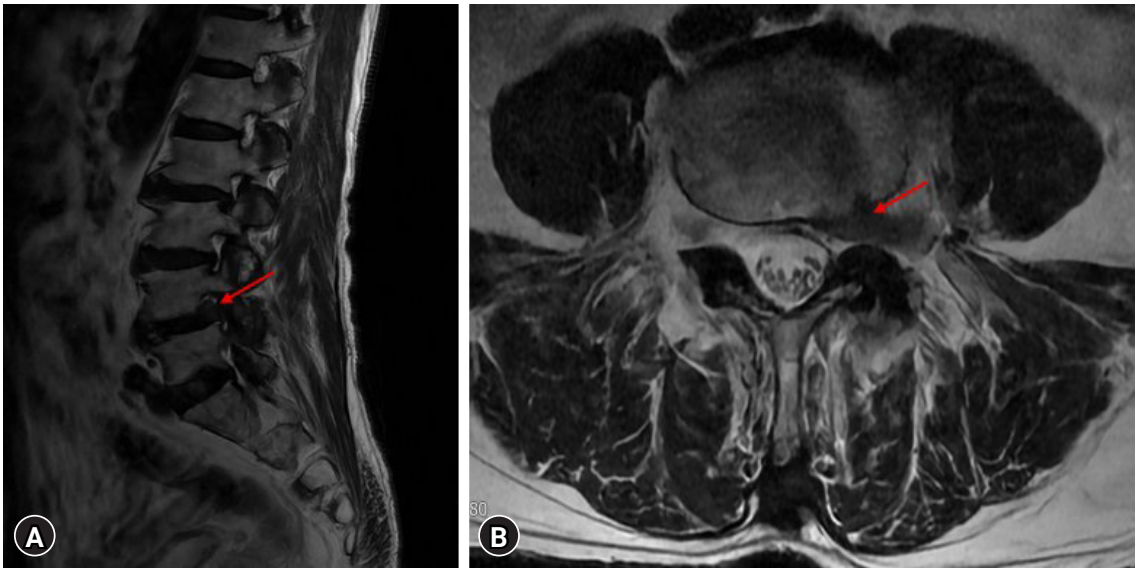

Fig. 3. Preoperative magnetic resonance imaging sagittal view (A) and axial view (B) showing a left-sided herniation at the L4–5 level (arrows).

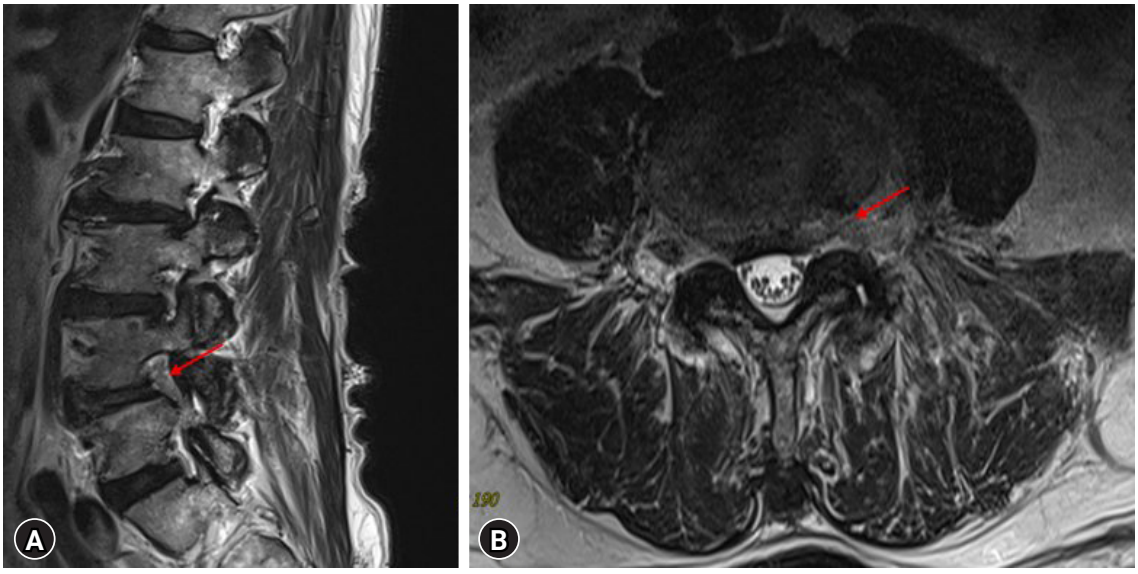

Fig. 4. Postoperative magnetic resonance imaging sagittal view (A) and axial view (B) showing adequate decompression at the L4–5 level after endoscopic discectomy (arrows).

https://doi.org/10.63858/jass.26.0029

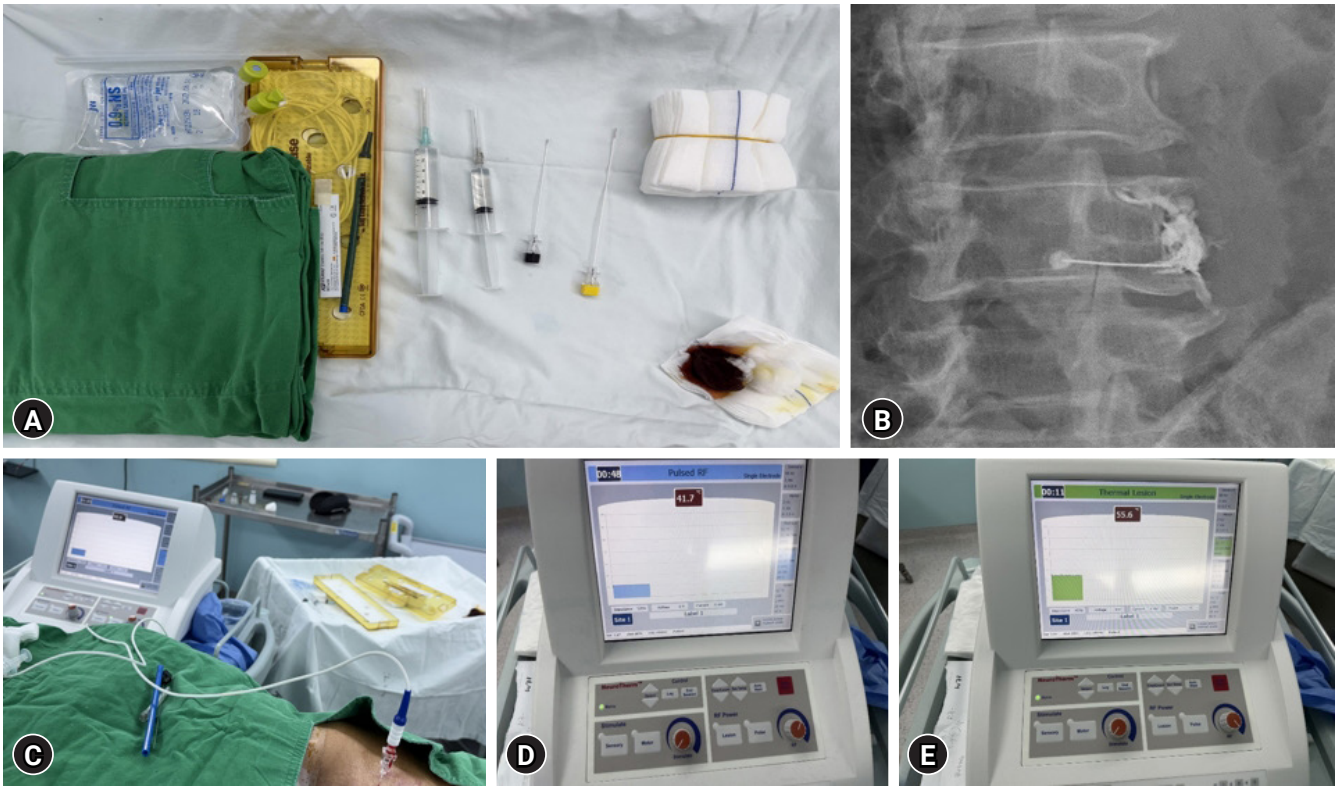

Fig. 5. Procedure of pulsed radiofrequency (PRF) and low-temperature thermal radiofrequency performed in case 2. (A) Instruments used for the procedure, including the radiofrequency (RF) electrode, RF needle, and a 10-mL syringe containing a mixture of lidocaine and steroid. (B) Fluoroscopic image showing selective nerve root targeting and contrast confirmation. (C) Intra-procedural image showing the RF electrode connected to the RF generator (IONIC RF Generator, Abbott Medical) during treatment. (D) Generator display during PRF (42°C, 120 seconds). (E) Generator display during low-temperature thermal radiofrequency (55°C, 60 seconds).

sterile preparation and local anesthesia, an RF needle (22-gauge, 10 cm, straight, 5 mm active tip) was advanced to the target nerve root. Contrast injection was used to confirm accurate positioning of the needle tip (Fig. 5B). An RF electrode (10 cm reusable stainless-steel electrode) was then inserted through the needle and connected to the RF generator (IONIC RF Generator, Abbott Medical, St. Paul, MN, USA) (Fig. 5C). Sensory stimulation (monopolar, maximum voltage 3 V, frequency 50 Hz, pulse width 1 ms) was performed to confirm correct targeting of the symptomatic nerve root. PRF was applied first at a maximum temperature of 42°C for 120 seconds (monopolar, maximum voltage 45 V, frequency 2 Hz, pulse width 20 ms) (Fig. 5D). Subsequently, the system was switched to lesion mode, and low-temperature thermal radiofrequency was applied at a target temperature of 55°C for 60 seconds (monopolar) (Fig. 5E). After completion of the procedure, a total of 10 mL of mixed solution (2 mL of 2% lidocaine, 1 mL of dexamethasone, and 7 mL of normal saline) was injected around the target nerve root. Written informed consent for publication was obtained from the patients.

Discussion

Postoperative radicular pain is a complex condition that cannot be explained solely by mechanical compression. In the present cases, radicular symptoms were observed despite adequate decompression, suggesting the involvement of additional non-compressive mechanisms. Previous studies have shown that inflammatory mediators around the intervertebral disc can induce radiculitis, increasing nerve root sensitivity.[1,2] Repeated or sustained neural irritation may also lead to hyperexcitability of the dorsal root ganglion (DRG), resulting in spontaneous neuronal firing and amplification of pain signals.[8,9] In addition, neuropathic pain arising from abnormal neural signaling pathways plays a significant role in radicular symptoms.[3] Therefore, the combined approach in this study was primarily aimed at modulating DRG sensitization and neuropathic pain components.

PRF is a neuromodulation technique that exerts its effect through electric fields rather than thermal nerve destruction, thereby minimizing structural damage while modulating pain

transmission.[6,8] It is believed to interfere with nociceptive signal transmission from peripheral nerves to the central nervous system.[10] Although some studies have reported limited high-quality evidence supporting PRF, the reported benefits have often been limited to short-term efficacy.[11-15] Other studies have shown clinically meaningful pain relief following PRF applied to the DRG in patients with radicular pain.[4,8,16,17] A recent systematic review suggested that PRF may provide superior pain relief compared with lumbar epidural block at three months post-procedure, although the overall level of evidence remains limited.[11]

According to experimental studies analyzing the phenomena occurring at the RF electrode tip, transient temperature elevations may occur during PRF application; however, these thermal effects are generally insufficient to achieve the level of ablation typically intended in conventional radiofrequency treatment.[6,7,18] In contrast, conventional RF is usually applied at higher temperatures (80°C–90°C), inducing neural suppression through protein denaturation, but it carries a relatively higher risk of irreversible neural injury.[6,7,18] In this context, we considered the addition of a controllable low-temperature thermal component to complement the neuromodulatory effects of PRF. At a relatively low target temperature of 55°C, this approach can be interpreted as a form of thermal modulation rather than conventional lesioning and may enhance clinical efficacy while maintaining procedural safety. Therefore, the combined application of PRF and low-temperature thermal RF may represent a rational and clinically applicable treatment strategy, integrating neuromodulatory effects with a controlled thermal component to overcome the limitations of each modality when used alone.

To the best of our knowledge, there are no previous reports describing the combined use of PRF and low-temperature thermal radiofrequency in this context, which represents a notable aspect of this study. Various treatment options have been proposed for postoperative radicular pain, including repeated nerve block, revision surgery, spinal cord stimulation (SCS), and DRG stimulation. Repeated nerve block may provide temporary symptom relief; however, recurrence of pain is common and long-term efficacy is often limited. Revision surgery may not be appropriate in the absence of a definite compressive lesion, while neuromodulation techniques such as SCS and DRG stimulation are relatively invasive and costly despite their demonstrated clinical efficacy in refractory neuropathic pain conditions.[9,19] In this context, combined PRF and low-temperature thermal radiofrequency may represent a feasible minimally invasive alternative in carefully selected patients. This approach may be particularly applicable in patients with radicular pain who demonstrate a positive response to SNRB despite the absence of clear surgical indications. However, this report is limited by the small number of cases and the absence of a control group. Therefore, further studies are required to better define the appropriate indications for this procedure and to validate its safety and clinical effectiveness.

Combined PRF and low-temperature thermal radiofrequency may represent a feasible minimally invasive treatment option for postoperative radicular pain. Further studies are needed to clarify its effectiveness and indications.

Author contributions

Conceptualization: CHK. Data curation: CSK. Formal analysis: CSK. Investigation: CSK. Methodology: CIJ. Project administration: JHS. Supervision: CHK. Validation: SWH. Visualization: PK. Writing – original draft: CSK. Writing – review & editing: CHK.

Conflict of interest

The authors have no conflicts of interest to declare.

Funding

None.

Acknowledgments

None.

ORCID

Cheol Sik Kim, https://orcid.org/0009-0005-5518-8842
Jong Hun Seo, https://orcid.org/0009-0006-6802-3403
Pius Kim, https://orcid.org/0000-0001-5514-9257
Sang Woo Ha, https://orcid.org/0000-0002-0409-2737
Chang Il Ju, https://orcid.org/0000-0001-9123-2808
Chi Ho Kim, https://orcid.org/0000-0002-9955-5107

References

1. Olmarker K, Rydevik B. Pathophysiology of sciatica. Orthop Clin North Am 1991;22:223-34.
2. McCarron RF, Wimpee MW, Hudkins PG, Laros GS. The inflammatory effect of nucleus pulposus: a possible element in the pathogenesis of low-back pain. Spine (Phila Pa 1976) 1987;12:760-4.
3. Freynhagen R, Baron R. The evaluation of neuropathic components in low back pain. Curr Pain Headache Rep 2009;13:185-90.
4. Cho JH, Lee JH, Song KS, Hong JY. Neuropathic pain after spinal surgery. Asian Spine J 2017;11:642-52.

https://doi.org/10.63858/jass.26.0029

5. Sam J, Catapano M, Sahni S, Ma F, Abd-Elsayed A, Visnjevac O. Pulsed radiofrequency in interventional pain management: cellular and molecular mechanisms of action - an update and review. Pain Physician 2021;24:525-32.
6. Cosman ER Jr, Cosman ER Sr. Electric and thermal field effects in tissue around radiofrequency electrodes. Pain Med 2005;6:405-24.
7. Walsh T, Malhotra R, Sharma M. Radiofrequency techniques for chronic pain. BJA Educ 2022;22:474-83.
8. Chua NH, Vissers KC, Sluijter ME. Pulsed radiofrequency treatment in interventional pain management: mechanisms and potential indications: a review. Acta Neurochir (Wien) 2011;153:763-71.
9. Deer TR, Hunter CW, Mehta P, et al. A systematic literature review of dorsal root ganglion neurostimulation for the treatment of pain. Pain Med 2020;21:1581-9.
10. Abd-Elsayed A, Hughes M, Narel E, Loebertman MD. The efficacy of radiofrequency ablation for pain management in patients with pre-existing hardware at the site of ablation. Pain Ther 2020;9:709-16.
11. Park S, Park JH, Jang JN, et al. Pulsed radiofrequency of lumbar dorsal root ganglion for lumbar radicular pain: a systematic review and meta-analysis. Pain Pract 2024;24:772-85.
12. Shanthanna H, Chan P, McChesney J, Thabane L, Paul J. Pulsed radiofrequency treatment of the lumbar dorsal root ganglion in patients with chronic lumbar radicular pain: a randomized, placebo-controlled pilot study. J Pain Res 2014;7:47-55.
13. Vuka I, Dosenovic S, Marcius T, et al. Efficacy and safety of pulsed radiofrequency as a method of dorsal root ganglia stimulation for treatment of non-neuropathic pain: a systematic review. BMC Anesthesiol 2020;20:105.
14. Malik K, Benzon HT. Radiofrequency applications to dorsal root ganglia: a literature review. Anesthesiology 2008;109:527-42.
15. Hussain AM, Afshan G. Use of pulsed radiofrequency in failed back surgery syndrome. J Coll Physicians Surg Pak 2007;17:353-5.
16. Tsou HK, Chao SC, Wang CJ, et al. Percutaneous pulsed radiofrequency applied to the L-2 dorsal root ganglion for treatment of chronic low-back pain: 3-year experience. J Neurosurg Spine 2010;12:190-6.
17. Van Zundert J, Patijn J, Kessels A, Lame I, van Suijlekom H, van Kleef M. Pulsed radiofrequency adjacent to the cervical dorsal root ganglion in chronic cervical radicular pain: a double blind sham controlled randomized clinical trial. Pain 2007;127:173-82.
18. Perret DM, Kim DS, Li KW, et al. Application of pulsed radiofrequency currents to rat dorsal root ganglia modulates nerve injury-induced tactile allodynia. Anesth Analg 2011;113:610-6.
19. North RB, Kidd DH, Farrokhi F, Piantadosi SA. Spinal cord stimulation versus repeated lumbosacral spine surgery for chronic pain: a randomized, controlled trial. Neurosurgery 2005;56:98-106.

Case Report

J Adv Spine Surg 2026;16(1):62-67
https://doi.org/10.63858/jass.26.0033
pISSN 2234-0637 • eISSN 3140-0663

JASS
JOURNAL OF ADVANCED SPINE SURGERY

Delayed Surgical Management of Initial Cauda Equina Syndrome Due to Concurrent Giant Ovarian Teratomas: A Case Report and Literature Review

Joon-Young Jung, M.D.*, Jae-Won Hur, M.D.*, Se-Jun Park, M.D., Ph.D., Dong-Ho Kang, M.D., Jin-Sung Park, M.D., Ph.D.

Department of Orthopedic Surgery, Samsung Medical Center, Sungkyunkwan University School of Medicine, Seoul, Korea

Dysplastic spondylolisthesis is a developmental subtype characterized by congenital lumbosacral abnormalities and progressive instability. Primary presentation with cauda equina syndrome (CES) has rarely been reported. We report a rare case of CES associated with high-grade dysplastic spondylolisthesis in a patient with concurrent giant ovarian teratomas, which contributed to delayed diagnosis and treatment because of overlapping pelvic symptoms. The patient presented with progressive urinary dysfunction, saddle anesthesia, and lower-extremity symptoms. Radiographic evaluation demonstrated high-grade L5–S1 dysplastic spondylolisthesis with severe canal compromise and lumbosacral deformity. Surgical treatment involved neural decompression and controlled deformity correction with sacral dome osteotomy and interbody fusion performed under provisional stabilization. Postoperatively, the patient demonstrated meaningful neurological recovery with improvement of urinary symptoms and restoration of lumbosacral alignment. This case highlights that CES can occur as an initial manifestation of dysplastic spondylolisthesis and underscores the importance of early spinal evaluation and timely surgical treatment with appropriate reduction techniques to prevent further neurological deterioration in patients with persistent neurological symptoms.

Keywords: Dysplastic spondylolisthesis, Cauda equina syndrome, Giant ovarian teratoma, Sacral dome osteotomy, High grade spondylolisthesis

Introduction

Dysplastic spondylolisthesis is a developmental subtype characterized by congenital abnormalities of the lumbosacral junction, including facet joint dysplasia, sacral dome deformity, and posterior element deficiency, resulting in inherent instability and progressive anterior translation of L5 on S1.[1-3] It predominantly affects pediatric and adolescent patients and has a higher propensity for progression to high-grade slippage.[1,2] Dysplastic spondylolisthesis is also commonly associated with lumbosacral kyphosis and abnormal spinopelvic alignment, which may further contribute to deformity progression and biomechanical instability.[4] Neurologi-

Received: May 15, 2026; Revised: June 5, 2026; Accepted: June 9, 2026
Corresponding author: Jin-Sung Park, M.D., Ph.D.
Department of Orthopedic Surgery, Samsung Medical Center, Sungkyunkwan University School of Medicine , 81 Irwon-ro, Gangnam-gu, Seoul 06351, Korea
TEL: +82-2-3410-1583, FAX: +82-2-3410-0061, E-mail: jinsungosspine@gmail.com, jinsungosspine.park@samsung.com

*These authors contributed equally to this work.

cal manifestations in dysplastic spondylolisthesis are typically gradual and most commonly present as radiculopathy related to foraminal narrowing or nerve root stretching1. In contrast, primary presentation with cauda equina syndrome (CES) is exceedingly rare in dysplastic spondylolisthesis. Most previously reported cases have occurred in the postoperative setting following in situ fusion or reduction procedures.[5,6]

The optimal surgical management of high-grade dysplastic spondylolisthesis remains controversial, particularly regarding the degree of reduction and the risk of neurological complications.[1,7] Recent studies have emphasized the role of sacral dome osteotomy and careful deformity correction techniques in facilitating safe reduction while minimizing neural tension.[7,8]

Herein, we report a rare case of CES associated with dysplastic spondylolisthesis in a patient with concurrent giant ovarian teratomas, in whom overlapping pelvic pathology contributed to delayed spinal diagnosis and surgical treatment. This case highlights that CES can occur as an initial manifestation of dysplastic spondylolisthesis and underscores the importance of maintaining suspicion for spinal pathology in patients with persistent neurogenic symptoms despite treatment of concomitant pelvic disease.

Case Report

A 19-year-old female presented to the emergency department with a 6-month history of urinary incontinence. The symptoms worsened during the preceding month. Neurological examination revealed sensory deficits in the bilateral S1–3 dermatomes, with approximately 30%–40% decreased sensation. Motor function of both lower extremities was intact without definite weakness. Initial abdominal-pelvic computed tomography demonstrated large bilateral mature cystic ovarian teratomas measuring approximately 14 cm in diameter (Fig. 1). Initially, the urinary symptoms were presumed to be secondary to compression by the large pelvic masses and the patient underwent bilateral ovarian cystectomy for bilateral mature cystic ovarian teratomas on the day of admission. However, the urinary symptoms persisted postoperatively. Because symptoms failed to improve after gynecologic surgery, orthopedic consultation was obtained. Standing radiographs and computed tomography (CT) demonstrated high-grade dysplastic spondylolisthesis at L5–S1 (Meyerding grade III) with a preoperative slip percentage of 55%. Magnetic resonance imaging demonstrated severe central canal stenosis and bilateral L5 nerve root compression (Figs. 2, 3). Characteristic radiographic features, including vertically oriented facet joints, sacral dome deformity, and elongation of the L5 pars interarticularis, were identified on CT (Fig. 4). CES secondary to dysplastic spondylolisthesis was considered the most likely diagnosis.

The patient subsequently underwent L5–S1 posterior lumbar interbody fusion with neural decompression. Direct decompression alone was considered hazardous because further slippage during surgery could worsen neural compression. Therefore, temporary fixation using reduction pedicle screws and bilateral rod fixation was performed before decompression to stabilize the lumbosacral segment and prevent further slippage during surgery. After provisional stabilization, decompression was carefully performed. Intraoperatively, marked dural tension was observed. Because reduction alone was insufficient to relieve neural tension

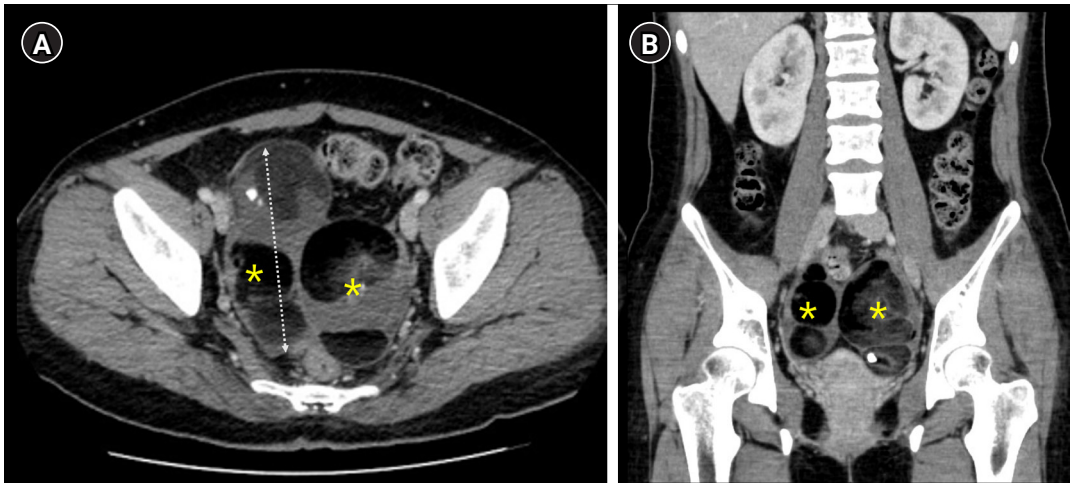

Fig. 1. Abdominal-pelvic computed tomography demonstrating bilateral mature cystic teratomas occupying the pelvic cavity. (A) Axial computed tomography (CT) image showing bilateral cystic masses (asterisks) with internal heterogeneous components, measuring approximately 14 cm in diameter (dashed line). (B) Coronal CT image demonstrating bilateral pelvic masses (asterisks) causing mass effect within the pelvic cavity.

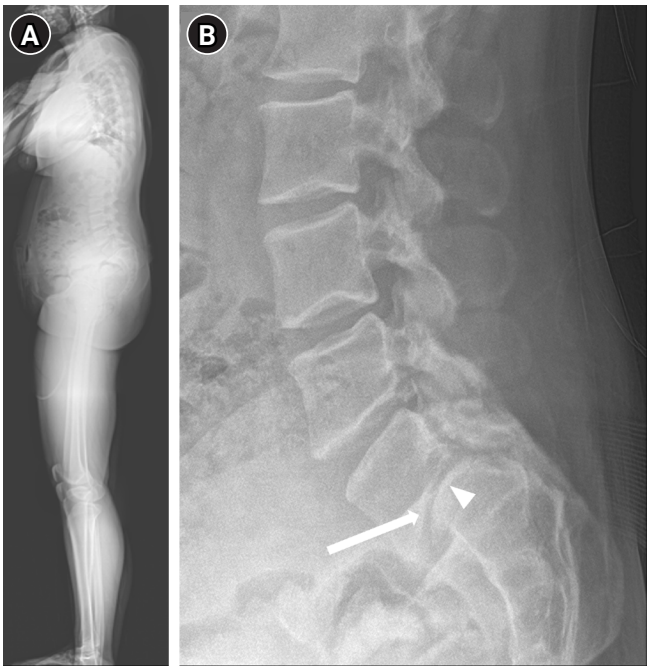

Fig. 2. Whole-spine standing lateral radiograph and simple lateral radiograph demonstrating dysplastic spondylolisthesis at the L5–S1 level. (A) Whole-spine standing lateral radiograph showing a stooped sagittal posture, resulting in a characteristic appearance associated with high-grade L5–S1 dysplastic spondylolisthesis. (B) Simple lateral lumbar radiograph demonstrating high-grade anterior slippage of L5 on S1 (arrow) and sacral dome deformity (arrowhead).

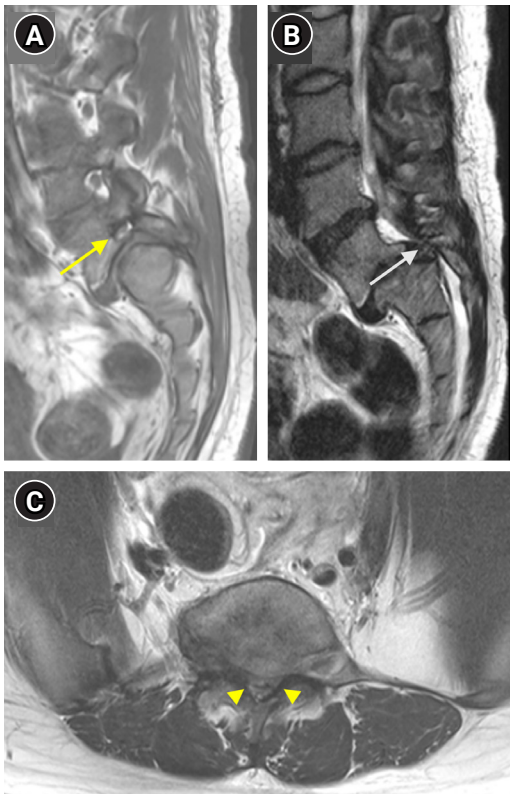

Fig. 3. Lumbar spine magnetic resonance imaging demonstrating severe central canal stenosis and foraminal stenosis associated with dysplastic spondylolisthesis at the L5–S1 level. (A) Sagittal T1-weighted magnetic resonance image demonstrating high-grade L5–S1 dysplastic spondylolisthesis with severe foraminal stenosis (yellow arrow). (B) Sagittal T2-weighted magnetic resonance image showing severe central canal stenosis at the L5–S1 level (white arrow). (C) Axial T2-weighted magnetic resonance image demonstrating severe central canal stenosis (yellow arrowheads).

and restore spinopelvic alignment, sacral dome osteotomy was additionally performed. After sacral dome osteotomy, the set screws were partially loosened, and further reduction was gradually performed using a unilateral blunt dilator. Bilateral interbody cages were then inserted sequentially on each side during the reduction maneuver. Postoperative radiographs demonstrated improvement in lumbosacral alignment, including correction of the Spinal Deformity Study Group lumbosacral angle and slip angle (Fig. 5). Urinary symptoms and sensory deficits gradually improved without postoperative neurologic deterioration. Radiographic alignment and instrumentation were well maintained at the 3-month and 1-year follow-up evaluations, with sustained clinical improvement.

Discussion

Dysplastic spondylolisthesis has a higher propensity for progression to high-grade slippage and is frequently associated with lumbosacral kyphosis and biomechanical instability.[1,4] Neurological manifestations of dysplastic spondylolisthesis are typically gradual and most commonly present as radiculopathy, whereas CES is rare and has been reported predominantly in the postoperative setting rather than as a primary presentation.[5,6] In the present case, concurrent giant ovarian teratomas further complicated the diagnostic process because the patient's progressive urinary dysfunction and saddle anesthesia initially overlapped with symptoms potentially attributable to pelvic pathology. Previous reports have described CES following in situ fusion or reduction procedures in high-grade spondylolisthesis, suggesting vulnerability of the neural elements to mechanical stress and stretch injury.[5,6] In contrast, the present case presented with CES as the primary presentation without prior surgical intervention, indicating that dysplastic spondylolisthesis itself may cause critical neural compression in the setting of progressive deformity and instability.

The mechanisms underlying CES in this setting likely involve central canal compromise from anterior translation and dynamic neural tension related to lumbosacral kyphosis and abnormal

https://doi.org/10.63858/jass.26.0033

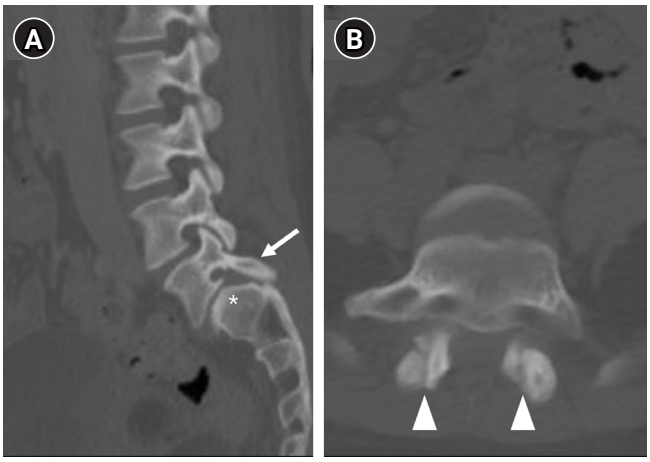

Fig. 4. Computed tomography demonstrating characteristic dysplastic features at the L5–S1 level. (A) Sagittal computed tomography (CT) image demonstrating elongation of the L5 pars interarticularis (arrow) and sacral dome deficiency (asterisk). (B) Axial CT image demonstrating vertically oriented L5–S1 facet joints (arrowheads).

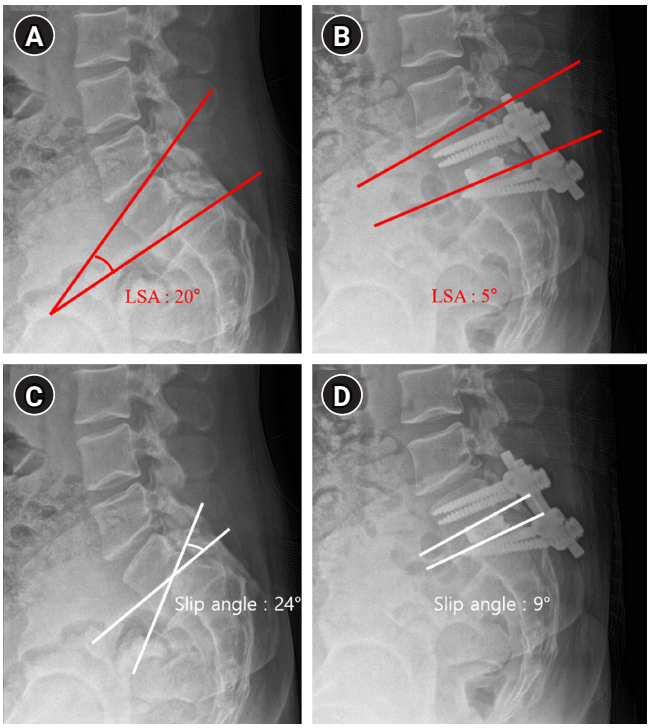

Fig. 5. Preoperative and postoperative lateral radiographs demonstrating changes in lumbosacral alignment following surgical correction. (A, B) Measurement of the Spinal Deformity Study Group (SDSG) lumbosacral angle (LSA) on preoperative and postoperative radiographs, respectively. The SDSG LSA, measured between the superior endplate of L5 and the superior endplate of S1, improved from 20° preoperatively to 5° postoperatively (red lines). (C, D) Measurement of slip angle on preoperative and postoperative radiographs, respectively. The slip angle, measured between the inferior endplate of L5 and the superior endplate of S1, improved from 24° preoperatively to 9° postoperatively (white lines).

sacral morphology.[4,9] These considerations are supported by prior reports of CES following in situ fusion or reduction procedures in high-grade spondylolisthesis, highlighting the vulnerability of the cauda equina to mechanical stress and stretch.[6] Interestingly, despite a delay in surgical treatment, the patient demonstrated meaningful recovery of cauda equina symptoms following decompression and reduction. This observation may suggest that neural compromise was influenced not only by static canal narrowing, but also by dynamic or positional mechanical compression related to instability at the lumbosacral junction.

Surgical management of high-grade dysplastic spondylolisthesis has evolved from traditional in situ fusion toward deformity correction and reduction techniques with increasing emphasis on restoration of sagittal alignment.[9-11] Hoel et al.[9] and Polly et al.[11] emphasized that high-grade dysplastic spondylolisthesis should be regarded as a sagittal deformity driven by lumbosacral kyphosis and spinopelvic imbalance, with restoration of lumbosacral lordosis and pelvic alignment representing the principal surgical goal. Although in situ fusion was historically favored to minimize neural traction, reduction and deformity correction techniques are increasingly performed to restore sagittal alignment.[10,11] Concerns regarding neural stretch injury remain. However, recent studies have demonstrated favorable clinical and radiological outcomes following partial or complete reduction.[12,13] Min et al.[8] and Faldini et al.[7] emphasized that sacral dome osteotomy facilitates reduction by shortening the posterior column and minimizing neural tension during deformity correction. In addition, Ye et al.[13] reported favorable clinical and radiographic outcomes after complete reduction and posterior L5–S1 fusion in pediatric high-grade dysplastic spondylolisthesis. This concept is consistent with our surgical strategy, in which sacral dome osteotomy allowed safe reduction while effectively addressing neural compression. Similarly, Takeda et al.[14] and Tatsumura et al.[15] also reported satisfactory radiographic and clinical outcomes after posterior lumbar interbody fusion with reduction (Table 1).

Despite these favorable outcomes, reduction in high-grade spondylolisthesis carries a theoretical risk of nerve root stretch injury, particularly involving the L5 nerve root and the cauda equina. In this context, sacral dome osteotomy has been proposed as a valuable adjunct to facilitate safe reduction by shortening the posterior column and reducing tension on neural elements. Previous studies have suggested that resection of the sacral dome can decrease neural stretch over the posterosuperior sacral margin and thereby reduce the risk of neurological complications during de-

Table 1. Representative studies of reduction strategies for high-grade dysplastic spondylolisthesis

Study	No.	Technique	SDO	Radiographic outcome	Neurologic outcome
Shufflebarger and Geck (2005)[2]	18	Monosegmental PLIF	Yes	Slip 77→13%, SA 35→4°	No permanent deficit
Lamartina et al. (2009)[1]	25	Posterior reduction+IF	No	Slip 73→14%, SA 34→−2°	2 Transient L5 deficits
Min et al. (2012)[8]	15	Posterior reduction+L4-S1 fixation	Yes	Slip 94→25%, LSA 15→−6°	4 Transient L5 deficits
Martiniani et al. (2012)[16]	16	In situ fusion vs reduction+PLIF	No	PT 41→30°, SS 36→47°	2 Transient L5 deficits
Bouyer et al. (2014)[17]	12	Reduction+transsacral fixation	No	Slip 72→19%	5 Transient L5/S1 radiculopathies
Tian et al. (2015)[18]	13	Navigation-assisted monosegmental fusion	Yes	Slip 63→11%, LSA 18→−7°	1 Transient L5 deficit
Thomas et al. (2015)[19]	15	Posterior reduction+IF	No	Slip 73→17%, sagittal balance improved	5 Transient L5 deficits
Tatsumura et al. (2022)[15]	2	PLIF+lumbosacral fixation	No	Fusion achieved	Full neurologic recovery
Faldini et al. (2023)[7]	14	Posterior reduction+circumferential fusion	Yes	SA 34→6°, SVA improved	2 Transient L5 deficits
Takeda et al. (2024)[14]	20	Single-level PLIF+SDO	Yes	Slip 60→25%, PI-LL improved	4 Transient L5 deficits
Hadgaonkar et al. (2025)[20]	3	Navigation-assisted reduction+IF	Yes	LSK 24→4°, SVA improved	1 Revision; no permanent deficit
Ye et al. (2026)[13]	31	Complete reduction+single level fusion	Yes	Slip 61%→13%→9%, PI-LL improved	12.9% Transient sensory/radicular symptoms; no permanent motor deficit
Present case	1	Provisional stabilization+SDO+PLIF	Yes	SA 24→9°, LSA 20→5°	Urinary symptoms improved

SDO: sacral dome osteotomy, PLIF: posterior lumbar interbody fusion, SA: slip angle, IF: interbody fusion, LSA: lumbosacral angle, PT: pelvic tilt, SS: sacral slope, SVA: sagittal vertical axis, PI: pelvic incidence, LL: lumbar lordosis, LSK: lumbosacral kyphosis.

formity correction.[7,8] Although intraoperative neurophysiologic monitoring may serve as a useful adjunct during reduction procedures for high-grade dysplastic spondylolisthesis, its interpretation may be limited in patients with established CES because baseline neurophysiologic signals can already be affected by pre-existing neural dysfunction. In the present case, temporary stabilization with reduction pedicle screws and a bilateral rod was performed prior to decompression in order to prevent further slip progression and facilitate controlled reduction with sacral dome osteotomy and interbody fusion while minimizing neural tension. This strategy allowed decompression and sacral dome osteotomy to be performed under provisional stability before definitive reduction and fusion, which may be advantageous in dysplastic spondylolisthesis with coexisting canal compromise and lumbosacral instability. Progressive urinary dysfunction, particularly involuntary urinary leakage without urinary urge or subtle cauda equina symptoms should prompt early spinal evaluation and surgical consideration. Surgical strategies emphasizing provisional stabilization prior to decompression, followed by controlled reduction with sacral dome osteotomy and interbody fusion with further reduction, may help minimize neurological deterioration while achieving safe neural decompression and lumbosacral stabilization.

Although limited by the nature of a single case report, this case demonstrates that cauda equina syndrome, although exceedingly rare, can occur as an initial manifestation of dysplastic spondylolisthesis. This finding underscores the importance of early recognition and timely spinal evaluation in patients with progressive neurogenic symptoms. Carefully planned surgical strategies incorporating neural decompression, provisional stabilization, controlled reduction, and lumbosacral reconstruction may provide meaningful neurological recovery even in delayed presentations.

Author contributions

Conceptualization: JSP. Data curation: JYJ, JWH. Formal analysis: JYJ. Investigation: JYJ. Methodology: JSP. Project administration: JSP. Supervision: JSP. Validation: JSP, DHK, SJP. Visualization: JYJ. Writing – original draft: JYJ, JWH. Writing – review & editing: JSP, DHK, SJP.

https://doi.org/10.63858/jass.26.0033

Conflict of interest

Jin-Sung Park, a contributing editor of the *Journal of Advanced Spine Surgery*, was not involved in the editorial evaluation or decision to publish this article. All remaining authors have declared no conflicts of interest.

Funding

None.

Acknowledgments

None.

ORCID

Joon-Young Jung, https://orcid.org/0000-0002-8561-7522
Jae-Won Hur, https://orcid.org/0000-0002-5527-8005
Se-Jun Park, https://orcid.org/0000-0002-2412-9437
Dong-Ho Kang, https://orcid.org/0000-0002-9114-0150
Jin-Sung Park, https://orcid.org/0000-0001-6517-8609

References

1. Lamartina C, Zavatsky JM, Petruzzi M, Specchia N. Novel concepts in the evaluation and treatment of high-dysplastic spondylolisthesis. Eur Spine J 2009;18 Suppl 1:133-42.
2. Shufflebarger HL, Geck MJ. High-grade isthmic dysplastic spondylolisthesis: monosegmental surgical treatment. Spine (Phila Pa 1976) 2005;30(6 Suppl):S42-8.
3. Wiltse LL, Newman PH, Macnab I. Classification of spondylolisis and spondylolisthesis. Clin Orthop Relat Res 1976;117:23-9.
4. Labelle H, Mac-Thiong JM, Roussouly P. Spino-pelvic sagittal balance of spondylolisthesis: a review and classification. Eur Spine J 2011;20 Suppl 5:641-6.
5. Alzakri AA. Cauda equina syndrome a rare early surgical complication in a pediatric patient with dysplastic high-grade lumbosacral spondylolisthesis: a case report. J Musculoskelet Surg Res 2022;6:283-7.
6. Maurice HD, Morley TR. Cauda equina lesions following fusion in situ and decompressive laminectomy for severe spondylolisthesis: four case reports. Spine (Phila Pa 1976) 1989;14:214-6.
7. Faldini C, Barile F, Ialuna M, et al. High-grade dysplastic spondylolisthesis: surgical technique and case series. Musculoskelet Surg 2023;107:323-31.
8. Min K, Liebscher T, Rothenfluh D. Sacral dome resection and single-stage posterior reduction in the treatment of high-grade high dysplastic spondylolisthesis in adolescents and young adults. Eur Spine J 2012;21 Suppl 6:S785-91.
9. Hoel RJ, Brenner RM, Polly DW Jr. The challenge of creating lordosis in high-grade dysplastic spondylolisthesis. Neurosurg Clin N Am 2018;29:375-87.
10. Elias E, Daoud A, Elias C, Chiu RG, Sanchez JM, Nasser Z. Historical evolution, management, and outcome of surgical treatment for high-grade spondylolisthesis: a systematic review. J Neurosurg Spine 2025;42:784-96.
11. Polly DW Jr, Haselhuhn JJ, Soriano PB, Odland K, Jones KE. Management of high-grade dysplastic spondylolisthesis. Neurosurg Clin N Am 2023;34:567-72.
12. Stulik J, Geri G, Barna M, Klezl Z. High-grade high-dysplastic lumbosacral spondylolisthesis in children treated with complete reduction and single-level circumferential fusion: a prospective case series. Brain Spine 2022;2:100871.
13. Ye X, Guo D, Zhao Y, et al. Posterior L5-S1 fusion with complete reduction for pediatric high-grade dysplastic spondylolisthesis: a multicenter retrospective case series with exploratory analysis of residual sagittal imbalance. BMC Musculoskelet Disord 2026;27:314.
14. Takeda K, Suzuki S, Ozaki M, et al. Influence of slippage reduction and correction of lumbosacral kyphosis by single-level posterior lumbar interbody fusion on spinal alignment in patients with dysplastic spondylolisthesis. Spine Deform 2024;12:1761-72.
15. Tatsumura M, Funayama T, Eto F, Nagashima K, Takeuchi Y, Yamazaki M. Posterior lumbar interbody fusion for dysplastic lumbar spondylolisthesis with high-grade slippage in two adolescent siblings: two case reports. J Med Case Rep 2022;16:331.
16. Martiniani M, Lamartina C, Specchia N. "In situ" fusion or reduction in high-grade high dysplastic developmental spondylolisthesis (HDSS). Eur Spine J 2012;21 Suppl 1:S134-40.
17. Bouyer B, Bachy M, Courvoisier A, Dromzee E, Mary P, Vialle R. High-grade lumbosacral spondylolisthesis reduction and fusion in children using transsacral rod fixation. Childs Nerv Syst 2014;30:505-13.
18. Tian W, Han XG, Liu B, et al. Posterior reduction and monosegmental fusion with intraoperative three-dimensional navigation system in the treatment of high-grade developmental spondylolisthesis. Chin Med J (Engl) 2015;128:865-70.
19. Thomas D, Bachy M, Courvoisier A, Dubory A, Bouloussa H, Vialle R. Progressive restoration of spinal sagittal balance after surgical correction of lumbosacral spondylolisthesis before skeletal maturity. J Neurosurg Spine 2015;22:294-300.
20. Hadgaonkar S, Nagpal S, Bhute AR, Sancheti P. Navigation-assisted reduction and fusion for 3 cases of high-grade pediatric dysplastic spondylolisthesis: a technical note. Surg Neurol Int 2025;16:381.

Instructions for authors

JASS
Journal of Advanced Spine Surgery

Revised: May 1, 2025
Last revision: June 1, 2026

Journal of Advanced Spine Surgery (JASS) is an open access, peer-reviewed, online journal published biannually on the last day of June and December. As the official journal of The Korean Society for the Advancement of Spine Surgery, JASS aims to promote communications among spine surgeons especially who are interested in advanced spine surgery and its related basic research.

Manuscripts should adhere to the Recommendations for the Conduct, Reporting, Editing, and Publication of Scholarly Work in Medical Journals, issued by the International Committee of Medical Journal Editors (ICMJE; http://www.icmje.org/recommendations/), unless otherwise specified.

1. Article Processing Charge

There are no author submission fees or other publication-related charges. All cost for the publication process is supported by the Publisher.

2. Research and Publication Ethics

It is available at: https://e-jass.org/policy/ethics.php

3. Editorial Policies

It is available at: https://e-jass.org/policy/publishing.php

4. Submission and Peer Review Process

A. Submission

Authors should submit their manuscripts online through the JASS submission system at https://submit.e-jass.org/. Once logged in, the system will guide you through the submission process step-by-step. Detailed submission instructions are available on the website, and all manuscripts must comply with these guidelines. Failure to do so may result in the return of the manuscript and potential delays in publication.

B. Peer review process

JASS reviews all submitted manuscripts. Each manuscript is first assessed for format and relevance to the journal's aims and scope. If it meets these criteria, it is sent to two experts in the relevant field for review. JASS uses a double-blind process, where reviewer identities are concealed from the author, but both are visible to the decision-making editor. Reviewers make one of four recommendations: accept, minor revision, major revision, or reject. A first decision is typically made within an average of 2 months of receiving the manuscript. In cases of review discrepancies, the editorial board will conduct an additional review to make a final determination. Authors are expected to revise their manuscripts based on reviewer feedback and provide explanations for any feedback they choose not to implement. The editorial board makes the final publication decision and may request further changes. For more information, please refer to our peer review policy at https://e-jass.org/policy/publishing.php

5. Manuscript Preparation

A. Article types

- Original articles: Original articles present results of research investigations related to basic and clinical research of fields of advanced spinal surgery.
- Review articles: Review articles should provide a comprehensive analysis of specific topics.
- Systematic reviews and Meta-analyses: Systematic reviews and Meta-analyses should follow the PRISMA (Preferred Reporting Items for Systematic Reviews and Meta-Analyses) guidelines. These reviews should rigorously assess and synthesize quantitative or qualitative data to answer specific research questions.
- Case reports: Case reports are published under exceptional circumstances to illustrate rare occurrences of clinical significance. They should address important issues for medical researchers and preferably include helpful illustrations. Informed consent from the patient is mandatory.
- Technical notes: Technical notes provide a brief description of a novel or modified surgical technique, instrumentation, or procedure. These should focus on the technical aspects and clinical utility of the innovation.
- Editorial: Editorials are most commonly invited by the editorial board. These provide a brief review of the articles in the journal and comment on recent developments and events in

the field of spine surgery.

- Correspondence: Correspondences provide a platform for discussing current issues in the spine, sharing brief observations, and offering professional opinions. Submissions may include short reports on novel findings, discussions on timely issues, or other scholarly contributions that do not fit the structure of full-length articles. If submitted as a Letter to the Editor, it presents opinions, findings, or responses directly related to articles published in the journal, fostering focused discussions.

Key features and limits of articles are summarized in Table 1 below. However, the limits are negotiable with the editor.

B. Reporting guidelines

For specific study designs, such as randomized controlled trials, diagnostic accuracy studies, meta-analyses, observational studies, and non-randomized studies, authors should follow the relevant reporting guidelines. Recommended sources include the EQUATOR Network (https://www.equator-network.org/) and the National Library of Medicine (https://www.nlm.nih.gov/services/research_report_guide.html). Table 2 summarizes reporting guidelines for listed article types.

C. General requirements

- **Language:** Manuscripts should be submitted in English or Korean. Medical terminology should be written based on the most recent edition of Dorland's Illustrated Medical Dictionary or the medical terminology published by the Korean Medical Association.
- **Cover letter:** The cover letter must confirm that all authors approved the final manuscript, that the work is original and not under review elsewhere.
- **Format:** Manuscripts should be prepared using Microsoft Word (doc or docx format). Texts should be double-spaced with the same normal, plain font throughout, preferably 11-point Times New Roman. Manuscripts should include continuous line numbers and page numbers to facilitate the review process.
- **Anonymization:** Submit the title page and manuscript as separate files. The manuscript must be anonymized for double-blind peer review; do not include authors' names or affiliations.

Table 1. Key features and limits of articles

Type of article	Word count*	Abstract	Text structure	References	Tables and figures
Original article	≤ 4,000	≤ 350 words (structured)	Introduction, Methods, Results, Discussion	30	8
Review article	≤ 5,000	≤ 350 words (unstructured)	Introduction, Body text, Conclusion	100	No limit
Systematic review and Meta-analysis	≤ 5,000	≤ 350 words (structured)	Follow the PRISMA guidelines	100	No limit
Case report	≤ 2,000	≤ 200 words (unstructured)	Introduction, Case report, Discussion	20	5
Technical note	≤ 2,000	≤ 200 words (unstructured)	Introduction, Technical note, Discussion	20	5
Editorial	≤ 1,000	Not required	Single section with no headings	10	2
Correspondence	≤ 1,000	Not required	Single section with no headings	10	2

*Excluding abstract, references, tables, and figure legends.

Table 2. Reporting guidelines for specific study designs

Initiative	Type of study	Source
CONSORT	Randomized controlled trials	https://www.equator-network.org/reporting-guidelines/consort/
TREND	Non-randomized controlled studies	https://www.cdc.gov/hivpartners/php/trend-statement/index.html
STROBE	Observational studies	https://www.equator-network.org/reporting-guidelines/strobe/
STARD	Diagnostic/prognostic studies	https://www.equator-network.org/reporting-guidelines/stard/
PRISMA	Systematic reviews and meta-analyses	https://www.equator-network.org/reporting-guidelines/prisma/
CARE	Case reports	https://www.equator-network.org/reporting-guidelines/care/

- **Abbreviations:** Abbreviations should be avoided as much as possible. Abbreviations should be defined at their first occurrence in the text and used consistently thereafter. Abbreviations should not be present in the title. Common abbreviations, such as DNA or COVID-19, however, may be used.
- **Units:** The use of International Standardized (SI) units (https://www.nist.gov/pml/owm/metric-si/si-units/) is encouraged.
- **Machines and equipment:** When the use of reagents or devices is reported in the text, the name of the manufacturer should be indicated.
- **Statistics:** Statistical methods must be described and the program used for analysis and its source should be stated. P-values should be reported to three decimal places (e.g., P = 0.005).
- **Use of generative artificial intelligence (AI):** Please refer to our AI policy at https://e-jass.org/policy/publishing.php

D. Manuscript structure and format

- **Organize your manuscript file as follows:**

- Title page
- Manuscript file: (1) Abstract & keywords, (2) Body text, (3) References list (4) Tables (each beginning on a new page), (5) Figures legends (upload figures in separate files)
- Supplementary materials (upload separately)

- **Title page**

Title: The article title should be concise and precise. The title should also indicate the study design. If the study involved human participants, the country where the study was conducted should be included.

Running title: Less than 50 characters.

Authors names: Each author's full given name, surname and degrees–MD, PhD, etc. should be provided. All authors must meet the authorship criteria of the ICMJE (www.icmje.org).

Affiliations: Departments and institutions of the authors. If from multiple institutions, use superscript numbers (e.g., [1], [2], [3]) to indicate specific affiliations.

Corresponding author: Full name, institutional affiliation, postal address, and email address.

Co-first authors and co-corresponding authors may be designated when applicable. Such designations must be explicitly stated on the title page at submission. However, the designation of an excessive number of authors may not be permitted.

ORCID: Providing ORCID iDs for all authors is required (https://orcid.org/).

Authors' contributions: Describe contributions using the Contributor Roles Taxonomy (CRediT; https://credit.niso.org/). Contributors must meet at least one core role (conceptualization, data curation, formal analysis, investigation, methodology, software, validation) and one writing role (original draft preparation, review, and editing). Authors who do not meet these requirements will not qualify for authorship.

Conflict of interest: Disclose any potential conflicts of interest, including employment, consultancy, ownership, or close relationships with organizations affected by the manuscript.

Funding: Funding for the research should be detailed here. Provision of a FundRef ID is recommended, including the name of the funding agency, country, and (if available) the number of the grant provided by the funding agency. If the funding agency lacks a FundRef ID, please ask that agency to contact the FundRef registry (email: fundref.registry@crossref.org).

Data availability: Include a statement indicating where the data supporting the article's results can be found, with hyperlinks to publicly archived datasets if applicable.

Acknowledgments: List individuals who contributed to the work but do not meet authorship criteria, and specify their contributions (e.g., technical assistance, data collection, analysis, or editorial support). Disclose any writing assistance and the entity that funded it.

If any of the sections are not relevant to the manuscript, please include the heading and write "Not applicable." for that section.

- **Abstract and keywords**

Abstract: For original articles and systematic reviews, provide a structured abstract of less than 350 words. The abstract must include the following headings: Purpose, Methods, Results, and Conclusion. Study Design and Overview of Literature may be included, if applicable.. For review articles, provide an unstructured abstract of up to 350 words. For case reports, provide an unstructured abstract of up to 200 words.

- Keywords: List up to three to five keywords at the bottom of the abstract. Refer to Medical Subject Headings (MeSH, http://www.ncbi.nlm.nih.gov/mesh/MBrowser.html) for keyword selection.

- **Main Text**

The main text of an original article should be divided into 4 sections: Introduction, Methods, Results, and Discussion.

Introduction: State the background or problem that led to the initiation of the study. Lead systematically to the hypothesis of the study and finally, to a restatement of the study objectives, which should match that in the abstract. Do not include con-

clusions in the Introduction.

Methods:

- Ethics: Statement of Ethics Committee/IRB approval and informed consent must be included.
- Study design: Describe the design (e.g., prospective, retrospective, randomized controlled), inclusion/exclusion criteria, and study period.
- Procedures: Provide enough detail to enable replication. Reference reporting guidelines such as CONSORT for clinical trials or STROBE for observational studies are encouraged.
- Statistical analysis: Clearly describe the statistical methods used, including the software and the level of significance (e.g., $p < 0.05$).

Results: Present the findings in a logical sequence. Avoid repeating all the data from tables or figures in the text; instead, emphasize or summarize the most important observations.

Discussion: Data should be interpreted to demonstrate whether they affirm or refute the original hypothesis. Discuss elements related to the purpose of the study and present the rationales that support the conclusion drawn by referring to relevant literature. Care should be taken to avoid information obtained from books, historical facts, and irrelevant information. A discussion of study weaknesses and limitations should be included. Conclusions derived from the results should be described in one to two sentences and must match the study objectives.

• References

All references should be listed in the order of citation in the text, with corresponding numbers.

- Identify references in the main text by superscript Arabic numerals and numbered in consecutive order, as they appear in the main text. Use "-" when there are more than 3 references to be cited; for example, 4-7).
- In the references section, list all authors' names for a reference with up to 6 authors; list first 3 authors' names followed by 'et al.' if more than 6 authors.
- Journals should be abbreviated according to the style used in the list of journals indexed in the NLM Journal Catalog (https://www.ncbi.nlm.nih.gov/nlmcatalog/journals/). Journal titles that are not listed in the Catalog should follow the ISO abbreviation as described in Access to the LTWA (List of Title Word Abbreviations; https://www.issn.org/services/online-services/access-to-the-ltwa/).
- References should follow the NLM Style Guide for Authors, Editors, and Publishers (https://www.ncbi.nlm.nih.gov/books/NBK7256/) if not specified below.

Journal articles

1. Park TG, Baek SN, Kim MS, Choi YS. The interplay between frailty, skeletal muscle mass, and bone mineral density in osteoporotic vertebral fractures. J Adv Spine Surg 2024;14:41-7.
2. Feng C, Wang L, Yang S, et al. A new pilot hole preparation system for percutaneous pedicle screw placement: a randomized controlled study. Spine (Phila Pa 1976) 2025;50:115-21.

Books

3. Baaj AA, Mummaneni P, Uribe JS, Vaccaro AR, Greenberg MS. Handbook of spine surgery. 3rd ed. Thieme; 2025.
4. Kim SW, McAfee PC. Cervical disc replacement combined with cervical laminoplasty. In: Yue JJ, Bertagnoli R, editors. Motion preservation surgery of spine. Saunders Elsevier; 2008. p. 595-603.

Online sources

5. World Health Organization (WHO). World health statistics 2023: a visual summary [Internet]. WHO; 2023 [cited 2025 Feb 1]. Available from: https://www.who.int/data/stories/world-health-statistics-2023-a-visual-summary
6. Sharma N, Sharma P, Basu S, et al. The seroprevalence and trends of SARS-CoV-2 in Delhi, India: a repeated population-based seroepidemiological study [Preprint]. Posted 2020 Dec 14. medRxiv 2020.12.13.20248123. https://doi.org/10.1101/2020.12.13.20248123

• Tables

Each table should begin on a new page, with the table number and title above the table and explanatory notes below. Tables should be self-explanatory, and the data presented should not be duplicated in the text or figures.

- Table numbers must correspond to the order in which they are cited in the text.
- Designate all units of measurement and concentration.
- Indicate footnotes with symbols in the following order: a), b), c), d).
- List abbreviations in the footnote under the table.
- Use only horizontal lines; longitudinal (vertical) lines must be avoided. A standard three-line format (top line, line below column headings, and bottom line) is highly encouraged.
- When reporting data, specify the measures of variability (e.g., mean ± SD or median [IQR]).

- If using previously published tables, the original source must be cited in the footnote. For copyrighted materials, authors are responsible for obtaining official permission from the copyright holder.

• **Figures**

- Each figure should be submitted as a separate file. Preferred formats are TIFF, EPS, or high-quality JPG. Figures must have a minimum resolution of 300 DPI for color/grayscale images and 600–1,200 DPI for line art. GIF format is not recommended.
- All identifying information (e.g., patient names, hospital IDs, dates) must be removed from radiographs, scans, and clinical photographs.
- Citations: Figure numbers must correspond to the order in which they are mentioned in the text.
- If a figure consists of multiple panels, label them with upper-case letters (A, B, C, etc.) in the top-left corner.
- Figure legends should be listed on a separate page after the reference list. Abbreviations used in the figure must be defined in alphabetical order at the end of each legend.
- All symbols used (e.g., arrows, asterisks) must be clearly explained in the legend.
- For previously published figures, the original source must be cited in the legend, and authors are responsible for obtaining and submitting official written permission from the copyright holder.

• **Supplementary materials**

- Supplemental materials (e.g., extra tables, appendices, or video clips) that enhance the article but are not essential for understanding the main text may be published online.
- Supplemental files should be named and cited in the text as Supplementary Table S1, Supplementary Fig. S1, etc.
- List all supplemental materials at the end of the manuscript file. These materials are subject to peer review and should be provided in their final form at the time of submission.

6. Processing After Acceptance

A. Manuscript corrections

Before publication, the manuscript editor will correct the manuscript such that it meets the standard publication format. The author(s) must respond within 2 working days when the manuscript editor contacts the author for revisions. If the response is delayed, the manuscript's publication may be postponed to the next issue.

B. Galley proofs

Once all corrections have been completed, the corresponding author will receive the final version of the manuscript in PDF format.

Within 3 working days of receipt, authors must reply to the printing office of any errors found in the file. The proof may be revised more than once by the corresponding author, if needed. Authors should double-check for corrections in the content, title, affiliation, capitalization, locations of figures, and references.

7. Post-Publication Corrections

To correct errors in published articles, the corresponding author should contact the journal's editorial office with a detailed description of the proposed correction. Corrections that profoundly affect the interpretation or conclusions of the article will be reviewed by the editors. Corrections will be published as author correction or publisher correction in a later issue of the journal.

Minor errors will be corrected directly in the online version of the article. An indication of the correction, along with the date it was made, will be added to the article information in both the HTML and PDF versions. A separate correction note will not be published.

Contact Us

Editor-in-Chief: Jae Keun Oh, MD, PhD
Email: ohajekeun@gmail.com

Editorial Office: The Korean Society for the Advancement of Spine Surgery, 50-1, Yonsei-ro, Seodaemun-gu, Seoul 03722, Korea
Tel: +82-2-2228-0582
Email: office@e-jass.org

NOTICE: These instructions to authors will be effective from the June 2026 issue.

Author's checklist

JASS
Journal of Advanced Spine Surgery

Question	Yes	No
1) Manuscript in MS-WORD (.doc) format.		
2) Double-spaced typing with 10-point font.		
3) Sequence of title page, abstract and keywords, introduction, methods, result, discussion, acknowledgements, references, tables, and figure legends. All page numbered consecutively, starting with the abstract.		
4) Title page with article title, author's full name (s) and affiliation (s), address for correspondence (including telephone number, e-mail address, and fax number), running title (less than 10 words), and acknowledgements, if any.		
5) Abstract in structured format up to 350 words for original articles and unstructured format up to 200 words for case reports. Keywords (up to 5) from theeS MH list of Index Medicus.		
6) All table and figure number are found in the text		
7) Figure as separate files, in JPG, GIF, or PPT format.		
8) References listed in proper format. All reference listed in the reference section are cited in the text and vice versa.		
9) Covering letter signed by the corresponding author.		

Copyright transfer agreement

JASS
Journal of Advanced Spine Surgery

Manuscript title: _____

I. Copyright Transfer Form

The authors hereby transfer all copyrights in and to the manuscript named above in all forms and media, now or hereafter known, to the Korean Society for the Advancement of Spine Surgery effective if and when the paper is accepted for publication in the Journal of Advanced Spine Surgery. The authors reserve all proprietary right other than copyright, such as patent rights.

Everyone who is listed as an author in this article should have made a substantial, direct, intellectual contribution to the work and should take public responsibility for it.

This paper contains works that have not previously published or not under consideration for publication in other journals.

II. Conflict of Interest Disclosure Form

All authors are responsible for recognizing any conflict of interest that could bias their work in the acknowledgments, disclosing all financial support and any other personal connections.

Please check the appropriate box below:

☐ No author of this paper has a conflict of interest, including specific financial interests, relationships, and/or affiliations relevant to the subject matter or materials included in this manuscript.

OR

☐ The authors certify that all conflicts of interest, as applicable to each author, including specific financial interests, relationships, and/or affiliations relevant to the subject matter or materials are disclosed in the manuscript.

(Please describe in detail about these interests.)

_____

_____

_____

These interests may include one or more of the following: employment; consultancy within the past two years; ownership interests – including stock options – in a start-up company, the stock of which is not publicly traded; ownership interest - including stock options but excluding indirect investments through mutual funds and the like - in a publicly traded company; research funding; honoraria directly received from an entity; paid expert testimony within the past two years; any other financial relationship (e.g., receiving royalties); membership on another entity's Board of Directors or its advisory committees (whether for profit or not for profit).

☐ All authors certify that the work followed the research ethics and have approved the submission of the manuscript for publication.

Corresponding author	Signature	Date
_____	_____	_____

*This copyright agreement has been signed by the submitting/corresponding author on behalf of any and all co-authors.